

Uppsala University  
Signals and Systems

OPTIMAL DETECTORS FOR  
TRANSIENT SIGNAL FAMILIES  
AND NONLINEAR SENSORS  
Derivations and Applications

Daniel Asraf



UPPSALA UNIVERSITY 2003

Dissertation for the degree of Doctor of Philosophy  
in Signal Processing at Uppsala University, 2003.

#### ABSTRACT

Asraf, D., 2003. *Optimal Detectors for Transient Signal Families and Nonlinear Sensors: Derivations and Applications*, 201 pp. Uppsala. ISBN 91-506-1664-1.

This thesis is concerned with detection of transient signal families and detectors in non-linear static sensor systems. The detection problems are treated within the framework of likelihood ratio based binary hypothesis testing.

An analytical solution to the noncoherent detection problem is derived, which in contrast to the classical noncoherent detector, is optimal for wideband signals. An optimal detector for multiple transient signals with unknown arrival times is also derived and shown to yield higher detection performance compared to the classical approach based on the generalized likelihood ratio test.

An application that is treated in some detail is that of ultrasonic nondestructive testing, particularly pulse-echo detection of defects in elastic solids. The defect detection problem is cast as a composite hypothesis test and a methodology, based on physical models, for designing statistically optimal detectors for cracks in elastic solids is presented. Detectors for defects with low computational complexity are also formulated based on a simple phenomenological model of the defect echoes. The performance of these detectors are compared with the physical model-based optimal detector and is shown to yield moderate performance degradation.

Various aspects of optimal detection in static nonlinear sensor systems are also treated, in particular the stochastic resonance (SR) phenomenon which, in this context, implies noise enhanced detectability. Traditionally, SR has been quantified by means of the signal-to-noise ratio (SNR) and interpreted as an increase of a system's information processing capability. Instead of the SNR, rigorous information theoretic distance measures, which truly can support the claim of noise enhanced information processing capability, are proposed as quantifiers for SR. Optimal detectors are formulated for two static nonlinear sensor systems and shown to exhibit noise enhanced detectability.

*Key-words:* Optimal detection, transient signals, noncoherent detection, unknown arrival time, ultrasonic nondestructive testing, nonlinear sensor, stochastic resonance.

*Daniel Asraf, Signals and Systems, Uppsala University, P O Box 528,  
SE-751 20 Uppsala, Sweden. Email: daniel.asraf@signal.uu.se.*

© Daniel Asraf 2003

ISBN 91-506-1664-1

Printed in Sweden by Elanders Gotab AB, Stockholm, March 2003.

Distributed by Signals and Systems, Uppsala University, Uppsala, Sweden.

*To Marie my wife to be  
and my family  
Abraham, Barbro, and Sabina*

## Acknowledgments

I want to express my sincere gratitude to my supervisor and dear friend, Dr. Mats Gustafsson, for his valuable guidance, co-operation, encouragement and support. Mats' broad and deep knowledge of signal processing has truly shaped me during my years as a Ph.D student, moreover, his enormous enthusiasm has also been a great source of motivation. It has been a pleasure and an honor to work with Mats and I am happy that we dedicated some of our countless discussions on topics other than science. I sincerely hope the future will bring several more opportunities for us to work together.

I would also like to thank, Dr. John Robinson, of the Swedish Defence Research Agency (FOI) for helpful guidance notably during the early stages of my Ph.D. studies. John's mathematical profile brought my interest to the rigorous and powerful tools associated with continuous-time stochastic calculus, which I hope to further pursue, mainly for the pure interest but also so that, I too, can become "kosher".

While working simultaneously at both FOI and the Signals and Systems group has proven challenging, I am deeply grateful to both institutions for allowing me to be part of their teams.

I want to thank all the people working at Signals and Systems for providing an open and creative research environment, especially the "basement click"; Fredrik Lingvall, Dr. Tomas Olofsson, Dr. Ping Wu, and Professor Tadeusz Stepinski for being invaluable sounding-boards and enduring my constant rambling about the biographies of various scientists. Additionally, I am very thankful to Professor Anders Ahlén for reading and constructively criticizing the manuscript.

I am particularly grateful to Dr. Johan Mattsson, of FOI, who provided me with an ultrasonic scattering code and helped me to absorb rudimentary elastodynamic wave propagation and scattering theory. I would also like to acknowledge Mattias Karlsson, Dr. Peter Krylstedt, Ron Lennartsson, Ingvar Nedgård, Dr. Leif Persson, Dr. Erland Sangfeldt, and Dan Öberg, of FOI, for being great colleagues and discussion partners. Due to my affiliation with FOI, I have had the opportunity to work with several international scientists, who I would like to acknowledge. In particular, Professor Melvin Hinich, of the University of Texas at Austin, for opening up my interest to other areas of signal processing and for being a dear friend. I also wish to thank Dr. Adi Bulsara, of SPAWAR Systems Center, and Professor Luca Gammaitoni, of the University of Perugia, for giving me a crash course on Stochastic Resonance and SQUIDS but also for spicing up the atmosphere by simply being themselves.

My reason for undertaking the “Ph.D.-endeavor” begun long before I decided to enroll as a Ph.D. student. This reason is due entirely to my parents, who brought me up to value education, have the confidence of free thinking and appreciate the importance of exploration and development. I am convinced that without this background, my sister Sabina’s constant encouragement and support, I would have most likely never written this thesis.

Finally, and most importantly, I would like to express my deepest gratitude to my fiancée, Marie, for enduring me all these years. You have been an incredible source of motivation with your never-ending patience and support. Thank you for making all this worth while and for opening up my heart, my soul, and my mind to all aspects of life. Marie, words can not express enough how grateful I am and always will be.

*Daniel Asraf*  
*Uppsala, February 2003.*



# Contents

<b>Acknowledgments</b>	<b>iv</b>
<b>COMPREHENSIVE SUMMARY</b>	<b>1</b>
<b>1 Introduction</b>	<b>3</b>
1.1 Derivations of optimal detectors . . . . .	4
1.1.1 Detection of transient signal families in Gaussian noise . .	5
1.1.2 Optimal detectors in nonlinear sensor systems . . . . .	6
1.2 The considered application areas . . . . .	8
1.2.1 Ultrasonic defect detection using piezoelectric transducers	8
1.2.2 Detection of a magnetic field by means of a nonlinear sensor	12
1.3 Problem formulations . . . . .	17
1.4 Contributions . . . . .	23
1.5 Outline of the thesis . . . . .	25
<b>2 Signal detection</b>	<b>27</b>
2.1 Signal detection in discrete time . . . . .	27
2.1.1 Detection of deterministic signals in Gaussian noise . . .	29
2.1.2 Detection of parameterized signals in Gaussian noise . . .	32
2.1.3 Detection of Gaussian signals in Gaussian noise . . . . .	36
2.2 Signal detection in continuous time . . . . .	38
2.2.1 Detection of deterministic signals in Gaussian noise . . .	40
2.2.2 Detection of parameterized signals in Gaussian noise . . .	41
2.3 Detection of non-Gaussian signals . . . . .	45
<b>3 Defect detection in ultrasonic nondestructive testing</b>	<b>47</b>
3.1 Elastodynamic preliminaries . . . . .	47

3.2	Modeling of the piezoelectric transducer . . . . .	49
3.3	Modeling of the crack echo . . . . .	51
3.3.1	Physical model in the frequency domain . . . . .	51
3.3.2	Phenomenological model in the time domain . . . . .	54
3.4	Modeling of clutter noise in metals . . . . .	57
3.5	Signal detection applied to nondestructive testing . . . . .	59
3.5.1	Physical model based crack echo detector . . . . .	60
3.5.2	Phenomenological model based crack echo detector . . . . .	62
<b>4</b>	<b>Detectors in nonlinear sensor systems</b>	<b>65</b>
4.1	The superconducting quantum interference device . . . . .	66
4.2	The magneto-resistive sensor . . . . .	68
4.3	Optimal detectors in static nonlinear sensor systems . . . . .	71
4.3.1	Detectability in nonlinear sensor systems . . . . .	71
4.3.2	Sensor optimization for detection . . . . .	73
<b>5</b>	<b>Concluding remarks and future work</b>	<b>75</b>
<b>A</b>	<b>Background on binary hypothesis testing</b>	<b>77</b>
A.1	Simple and composite binary hypothesis testing . . . . .	77
A.2	Bayesian optimality . . . . .	78
A.3	Neyman-Pearson optimality . . . . .	80
A.4	The generalized likelihood ratio strategy . . . . .	81
A.5	Detector performance evaluation . . . . .	82
<b>B</b>	<b>Sufficient statistics and statistical distance measures</b>	<b>85</b>
B.1	Sufficient statistics . . . . .	85
B.2	Statistical distance measures . . . . .	88
B.2.1	Information theoretic distance measures . . . . .	88
B.2.2	The deflection ratio . . . . .	91
	<b>Bibliography</b>	<b>93</b>

# **COMPREHENSIVE SUMMARY**



# Chapter 1

## Introduction

THE subjects of signal detection and information theory, in one way or another, deal with processing of information bearing signals in order to make inferences concerning the information they contain. These fields trace back to the classical work of Bayes, Gauss, Fisher [1], and Neyman and Pearson [2] but it was not until the 1930's and 1940's that Wiener [3], Shannon [4], and others, shaped the disciplines into the form we see today.

Ever since the early dawn of signal detection and information theory, the fields have been actively used in a multitude of applications ranging from communications and physics to economics. This progress is in many aspects due to the access of high performing computers, which open the possibilities to process, store and collect massive amounts of data in order to implement many of the computationally demanding methodologies within information theory and signal detection.

Still, several applications remain that can benefit from utilizing the general results that have been presented within these disciplines, both when it comes to pushing the envelopes of already existing methods but also in explaining and understanding new phenomena.

This introductory chapter is intended to give a brief overview of the general framework used to solve detection problems but also the different application areas considered in the thesis as well as the current state-of-the-art approaches and solutions to the problems under study. Section 1.1 outlines the generic approach to solve detection problems based on statistical binary hypothesis testing and also how this generic setting can be used to cast the specific problem of detecting transient signal families and signals acquired with nonlinear sensors. Section 1.2, presents the two considered application areas, which are magnetic field detection and defect detection by means of ultrasonic nondestructive testing. The specific problems

considered in the thesis are presented in Section 1.3, followed in Section 1.4 by a list of the contributions and publications on which the thesis is based. Finally, in Section 1.5, an outline of the thesis is given.

## 1.1 Derivations of optimal detectors

From a purely mathematical perspective the problem of optimal signal detection was solved once it was connected to statistical hypothesis testing and thereby the classical 1933 paper by Neyman and Pearson [2]. However, this insight only signaled the beginning of a new quest from an engineering point of view. The main objective of this engineering quest is to explicitly derive and apply optimal detectors for special, practically relevant problems.

The generic approach to solve detection problems is here briefly described by considering the binary hypothesis test. Binary hypothesis testing is concerned with deciding among two possible statistical hypotheses (situations), denoted  $H_0$  and  $H_1$  respectively, by processing the outcomes,  $y$ , of a stochastic variable  $Y$ . The stochastic variable  $Y$  is assumed to have two possible probability distributions  $P_0$  and  $P_1$  under  $H_0$  and  $H_1$ , respectively. This problem may be written as

$$\begin{aligned} H_0 : Y &\sim P_0 \\ \text{versus} & \\ H_1 : Y &\sim P_1, \end{aligned} \tag{1.1}$$

where  $Y \sim P$  denotes that  $Y$  has the probability distribution  $P$ . In [2] Neyman and Pearson present a general formalism for finding a decision rule with the highest probability of correct detection given a specified probability of false alarm. It is shown that the key quantity to compute is the likelihood ratio which is given by

$$L(y) = \frac{p_1(y)}{p_0(y)}, \tag{1.2}$$

where  $p_0$  and  $p_1$  are the probability density functions (pdfs) of  $Y$  under the  $H_0$  and  $H_1$  hypotheses, respectively. A comparison of the likelihood ratio to a threshold then yields the Neyman-Pearson optimal decision rule

$$\delta(y) = \begin{cases} 1 & \text{if } L(y) \geq \tau \\ 0 & \text{if } L(y) < \tau, \end{cases} \tag{1.3}$$

where the threshold  $\tau$  is selected to satisfy the imposed false alarm constraint. Hence, given an observation  $y$  the decision rule in (1.3) produces either  $\delta(y) = 0$  or  $\delta(y) = 1$  corresponding to  $H_0$  and  $H_1$ , respectively. Detection strategies where

the likelihood ratio is compared to a threshold is also the result of a number of other optimization criteria and is described in some more detail in Appendix A.

Thus, to derive an optimal detector one *only* has to cast the signal detection problem as a binary hypothesis test and then find an expression for the likelihood ratio between the considered hypotheses. Several practically relevant detection problems have been solved by using this methodology and proved useful in applications such as radar [5, 6, 7, 8, 9, 10], sonar [5, 6, 11], and communication [12, 13].

The ambition of this thesis is to contribute to the above mentioned engineering quest by focusing on deriving and applying optimal detectors for some problems associated with detecting transient signal families as well as signals acquired with nonlinear sensors.

### 1.1.1 Detection of transient signal families in Gaussian noise

The need to detect transient signals is apparent in applications such as radar [5, 6, 7, 8, 9, 10], sonar [5, 6, 11], communication [12, 13], and ultrasonic nondestructive testing (UNDT) [14], with the latter being studied in some detail in this thesis. Moreover, in many of the above mentioned applications it is common that the transient signal to be detected can exhibit different waveforms from one measurement to another.

In digital communication systems this situations arises, for example, when the symbol to be transmitted is represented by an amplitude modulated sinusoid. At the receiver the carrier frequency and the modulation might be known but the amplitude and phase may not. This yields that the transient signal to be detected can be represented by an explicit mathematical expression with the amplitude and phase as unknown parameters.

In the radar, sonar, and UNDT applications the transient signal to be detected is, for example, generated by the back-scattered echo from a potential object impinged by a transmitted pulse. The waveform of the received target echo is dependent on the the physical attributes involved in the scattering process such as the objects shape, location, orientation, material, etc.

Regardless of the signal generating mechanism, the transient signal family can be described by

$$\mathcal{S} = \{\bar{s}(\theta) | \theta \in \Lambda\}, \quad (1.4)$$

where  $\bar{s}(\theta) = [s_1(\theta), \dots, s_N(\theta)]^T$  is a vector<sup>1</sup> of samples from a transient signal,  $\theta$  represents explicit mathematical or underlying physical parameters and  $\Lambda$  is some

---

<sup>1</sup>In the discrete time problems treated in this thesis vectors are taken to be columnar and the superscript  $T$  denotes transposition.

space where  $\theta$  takes its values.

The problem of detecting a transient signal, randomly drawn from the family in (1.4), and corrupted by an additive noise can be formulated as a binary hypothesis test (1.1). A discrete time formulation of (1.1) may be expressed as

$$\begin{aligned} H_0 : \bar{Y} &= \bar{V} \\ \text{versus} \\ H_1 : \bar{Y} &= \bar{s}(\theta) + \bar{V}, \end{aligned} \tag{1.5}$$

where  $\bar{Y} \in \mathbb{R}^N$  is a stochastic vector representing a sampled version of the observed signal and  $\bar{V}$  is a vector of noise samples. In statistical hypothesis testing the problem in (1.5) is commonly referred to as a composite hypothesis test since the  $H_1$ -hypothesis is dependent on the unknown parameter  $\theta$ .

Thus, to find an optimal detector for (1.5) on the form (1.3) the likelihood ratio needs to be computed. This involves not only knowledge of the statistical properties of the noise  $\bar{V}$ , and the waveforms of the signals  $\bar{s}(\theta)$  but also the random law describing how the signals  $\bar{s}(\theta)$  are drawn from (1.4), i.e. the distribution of  $\theta$  on  $\Lambda$ . Even if all this knowledge is available and expressed by explicit mathematical expressions the derivation of the likelihood ratio is often a formidable task to perform analytically. Historically, the analytical approach was the main route to consider in order to achieve a practically useful detector, but due to the current access of high performing computers alternative approaches, based on numerical solutions, are opened up.

### 1.1.2 Optimal detectors in nonlinear sensor systems

Sensors are generally based on mechanisms where one physical quantity can be coupled to another, e.g. a magnetic field at the input to the sensor yields an electrical voltage at its output. Several of these physical mechanisms are nonlinear by nature and when designing sensors great effort and ingenuity are used to obtain a linearized regime within which the sensor is to be operated. However, in situations when a sensor is operated outside its linear regime, e.g. in very noisy environments, the interpretation of the sensor outputs becomes more complicated. This limits the original usability of the sensor to reach end objectives such as detection, estimation, prediction etc.

Recently a new approach for detecting a weak harmonic signal in additive Gaussian noise, measured by a nonlinear sensor, was proposed independently by Hibbs *et al.* [15] and Rouse *et al.* [16]. Their method utilizes the nonlinear characteristics of the super conductive quantum interference device (SQUID) to detect a weak magnetic field corrupted by an additive Gaussian noise. The key step in

their proposed detection strategy is to “tune” the SQUID to operate in the so-called stochastic resonance (SR) regime [17, 18].

In this context the SR effect yields the somewhat unintuitive phenomenon of increased detectability with increased noise strength. A generally accepted description of the SR phenomenon is that of a noise induced performance enhancement in terms of the system’s information processing capability [17, 18, 19, 20, 21]. Although SR has been observed in several different application areas and contexts, one of the most studied and exemplified is that of signal detection, mainly due to the unintuitive effect of noise enhanced detection performance. Recently a similar study has been presented in the signal processing community where Kay poses the question: “Can detectability be improved by adding noise?” in a paper with the same title [22].

As pointed out above, the approach taken by Hibbs *et al.* [15] and Rouse *et al.* [16] was based on the SR phenomenon and focused less on the signal processing methodologies associated with optimal detection. Therefore, it is of interest to explore the potential of deriving and applying statistically optimal detectors for nonlinear sensors. The fundamental problem considered is to detect if a weak signal is present in an additive Gaussian noise environment based on measurements acquired with a nonlinear sensor. This problem is naturally cast within the framework of binary hypothesis testing by modeling the hypotheses in (1.1) as

$$\begin{aligned} H_0 : Y_t &= g_\beta(V_t), \quad 0 \leq t \leq T \\ \text{versus} \\ H_1 : Y_t &= g_\beta(s_t + V_t), \quad 0 \leq t \leq T. \end{aligned} \tag{1.6}$$

Here  $s_t$  is the signal to be detected,  $V_t$  is the additive Gaussian noise,  $Y_t$  is the sensor output signal and  $g_\beta$  represents the nonlinear sensor, which can be “tuned” by means of the parameter  $\beta$ . Obviously, even if the noise  $V_t$  is Gaussian and the signal to be detected,  $s_t$ , is deterministic and known, the sensor output  $Y_t$  will be non-Gaussian under both  $H_0$  and  $H_1$  due to the nonlinear characteristic of  $g_\beta$ . Generally, non-Gaussian detection problems are analytically intractable and thereby usually attracts alternative types of signal processing, e.g. wavelet decompositions, neural networks, and higher order statistics. A comprehensive tutorial on non-Gaussian detection problems can be found in [23]. The preferred approach for a particular problem depends on the level of knowledge that can be used in describing the stochastic processes. In situations when little knowledge is at hand one has to retreat to suboptimal techniques which are tailor made for the particular problem. The approach taken by Hibbs *et al.* [15] and Rouse *et al.* [16] can be considered to belong to these suboptimal techniques since their method is based on qualitative reasoning concerning the spectral characteristics of the signal and not on the likelihood ratio.

When the sensor transfer characteristics  $g_\beta$ , the statistical properties of the noise  $V_t$  as well as the signal to be detected  $s_t$ , are all considered to be known there is no need to retreat to suboptimal procedures to solve (1.6). Instead the classical statistical hypothesis testing approach can be used to construct an optimal likelihood ratio detector. The statistical hypothesis testing formulation of the sensor-detector problem does not only have the benefit of ensuring optimality, it also provides a framework for an information theoretic (IT) view on the sensor “tuning” problem. Moreover, as is shown in this thesis, the IT formulation yields, as a “Bonus”, a generalization of the SR phenomenon.

Due to the development of digital signal processors (DSP) ubiquitous algorithms can be implemented in sensor systems to tackle problems such as “tuning” and detection. The signal processing approach can in this way enhance performance of nonlinear sensor systems by expanding the sensors operating regime and has the benefit of alleviating the constraints imposed by linearization and thereby reducing, for example, energy consumption, complicated and costly design procedures, the use of expensive materials etc.

## 1.2 The considered application areas

In this thesis the two considered application areas are defect detection by means of ultrasonic nondestructive testing (UNDT) and detection of magnetic fields measured by means of a nonlinear magnetic sensor. Although many of the utilized methodologies and results presented here are of general applicability this section is intended to give an overview of the two application areas as well as a brief description of some of the state-of-the art methods of particular interest for the problems treated in this thesis. The considered application areas are briefly presented next.

### 1.2.1 Ultrasonic defect detection using piezoelectric transducers

Most transducers used for ultrasonic nondestructive testing (UNDT) are based on piezoelectric materials due to their ability to convert electric energy to mechanical energy and vice versa. In this type of testing procedure, acoustic waves or pulses in the frequency range of 1 – 10 MHz, are transmitted into a test specimen and the reflected echoes are analyzed to make inferences about the condition of the specimen. Many materials, such as stainless steel and copper, consist of randomly configured and densely packed crystals or grains. These grains, as well as other micro-structural inhomogeneities, affect the acoustical impedance of the material. Therefore, when an acoustic pulse is emitted into a material the pulse will be scattered, not only by the defects, but also by a myriad of micro-structures that will

cause the received signal to exhibit a random behavior. This signal, which is induced by the backscattering from the material micro-structure is commonly called clutter.

Common UNDT objectives are to detect defects or to characterize the shape, location, and orientation of material inhomogeneities. Furthermore, material properties such as density and stiffness can also be estimated by means of an UNDT system. These objectives are of significant importance in many industrial branches such as nuclear power plants, aircrafts, and construction sites, where components of metal, composites, and concrete are tested for flaws. Yet another vast area where ultrasonics has been found very useful is medical diagnosis. Detection of tumors and monitoring of pregnancies (fetus) are two examples.

The main components of a typical UNDT measurement system are depicted in Figure 1.1. An electric pulser is used to excite one transducer (or an array of transducers), which converts the electric energy into a displacement field. The displacement field propagates into the test specimen where the wave is scattered by inhomogeneities in the solid. Parts of these scattered waves are received by a single transducer (or an array of transducers), which converts the scattered field into an electric signal. The signal is amplified in a receiver and can be viewed on an oscilloscope for instantaneous visual examination or discretized and stored in a computer.

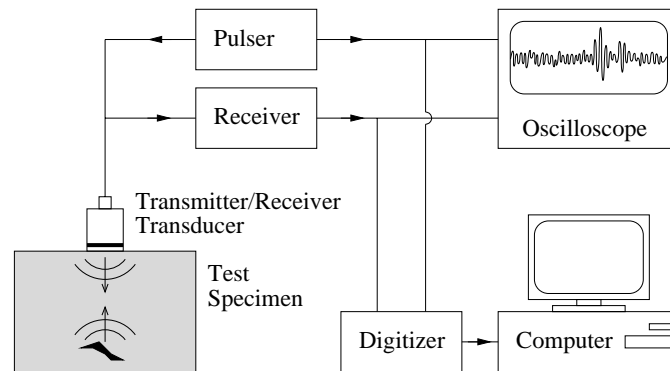


Figure 1.1: Schematic of an UNDT system.

There are three main transducer configurations used in ultrasonic contact testing scenarios. The applicability of the configurations depend on the end objective of the examination and the geometrical shape of the specimen being tested. These different configurations are depicted in Figure 1.2 and referred to as *pulse-echo*, *pitch-catch*, and *through-transmission*. A common test scenario is the so-called

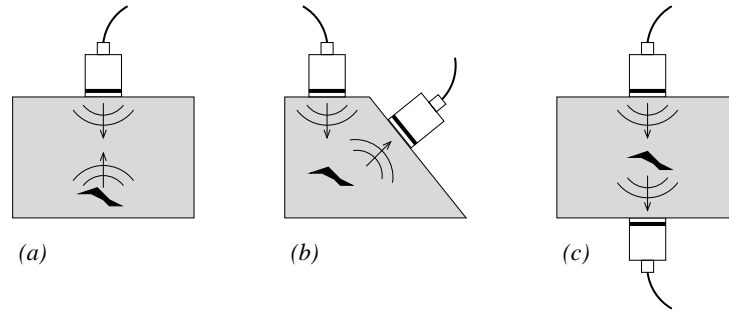


Figure 1.2: Different contact testing configurations: (a) pulse-echo setup, (b) pitch-catch set up, (c) through-transmission setup.

immersion testing whereby the object is immersed in water in order to achieve a “good” acoustic coupling between the object and the transducer. The UNDT contributions in this thesis exclusively considers the contact testing pulse-echo configuration, which also is the most common setup in industrial applications.

The physical mechanisms from pulser to receiver can in most cases be considered as linear and time invariant [14]. Thus, the whole measurement process from the electrical excitation pulse to the received electrical signal can be modeled as a series of linear time-invariant (LTI) systems. Due to the LTI properties, the systems can, mathematically, be treated individually and reconfigured when modeling/computing overall signal responses.

Often the operator of an UNDT system visually examines the raw signal to determine if a test specimen contains defects. This is a very time consuming process since the defect echoes can be severely obscured by the clutter noise and requires extensive experience in order to be successful in finding small defects. Moreover, this kind of screening process is colored by the operators subjectivity and ability to maintain attention through out the inspection of large amounts of data.

In order to alleviate the burden on the operator, to increase detection performance, and to reduce subjectivity and time consumption, appropriate signal processing algorithms can be utilized to aid the operator. Such signal processing algorithms have mainly been designed for reducing the clutter noise in the measured signals. Since the grains in a material specimen being tested have fixed locations, the clutter noise signal will not vary in time, thus simple averaging of multiple measurements will not reduce the clutter. However, the clutter noise signal is highly dependent on the position and the frequency characteristic of the transducer. These effects are employed in the two main approaches currently used for clutter suppression. In the first, the spatial diversity of the material grains is utilized by performing multiple measurements, each at a slightly different position. The resulting signals

are then averaged yielding a reduction of the clutter. This approach relies on the fact that the echo from a large defect will not change dramatically when moving the transducer slightly. The other approach utilizes the frequency diversity by using transducers with different center frequencies, whereby the clutter component in the signal will vary for different frequency bands while the echo from a large defect should remain relatively constant. Thus, both these approaches rely on the qualitative insights that the echo from a large defect is relatively unchanged over some specific frequency range as well as small shifts of the transducer position. However, these techniques are both costly and time consuming due to the need of multiple measurements and/or the use of several transducers.

One approach, known as split spectrum processing (SSP) [24, 25, 26, 27] utilizes the underlying idea in the frequency diversity approach by using one wide-band transducer and then synthetically segmenting the measured signal,  $\bar{y}$ , into separate sub-bands using a filter bank, see Figure 1.3. These sub-band signals are then combined, usually by some nonlinear operation, into a filtered signal, denoted  $\bar{z}$  in Figure 1.3. The SSP approach is qualitative since it is not based on any explicit assumptions of the physical properties of the defects other than that the echo signal from a large potential defect will contain spectral energies over a wide frequency band.

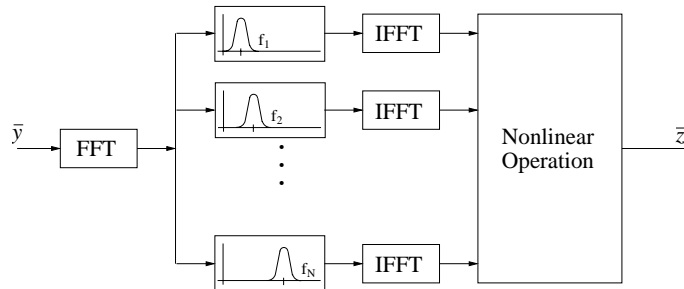


Figure 1.3: Schematic of an SSP system. The sampled signal received from the ultrasonic transducer  $y_n$  is filtered through a digitally implemented filter bank using the fast Fourier transform and the filter bank outputs are then processed by some memoryless nonlinear operation.

The SSP technique is dependent on several parameters, for example, the center frequencies of the bandpass filters, their bandwidth, and overlap in the frequency domain. Extensive research [24, 28, 29, 30] has been devoted to developing strategies for finding parameters yielding an output signal,  $\bar{z}$ , which clearly shows if a defect is present. The parameter optimization is mainly complicated by the nonlinear operation used to combine the output from the filter bank. One optimization

technique proposed in [28, 29, 30] is based on the so-called signal-to-noise ratio enhancement (SNRE), which is the ratio between the input- and the output SNR. The SNRE is defined by

$$\text{SNRE} = \frac{\text{SNR}_{\text{In}}}{\text{SNR}_{\text{Out}}} = \frac{E_1\{y_{n_0}\}}{\sqrt{E_0\{(y_{n_0})^2\}}} \bigg/ \frac{E_1\{z_{n_0}\}}{\sqrt{E_0\{(z_{n_0})^2\}}} \quad (1.7)$$

where  $y_{n_0}$  and  $z_{n_0}$  are the input and output signals, respectively,  $n_0$  is the sample number corresponding to the specific time instant of interest, and  $E_0\{\cdot\}$  and  $E_1\{\cdot\}$  denote the expectation under  $H_0$  and  $H_1$ , respectively. The basic idea in this optimization strategy is then simply to find the SSP parameters which maximize the SNRE in (1.7) when presented training data containing clutter contaminated defect echoes as well as only clutter.

### 1.2.2 Detection of a magnetic field by means of a nonlinear sensor

Magnetic sensors are useful in a wide area of application and for a variety of final objectives. There exist a multitude of magnetic sensor types, which are based on different physical mechanisms and which are applicable in situations depending on sensitivity requirements and environment of operation. The two types of magnetic sensors studied in this thesis are the magneto-resistive (MR) and the super conductive quantum interference device (SQUID), which both are inherently non-linear. Common application areas for both these sensors are nondestructive testing and geomagnetism. For both these applications the main objectives are detection, localization, and classification of either objects buried in the ground or defects residing in components. The MR sensor, in particular, is also often used for reading the magnetic stripe on, for example, credit cards and the SQUID sensor has been found very useful in naval warfare where again detection, classification and localization are the primary goals.

In this thesis the problem in focus is that of detecting a magnetic field  $s_t$ , contaminated by a strong additive ambient noise  $v_t$ , based on measurements,  $y_t$ , from the MR or the SQUID sensor, see Figure 1.4.

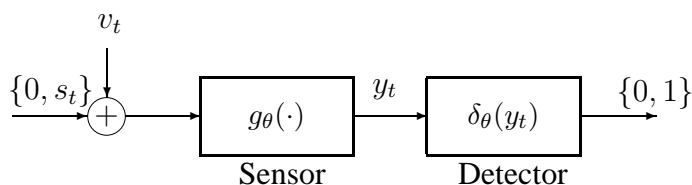


Figure 1.4: Schematic block structure of a sensor-detector system.

A complication encountered when applying these sensors in very noisy environments is their nonlinear transfer characteristics which makes it difficult to interpret the output signal  $y_t$ . This complication is often overcome by some means of sensor tuning where the transfer characteristic is altered so that the sensor produces valuable output signals. In Figure 1.4 the sensor transfer characteristic is denoted  $g_\beta$  where  $\beta$  denotes the tuning parameter.

There are several techniques of varying degree of sophistication for tuning magnetic sensors [31]. One simple, but efficient, way to tune a magnetic sensor is to inject a carefully chosen external magnetic field, thereby altering the working point of the sensor. In this case the tuning parameter  $\beta$  could, for example, correspond to the amplitude of the injected field.

A central problem is to find an appropriate value for the tuning parameter  $\beta$ . This should naturally be solved with the final objective in mind in order to reach the highest possible performance. As mentioned previously, a recently proposed method, presented in [15, 16], for improving the detectability of a weak harmonic signal in additive Gaussian noise, is based on tuning a nonlinear sensor to operate in the SR regime. This approach is briefly discussed in the proceeding section.

### Operating a sensor in the SR regime

The term stochastic resonance (SR) has been given to a phenomenon that may occur in nonlinear systems whereby some particular features of a weak input excitation is amplified by the assistance of a random signal, e.g. noise. This has rendered a multitude of publications where systems have been operated in the SR regime in order to exhibit noise induced enhancement of detection performance [19, 20, 21], channel capacity [32, 33], neuronal responses [34], image and signal processing [35, 36], etc. Due to the occurrence of SR in such a variety of contexts, different characterizations (definitions) of the SR effect have been proposed [18]. In many of these studies the quantifier for SR is tailor made for the specific application under study to exhibit and use the desired effect.

The role of SR in sensor-detector applications is one of the main topics of this thesis, which is further explained by an example given below. In this example the sensor is represented by a nonlinear dynamical system and the detector is intended to operate on the output from the sensor. The particular nonlinear dynamics used in the example is that of a double-well potential<sup>2</sup>. This particular dynamics is chosen since it is a classical example of the SR effect.

---

<sup>2</sup>Double-well potential means that the dynamical system has two local minima in the state space, see Figure 1.5

---

**EXAMPLE 1.1: SR IN A DOUBLE-WELL SENSOR**


---

Consider a sensor with a transfer function that can be described by the stochastic nonlinear differential equation (SNDE)

$$Y_t = Y_0 + \int_0^t \frac{d}{dy} f(Y_\tau) d\tau + s_t + \sigma V_t. \quad (1.8)$$

Here,  $Y_t$  is a stochastic process representing the sensor's output signal,  $f$  is a nonlinear function representing the double-well potential of the system,  $s_t$  is a periodic excitation signal, and  $V_t$  is a zero mean unit variance white Gaussian noise scaled by the noise strength parameter  $\sigma$ . The input signal,  $s_t$ , is taken to be harmonic and described by

$$s(t) = A_0 \cos(2\pi f_0 t), \quad (1.9)$$

where  $A_0$  determines the strength and  $f_0$  the frequency. Moreover, let the double-well potential,  $f$ , be represented by

$$f(x) = \frac{b}{4}x^4 - \frac{a}{2}x^2. \quad (1.10)$$

The dynamics in (1.10) has two potential minima located at  $\pm x_m = \pm\sqrt{a/b}$ . In the absence of noise, and when the system is unperturbed the minima are separated by a potential barrier with the height given by  $\Delta V = a^2/(4b)$ .

If the system in (1.8) is perturbed only by the harmonic signal in (1.9), then the potential minima are tilted up and down periodically, thereby lowering the potential barrier separating them. If the periodic forcing is strong, i.e. large amplitudes  $A_0$ , then the system's state will transit between the potential minima with a rate corresponding to half the forcing frequency  $f_0$ . This type of excitation is called *supra-threshold* forcing and is visualized in Figure 1.5. A periodic forcing with small amplitudes,  $A_0$ , will cause the system's state to rock back and forth in one of the potential wells. This is commonly called *sub-threshold*.

The output signal from the system in (1.10), when excited by a sub-threshold periodic forcing  $s_t$ , exhibits interesting behavior when altering the inherent noise strength  $\sigma$ . First consider the noise strength  $\sigma$  to be small, then only few transitions between the potential minima will occur, generating an output signal with the typical behavior presented in the lower left plot in Figure 1.6. On the other hand, if the noise strength is very high, several random transitions between the potential minima will occur, producing an output signal as in the upper left plot in

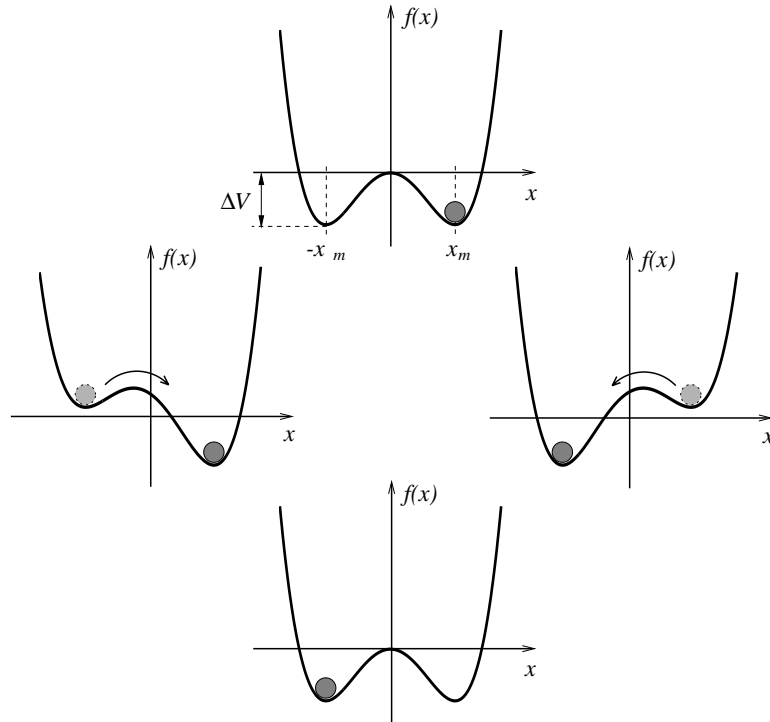


Figure 1.5: The double well potential in (1.10) excited by a periodic forcing.

Figure 1.6. For a moderate noise strength the system operates in an intermediate regime where the systems state transits between the wells with a rate synchronized with half of the periodic forcing. This is depicted in the middle left plot in Figure 1.6. Also presented in the right column of Figure 1.6 are the power spectra averaged over 500 realizations of the corresponding time domain signals.

Curiously, when the noise strength is increased and reaches some intermediate level the sensor output signal starts to oscillate between  $x_m$  and  $-x_m$  with a period equivalent to half the forcing frequency. This is the SR effect, which is also clearly visible in the frequency domain plots in Figure 1.6. Thus, if a frequency based detector, with a detection statistic represented by the amplitude of the power spectral component at half the forcing frequency, was to operate on the sensors output signal, then the detectability would be improved by adding noise.

---

In the light of the behavior of the signals presented in Figure 1.6 it is tempting to quantify the SR effect, and thereby the information processing capabilities of the system, in terms of spectrum based measures, since the barrier-crossing rate

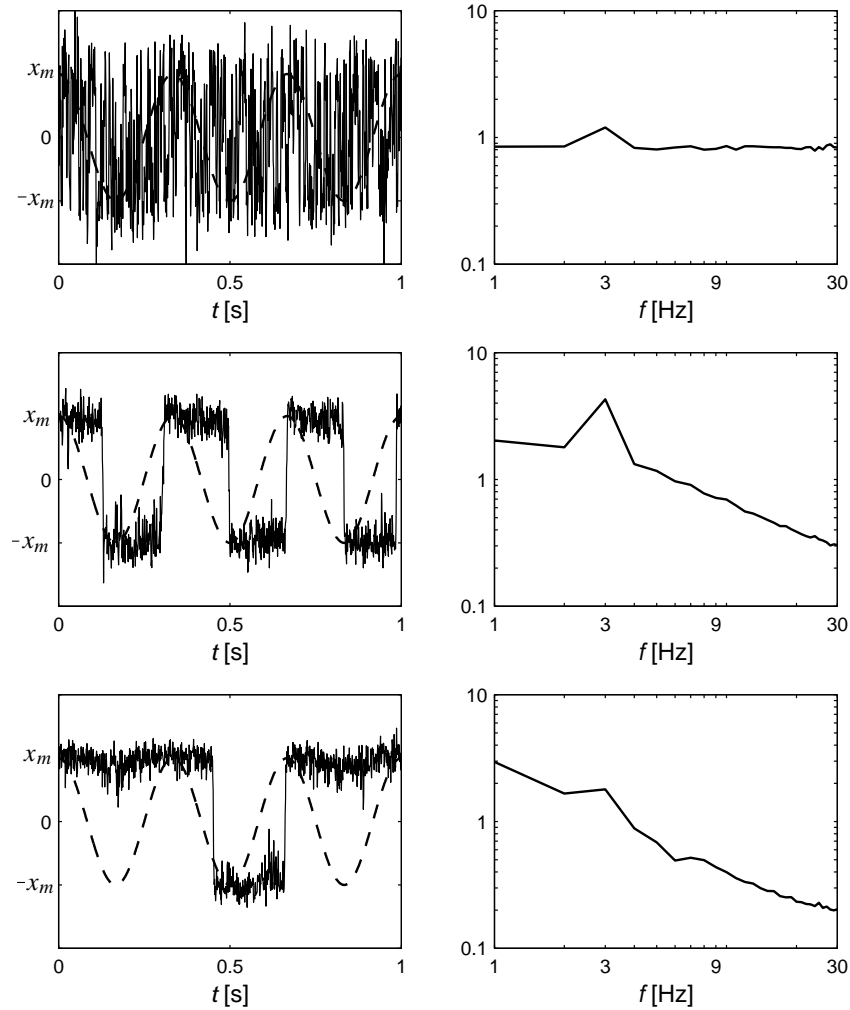


Figure 1.6: On the left the nonlinear sensor output signal is displayed for different noise strength parameter values  $\sigma$  (increasing values from the bottom row to the top row). Also depicted by the dashed line is the harmonic input signal, with a normalized amplitude. On the right the corresponding power spectra based on 500 realizations of the output signal is displayed.

depends critically on the noise strength  $\sigma$ . Indeed, the most common way to characterize SR is by means of a signal-to-noise ratio (SNR) of the system's output signal. This SNR is expressed in the spectral domain by exclusively considering the spectral component at the fundamental frequency given by the input excitation, which corresponds to  $f_0$  in Example 1.1. By assuming that the system has a sta-

tionary solution when the excitation signal  $s_t = 0$  and a cyclostationary solution when  $s_t$  is harmonic as in (1.9), this spectral based SNR measure may be expressed as [18]

$$d_{\text{SR}} = \frac{a}{S_V^0(f_0)}. \quad (1.11)$$

Here  $S_V^0(f_0)$  is the power spectral component at  $f_0$  of  $Y_t$  without any periodic excitation of the system and  $a = |c_1|^2/2\pi$ , where  $c_1$  is the first coefficient in the Fourier expansion  $\sum_{n \in \mathbb{Z}} c_n e^{i2\pi f_0 n t}$  of the ensemble averaged system response with a harmonic excitation of frequency  $f_0$ . Obviously, this approach makes most sense if the system under study can be described by a SNDS as in (1.8) and the excitation signal is harmonic. However, similar spectral based SNR measures has also been utilized for other types of systems and excitation signals [18].

The motivation for having a quantifier for the SR phenomenon and thereby the information processing capability of a nonlinear system lies not only in describing the phenomenon but also, and more importantly, in that such a measure can serve as a cost function when optimizing system performance. In many practical applications, altering of the noise strength is not an option to be considered. Instead, from a technical perspective, a similar effect can occur by “tuning” the system to operate in the intermediate regime where the SR effect becomes pronounced. For the double well potential this could, for example, be made by altering the barrier height  $\Delta V$ . As mentioned, Hibbs *et al.* [15] and Rouse *et al.* [16] managed to operate a SQUID in its SR regime. At the sensor output they utilized a frequency based detector, set to the fundamental frequency of the input signal, to detect harmonic magnetic fields. This system clearly showed better detectability with increased noise strength. Also, the spectral based SNR measure of the sensor output in [15, 16] indicated a similar performance enhancement. Based on the results from these studies general conclusions of noise enhanced detection performance were drawn. In this thesis, these types of general conclusions are reconsidered using optimal detectors instead of detectors based on suboptimal detection statistics.

### 1.3 Problem formulations

In several applications such as digital communications, radar and sonar, the signal family to be detected can be modeled by an amplitude modulated sinusoid. Thus, the signal family may be expressed as

$$s_t = A a_t \sin(2\pi f_c t + \phi) \quad (1.12)$$

where  $A$  is the amplitude,  $a_t$  is the envelope,  $f_c$  is the carrier frequency and  $\phi$  is the phase angle. For this case the unknown parameters  $\theta$  in (1.4), which spans the

signal family, can be various combinations of  $A$ ,  $f_c$ , and  $\phi$ .

Due to the wide applicability of the signal family in (1.12) significant research has been devoted to developing detectors for these types of signals, in particular when corrupted by an additive Gaussian noise. The resulting detection strategies focus on providing high performing and practical solutions to problems where  $\theta$  includes close to all permutations of the unknown parameters  $A$ ,  $f_c$  and  $\phi$ . A comprehensive display of several of these detectors and strategies can be found in [5, 7, 8, 12]. Some special cases, which have received extra attention, are listed below:

1.  $A$ ,  $a_t$ ,  $f_c$ , and  $\phi$  are completely known<sup>3</sup>
2.  $A$ ,  $a_t$ , and  $f_c$  are known and deterministic and  $\phi \sim U[0, 2\pi]$ , where  $U[\cdot, \cdot]$  denotes the uniform distribution.
3.  $a_t$  and  $f_c$  are known and deterministic,  $\phi \sim U[0, 2\pi]$  and  $A \sim R(\sigma_A)$ , where  $R(\sigma)$  denotes the Rayleigh distribution.

One well-known detector is the *noncoherent detector*, which is applicable for the case listed in item 2 above. However, in the derivations of the likelihood ratio for the noncoherent detection problem it is assumed that the envelope  $a_t$  satisfies the so-called *narrowband approximation*, which can be expressed as

$$\int_0^T a_t^2 \cos(4\pi f_c t + 2\phi) dt = 0, \quad \forall \phi \in [-\pi, \pi]. \quad (1.13)$$

This entails that the bandwidth of the envelope is narrow in comparison with the (carrier) frequency,  $f_0$ , of the sinusoid. In the case of wideband transient signals the envelope can not be considered to satisfy the narrowband approximation (1.13) and thereby the classical noncoherent detector will be suboptimal. This is the topic for the first problem statement described below.

### Problem 1: Wideband noncoherent detector

The objective is to derive an expression of the likelihood ratio for the noncoherent detection problem without imposing the narrowband approximation in (1.13). The objective is also to evaluate the performance of this detector compared to the classical noncoherent detector to find out the performance degradation caused by imposing the narrowband approximation.  $\square$

---

<sup>3</sup>This case simply yields the matched filter detector which is optimal regardless of the wave form of the signal [8].

An often encountered problem when detecting transient signals is that of unknown arrival time. This situation arises, for example, in the radar, sonar, and UNDT applications where the measured signal is generated by backscattered echoes due to a transmitted pulse. For this scenario, the arrival time of the received target echo is mainly dependent on the location of the object to be detected.

The objective is to find a detector which can determine if there is a transient signal, e.g. target echo, present anywhere within a measurement  $y_0^T = \{y_t; t \in [0, T]\}$ , taken over some specific time interval  $t \in [0, T]$ . As always, the key issue in formulating such a detector is to find a detection statistic, preferably the likelihood ratio. A common approach to obtain a detection statistic for this problem is by means of a maximum likelihood formulation [12]

$$\max_{\tau \in [0, T]} \{L(y_0^T | \tau)\}, \quad (1.14)$$

where  $L(y_0^T | \tau)$  is the likelihood ratio for the case of a single pulse with known arrival time. For the case of detecting a single pulse with an *a priori* known arrival time pdf  $p_\Upsilon$  the optimal detection statistic is given by [7, 37]

$$\int_0^T L(y_0^T | \tau) p_\Upsilon(\tau) d\tau. \quad (1.15)$$

An extension of the unknown arrival time problem discussed above is considered in the problem statement below and treats the case when the measured signal may consist of multiple pulses all with unknown arrival times. This scenario could, for example, also occur in the radar, sonar, and UNDT applications when there are multiple targets generating reflected echoes or a single target located in an environment with multi-path propagation. Yet another example is targets of extended spatial dimension with several reflecting surfaces generating multiple reflected pulses even if only one pulse was transmitted.

### **Problem 2: Multiple pulses with unknown arrival times**

The objective is to first derive an expression for the likelihood ratio when the signal to be detected can consist of multiple transient signals with unknown arrival times. Then compare the performance of a detector based on this likelihood ratio to one with the maximum likelihood ratio detection statistic in (1.14).  $\square$

Generally, formulating an optimal detector for a hypothesis problem such as (1.5) requires that an accurate representation of the signal family  $\mathcal{S}$  in (1.4) is accessible. In all practical detection problems the signals to be detected are, in one

way or another, generated by some underlying physical mechanisms. In some of these situations it is difficult to derive/obtain an explicit parameterized mathematical model of the signal family. A scenario where this difficulty may emerge is that of defect detection by means of UNDT which is the focus of the third problem statement below. As mentioned, common approaches to test for defects by means of a piezoelectric UNDT system are aimed at reducing the clutter noise in the measured signal and does not explicitly utilize the framework of binary hypothesis testing to solve the problem. Thus, a signal detection treatment of the ultrasonic defect detection problem seems appropriate and has the potential to contribute to the UNDT application area. The ambition is to add the UNDT problem as yet another field to the list of applications where optimal signal detection is useful.

**Problem 3: Physical model-based optimal UNDT detector for cracks**

The objective is to present a methodology for the design of statistically optimal UNDT detectors for cracks in elastic solids based on physical models. Subproblems to consider are:

- Formulate the crack detection problem as a one sided composite hypothesis test of the form (1.5).
- Utilize state-of-the-art numerical simulation programs to sample the crack echo family of interest to obtain transient signal family members to detect.
- Modify the state-of-the-art ultrasonic clutter model in [38] for the problem of interest and derive a numerically more efficient algorithm than that of [38].
- Unify the numerical crack echo and clutter models with the classical theory of signal detection to obtain an optimal detector for the special case of strip-like cracks with unknown orientation embedded in materials with a grainy micro-structure like steel and copper.
- Determine the performance of the optimal detector through Monte-Carlo simulations to obtain upper bounds on detectability provided that the physical models used are accurate.
- Compare the performance with the so-called generalized likelihood ratio test<sup>4</sup> (GLRT). □

The physical model-based approach outlined above can obviously be adopted for other detection problems where numerical physical models of the signal generating mechanisms are accessible. In some cases it may, however, be of to high

---

<sup>4</sup>The GLRT detection strategy is briefly described in Appendix A.

computational complexity for a practical detector implementation. In these situations one has to retreat to other alternatives when constructing detectors. Since the main difficulty lies in accurately representing the signal family, one alternative approach is to postulate a signal family which is tractable when deriving optimal detectors. Preferably, such a signal family should be representative for the underlying physical mechanisms and could, for example, be based on a phenomenological model<sup>5</sup>. The appeal of this approach is that the introduced assumptions are confined to the postulated signal model and thereby any deviations from optimal detection performance can be directly traced to the assumed signal family.

This type of phenomenological signal modeling approach was adopted early in the development of detectors for the radar and sonar applications. In particular, a signal model described by the amplitude modulated sinusoid in (1.12) has been frequently used to represent both radar and sonar echoes when deriving detectors which have been proved to work successfully in both application areas. However, this methodology has not been fully embraced in the field of UNDT for the problem of detecting defects.

#### **Problem 4: Phenomenological model-based UNDT detectors for cracks**

Employ a simple phenomenological signal model, based on (1.12), for the crack echoes to derive and apply low-complexity signal family detectors. In this context, utilize the solution to Problem 2, which makes it possible to consider multiple transients with unknown arrival times. Compare the performance of these low-complexity detectors to the physical model-based optimal detector in Problem 3. Moreover, due to the wideband character of the ultrasonic echoes it is also of interest to utilize the knowledge gained from solving Problem 1 when evaluating the applicability of the low-complexity detectors.  $\square$

Problem 5 stated below concerns the information processing capability in nonlinear sensor-detector systems in particular as well as the concept of quantifiers for SR in general. As pointed out previously, general claims of noise enhanced information processing capability based on the SR effect, when the SNR in (1.11) serves as a quantifier, has been presented in many different scenarios and reported to occur in a wide class of nonlinear systems [18]. One scenario which has been vigorously studied in the SR community, and is also of specific interest in this thesis, is that of signal detection. In this scenario the nonlinear system constitutes a sensor and the information to be passed through the system is the presence or

---

<sup>5</sup>By phenomenological modeling we mean modeling which is qualitative, i.e. which does not rely on an underlying detailed physical model but rather based on a combination of observed measurements and physical qualitative reasoning.

absence of a signal contaminated by an additive Gaussian noise. The traditional SR based approach to the detection problem does not utilize all information available in the sensors input signal, by simply constructing a frequency based detector. Therefore it is of interest to instead pursue an optimal signal detection approach based on a likelihood ratio detector. It is also of interest to scrutinize if the SR phenomenon, when quantified with the SNR in (1.11), generally can support the claim of noise enhanced information processing capability of nonlinear systems.

**Problem 5: Noise enhanced detectability in nonlinear sensor systems**

Reconsider the problem of detecting signals contaminated by additive Gaussian noise acquired with a nonlinear sensor in the context of optimal detection theory. Subproblems to consider are:

- Derive an optimal detector which relies on the whole probabilistic structure of the problem by casting it as a binary hypothesis test.
- Determine if the SR phenomenon exist in an information theoretic sense by employing information measures from the Ali-Silvey class<sup>6</sup>. Also evaluate the performance of the optimal detector in terms of Receiver Operating Characteristics<sup>7</sup> (ROCs) and the minimum achievable probability of error.
- If the SR phenomenon exist, then determine a criteria for “true” (or generalized) SR. □

The final problem statement is dedicated to performance optimization of nonlinear sensors and detectors, and is essentially an application of the results from the previous problem. The approach to optimize the performance of detecting a magnetic field by means of a SQUID, presented in [15, 16], focuses on tuning the sensor to operate in the SR regime by maximizing the SNR in (1.11). An, in some aspects, similar technique is also employed in the application area of UNDT and presented in [24, 25, 26, 27], where the detection performance of the parameterized and nonlinear SSP detector is optimized by maximizing the SNRE in (1.7). Although the two application areas discussed above are quite different, there are similarities between the two optimization approaches. In particular the utilization of an optimization criterion which is based on some type of second order statistic, namely the SNR in (1.11) for sensor tuning and the SNRE in (1.7) for the SSP tuning.

---

<sup>6</sup>The Ali-Silvey class of information measures [39, 40], is also commonly called Csiszár  $f$ -divergences [41, 42], and can be interpreted as distance measures between two probability distributions. These are further discussed in Appendix B.

<sup>7</sup>Detection performance evaluation by means of ROCs is briefly described in Appendix A.

However, an important issue to consider is that various types of SNRs does not generally reflect the detectability accurately<sup>8</sup> [8, 40, 43]. Thus, in order to undertake the task of tuning nonlinear sensors and detectors, with respect to optimal detection performance, it is essential to employ adequate and reliable measures as cost functions.

**Problem 6: Optimization of nonlinear sensors and detectors**

The objective is to employ adequate and reliable measures for detectability for both performance comparisons and parameter tuning. The specific subproblems to consider are:

- Employ information measures from the Ali-Silvey class [39, 40] for tuning nonlinear sensors.
- Use the probability of error when selecting parameters for the phenomenological model-based detectors (Problem 4). □

## 1.4 Contributions

The solution to the wideband noncoherent detector (Problem 1) is described in Paper I:

Daniel E. Asraf and Mats G. Gustafsson, “An Analytical Series Expansion Solution to the Problem of Noncoherent Detection,” submitted to *IEEE Transactions on Information Theory*.

This result provides a generalization of the noncoherent detector where the narrowband condition previously imposed on the amplitude modulation has been relaxed.

The derivation of a detector for multiple transient signals with unknown arrival times (Problem 2) is treated in Paper II:

Daniel E. Asraf and Mats G. Gustafsson, “Detection of Multiple Transient Signals with Unknown Arrival times,” submitted to *IEEE Transactions on Information Theory*.

The presented solution generalizes the single pulse detection approach given in [7, 37] by allowing for a random number of pulses of unknown arrival times. Hence, it includes the case of a single pulse with unknown arrival time as a special case.

---

<sup>8</sup>Detectability quantified with SNRs is further discussed in Appendix B.

The physical model-based transient signal detection strategy for cracks in elastic solids (Problem 3) is presented in Paper III:

Daniel E. Asraf and Mats G. Gustafsson, “Optimal Detection of Crack Echo Families in Elastic Solids”, accepted for publication in *The Journal of the Acoustical Society of America*.

The phenomenological model-based transient signal detection strategy for cracks in elastic solids (Problem 4) is presented in Paper IV:

Daniel E. Asraf and Mats G. Gustafsson, “Phenomenological Detectors for Crack Echo Families in Elastic Solids” submitted to *The Journal of the Acoustical Society of America*.

The proposed parameterized detectors are “tuned” based on the probability of error criterion (Problem 6).

The influence of noise on performance of an optimal detector for signals acquired with a nonlinear sensor (Problem 5) is presented in Paper V:

John W.C. Robinson, Daniel E. Asraf, Adi R. Bulsara and Mario E. Inchiosa, “Information-Theoretic Distance Measures and a Generalization of Stochastic Resonance” *Physical Review Letters*, vol. 81, no. 14, pp. 2850–2853, Oct. 1998.

A new definition of the SR phenomenon is proposed, which generalizes the original formulation, and the methodology is exemplified by studying signal detection by means of the SQUID sensor. Also pointed out is the need for accurate performance measures when tuning both the sensor and the detector (Problem 6).

The problem of sensor tuning by means of information theoretic distance measures (Problem 6) is studied in Paper VI:

Karl Stranne, Daniel E. Asraf, John W.C. Robinson, Peter Lindqvist and Peter Sigray, “Information-Theoretic Characterization of System Performance for a Nonlinear Magneto-Resistive Sensor”, *Stochastic and Chaotic Dynamics in the Lakes, AIP Conference Proceedings 502*, Melville, NY, 2000, pp 603–608.

In this study the magneto-resistive sensor is used to exemplify the proposed approach but the methodologies are generic and can be adopted in tuning also other types of nonlinear sensors.

## 1.5 Outline of the thesis

The different chapters in this comprehensive summary are intended to provide the reader with the background and the surrounding theories on which the papers are based. The main contributions of the papers are also presented in the chapters. A brief outline of each chapter is given below.

### **Chapter 2: Signal detection.**

This chapter presents the core of the signal detection concepts that has been used in both application areas; defect detection by means of UNDT and detectors for nonlinear sensors. It includes signal detection in discrete time as well as continuous time and a non-Gaussian signal detection problem. Also briefly summarized are the two application independent contributions in Paper I and Paper II.

### **Chapter 3: Defect detection in ultrasonic nondestructive testing.**

This chapter contains a brief description of the ultrasonic models employed for the transducer, the defect scattering as well as the clutter noise. Thereafter, the detection approaches taken in Paper III and Paper IV are summarized.

### **Chapter 4: Detectors in nonlinear sensor systems.**

This chapter contains a brief description of two static nonlinear sensors, namely the super conductive quantum interference device (SQUID) and the magneto-resistive (MR) sensor, that have been used in Paper V and Paper VI. Thereafter, the contributions in Paper V and Paper VI are summarized.

### **Chapter 5: Concluding remarks and future work.**

In this chapter some additional conclusions, of more general nature, concerning the presented studies are given. Also briefly discussed are suggestions for both interesting and necessary directions for future work.



## Signal detection

THE field of signal detection sprung, in many aspects, from the theoretical problems associated with the application and development of the radar, in which the problem is to detect the presence or absence of a target. In a 1943 report, dedicated to the radar detection problem, D.O. North presented, among several other remarkable discoveries, for the first time the so-called matched filter principle [44]. Ever since then, signal detection has also been found useful for applications such as sonar, communication, seismology and radio astronomy. Some of the other early pioneers in the field of signal detection who developed several results of significant importance are Van Trees [5, 6, 45], Helstrom [7], and Woodward [9].

This chapter is intended to give the framework for the signal detection problems treated in the thesis. Overall, the chapter is colored by the considered application areas and in particular the problem formulations presented in the previous chapter. This chapter begins in Section 2.1 by treating the problem of signal detection in discrete time and is followed in Section 2.2 by signal detection in continuous time. In Section 2.3, a non-Gaussian detection problem of particular interest for the nonlinear sensor application is briefly presented.

### 2.1 Signal detection in discrete time

This section presents the basic principles for discrete time signal detection, which has been employed in Paper III and Paper IV for the problem of detecting strip-like cracks. The UNDT defect detection problem is further developed in Chapter 3, where several concepts from this section are employed.

The underlying observation model is that of a continuous time waveform consisting of either a signal corrupted by additive noise, or noise only. Moreover, the

observed continuous time signal is considered to be discretized into a vector of  $N$  samples and the objective is to process these  $N$  samples to determine if the observation contains only noise or a noise contaminated signal. Hence, the hypothesis for the discrete time signal detection problem can be described by

$$\begin{aligned} H_0 : \bar{Y} &= \bar{V} \\ H_1 : \bar{Y} &= \bar{S} + \bar{V}, \end{aligned} \quad (2.1)$$

where  $\bar{Y} = [Y_1, \dots, Y_N]^T$  is a stochastic vector representing the observation,  $\bar{S} = [S_1, \dots, S_N]^T$  is the signal to be detected, and  $\bar{V} = [V_1, \dots, V_N]^T$  is the additive noise with a pdf denoted  $p_V$ . In this discrete time setting the observation space is the set of  $N$ -dimensional vectors with real components, i.e.  $\bar{Y} \in \mathbb{R}^N$ .

A decision rule for the hypotheses in (2.1) which is optimal in the NP or Bayes' sense<sup>1</sup> is

$$\delta(\bar{y}) = \begin{cases} 1 & \text{if } L(\bar{y}) \geq \tau \\ 0 & \text{if } L(\bar{y}) < \tau. \end{cases} \quad (2.2)$$

Here  $\bar{y}$  is a realization of  $\bar{Y}$ ,  $\tau$  is a detection threshold, and  $L(\bar{y}) = p_1(\bar{y})/p_0(\bar{y})$  is the likelihood ratio, where  $p_0$  and  $p_1$  denotes the pdfs of  $\bar{Y}$  under  $H_0$  and  $H_1$ , respectively. The pdf of  $\bar{Y}$  under the null hypothesis in (2.1) is simply

$$p_0(\bar{y}) = p_V(\bar{y}), \quad (2.3)$$

whereas  $p_1$  depends on  $p_V$  as well as the statistical nature of the signal  $\bar{S}$ .

Following the formalism presented by Garth and Poor [23], signal detection problems are categorized within a hierarchical framework. The hierarchy begins with a completely known and deterministic signal and ranges through parameterized signals, stochastic signals, both fully and incompletely modeled, and ends at unstructured signals. For the cases of interest in this thesis the statistical properties of the signal  $\bar{S}$  are considered to be known and based on this assumption the pdf of  $\bar{Y}$  under  $H_1$  can be computed. In particular, given a realization  $\bar{s}$  of  $\bar{S}$  the conditional pdf of  $\bar{Y}$  is

$$p_1(\bar{y}|\bar{s}) = p_V(\bar{y} - \bar{s}). \quad (2.4)$$

Thus, a general expression for  $p_1$  is

$$p_1(\bar{y}) = E_{\bar{S}}\{p_V(\bar{y} - \bar{S})\}, \quad (2.5)$$

where  $E_{\bar{S}}$  denotes the average with respect to the signal  $\bar{S}$ . Hence, based on (2.3) and (2.5) the likelihood ratio can expressed as

$$L(\bar{y}) = E_{\bar{S}}\left\{\frac{p_V(\bar{y} - \bar{S})}{p_V(\bar{y})}\right\} = E_{\bar{S}}\{L(\bar{y}|\bar{S})\}, \quad (2.6)$$

---

<sup>1</sup>The NP and Bayes' optimality criteria are discussed in Appendix A.

where  $L(\bar{y}|\cdot)$  denotes the conditional likelihood ratio.

Not much can be said about tests based on (2.6) without making further simplifying assumptions. The assumption that will be used throughout the remainder of this section is that the additive noise,  $\bar{V}$  in (2.1), is zero mean colored Gaussian with a known covariance matrix  $\Sigma_V$ . The pdf of a Gaussian random vector  $\bar{X}$  with realizations  $\bar{x} \in \mathbb{R}^N$  can be described by

$$p_X(\bar{x}) = \frac{1}{(2\pi)^{N/2} |\Sigma_X|^{1/2}} \exp \left\{ -\frac{1}{2} (\bar{x} - \bar{\mu}_X)^T \Sigma_X^{-1} (\bar{x} - \bar{\mu}_X) \right\}, \quad (2.7)$$

where  $\bar{\mu}_X \triangleq E\{\bar{X}\}$  is the mean,  $\Sigma_X \triangleq E\{(\bar{x} - \bar{\mu}_X)(\bar{X} - \bar{\mu}_X)^T\}$  is the covariance matrix,  $|\Sigma_X|$  denotes the determinant of  $\Sigma_X$  and  $\Sigma_X^{-1}$  denotes the inverse of  $\Sigma_X$ . The notation that will be used to describe a random variable with a pdf on the form (2.7) is  $\mathcal{N}(\bar{\mu}_X, \Sigma_X)$ . Thus, the noise,  $\bar{V}$  in (2.1), is  $\bar{V} \sim \mathcal{N}(0, \Sigma_V)$ .

In the considered UNDT application the clutter noise can in many cases be accurately modeled by a colored Gaussian process [46, 47, 48, 49, 50]. This is also the property for the physics based clutter noise model derived in Paper III and briefly presented in Chapter 3. However, in the nonlinear sensor-detector application, considered in this thesis, the statistical properties under both hypotheses will be non-Gaussian yielding that other approaches than those presented in this section have to be considered. These techniques are discussed in Section 2.3.

### 2.1.1 Detection of deterministic signals in Gaussian noise

The first category in the hierarchy mentioned above is when the signal to be detected in (2.1) is known and deterministic. This scenario is commonly known as the *coherent* detection problem and is particularly favorable analytically since the likelihood ratio can be obtained regardless of the waveform of the signal to be detected. In the light of the UNDT defect detection problem this could correspond to detection of one type of defect with an a priori known shape and location. Since if only defects of the same shape and location can occur, and the transmitting and receiving transducers have fixed locations, then the received waveform generated by the defect echo will not exhibit any variations.

The hypothesis for the coherent detection problem can be expressed as (2.1), where  $\bar{S}$  is replaced by a known and deterministic signal  $\bar{s}$ . In order to obtain the NP or Bayes optimal decision rule for the coherent detection problem the likelihood ratio has to be computed. Since the noise is zero mean Gaussian with a known covariance matrix the pdf of the null hypothesis,  $p_0(\bar{y})$ , is immediately obtained from (2.3). Furthermore, since the signal is considered to be completely known and deterministic the expectation in (2.5) can be dispensed off, which yields the

pdf for the alternative hypothesis  $p_1(\bar{y}) = p_V(\bar{y} - \bar{s})$ . Thus, the discrete time likelihood ratio for the coherent detection problem is given by

$$\begin{aligned} L(\bar{y}) &= \frac{p_1(\bar{y})}{p_0(\bar{y})} = \frac{\frac{1}{(2\pi)^{N/2}|\Sigma_V|^{1/2}} \exp\{-\frac{1}{2}(\bar{y} - \bar{s})^T \Sigma_V^{-1}(\bar{y} - \bar{s})\}}{\frac{1}{(2\pi)^{N/2}|\Sigma_V|^{1/2}} \exp\{-\frac{1}{2}\bar{y}^T \Sigma_V^{-1}\bar{y}\}} \\ &= \exp\left\{\bar{s}^T \Sigma_V^{-1}\bar{y} - \frac{1}{2}\bar{s}^T \Sigma_V^{-1}\bar{s}\right\}. \end{aligned} \quad (2.8)$$

The natural logarithm<sup>2</sup> of (2.8) yields

$$\ln\{L(\bar{y})\} = \bar{s}^T \Sigma_V^{-1}\bar{y} - \frac{1}{2}\bar{s}^T \Sigma_V^{-1}\bar{s}, \quad (2.9)$$

and since the second term in (2.9) is independent of the observations  $\bar{y}$  it can be included in the detection threshold  $\tau$ . This yields a detection statistic on the form

$$T(\bar{y}) = \bar{s}^T \Sigma_V^{-1}\bar{y}. \quad (2.10)$$

Hence, the NP and Bayes optimal decision rule can be expressed as

$$\delta(\bar{y}) = \begin{cases} 1 & \text{if } T(\bar{y}) \geq \tau' \\ 0 & \text{if } T(\bar{y}) < \tau', \end{cases} \quad (2.11)$$

where

$$\tau' = \log\{\tau\} + \frac{1}{2}\bar{s}^T \Sigma_V^{-1}\bar{s}. \quad (2.12)$$

In the NP case the threshold  $\tau$  is determined from the imposed false alarm constraint and in the Bayes case  $\tau$  depends on the assigned costs as well as the hypotheses a priori probabilities (for details see Appendix A).

### Coherent detection performance

Another appealing feature of the coherent detector is that both the NP and Bayes detection performance can be analyzed analytically. This analytical tractability comes from the fact that the detection statistic  $T(\bar{y})$  in (2.10) is Gaussian under both  $H_0$  and  $H_1$ , since it is a linear combination of Gaussian random variables. Thus, to evaluate the performance of an NP or Bayes optimal detector one can determine the pdfs of the detection statistic and then calculate either the Bayes risk, or in the NP case, the probability of detection versus the probability of false

<sup>2</sup>Any monotone function of the likelihood ratio can equally well serve as a detection statistic (for details see Appendix A).

alarm. Since the pdfs of  $T$  under both  $H_0$  and  $H_1$  are Gaussian it is sufficient to find the means and variances. The mean under  $H_0$  and  $H_1$  is

$$E\{T(\bar{Y})|H_0\} = 0 \quad \text{and} \quad E\{T(\bar{Y})|H_1\} = \bar{s}^T \Sigma_V^{-1} \bar{s}, \quad (2.13)$$

respectively. The variance is the same under both hypotheses and is given by

$$\text{Var}\{T(\bar{Y})|H_j\} = \bar{s}^T \Sigma_V^{-1} \bar{s}, \quad j = 0, 1. \quad (2.14)$$

By defining

$$d^2 \triangleq \bar{s}^T \Sigma_V^{-1} \bar{s}, \quad (2.15)$$

the probability of detection for the decision rule in (2.11) can be expressed as [5]

$$P_D(\delta) = 1 - \Phi\left(\frac{\ln\{\tau\}}{d} - \frac{d}{2}\right). \quad (2.16)$$

Here  $\Phi$  denotes the cumulative probability distribution function (cdf) of a  $\mathcal{N}(0, 1)$  random variable. The probability of false alarm can also be expressed in terms of the cdf of a  $\mathcal{N}(0, 1)$  random variable, yielding [5]

$$P_F(\delta) = 1 - \Phi\left(\frac{\ln\{\tau\}}{d} + \frac{d}{2}\right). \quad (2.17)$$

For an  $\alpha$ -level NP test the probability of false alarm is  $P_F(\delta) = \alpha$  and since  $\Phi$  is a monotonically increasing function it has an inverse, yielding that the natural logarithm of the threshold can be expressed as

$$\ln\{\tau\} = d\Phi^{-1}(1 - \alpha) - \frac{d^2}{2}. \quad (2.18)$$

Now by using (2.18) in (2.16) the probability of detection can be expressed in terms of  $\alpha$  as

$$P_D(\delta) = 1 - \Phi(\Phi^{-1}(1 - \alpha) - d). \quad (2.19)$$

Since  $\Phi$  is a monotonically increasing function the performance of an  $\alpha$ -level NP detector for the coherent detection problem will improve monotonically with increasing  $d$ .

A similar conclusion is also arrived at when evaluating the performance of the Bayes decision rule with uniform cost and equal priors [5]. Thus, the quantity which is intimately related to the detection performance is  $d$  in (2.15), which can be interpreted as a measure of the signal-to-noise ratio (SNR).

The notion of signal-to-noise ratio appears in many different manifestations and has been, and is still, used for several purposes also outside the scope of detection of deterministic signals in Gaussian noise. In the SR application, mentioned in

the previous chapter, a SNR measure expressed in a narrowband in the frequency domain is used to measure performance of nonlinear systems. Also mentioned in the previous chapter is the employment of an SNR enhancement for parameter optimization of the SSP detector. From the derivations above it is clear that the ability of the SNR measure in (2.15) to reflect optimal performance depends heavily on the assumption of Gaussianity. Since the systems in the SR and SSP applications are nonlinear and thereby, in the general case, yields non-Gaussian signals it is questionable if these SNR measures serve the purpose of which they are intended.

### 2.1.2 Detection of parameterized signals in Gaussian noise

In the previous section the signal to be detected was considered known and deterministic. A generalization of this case arises when the waveform of the signal is allowed to vary. This is often a more realistic model in particular when the signal is generated by some underlying physical mechanism which in one way or another can vary and thereby produce signals of different waveforms. For the case of defect detection by means of UNDT this framework, in contrast to the coherent detection problem, can be applied in such a way that the defects to be detected are allowed to have different shapes and/or locations. This idea is used in Paper III of this thesis where the problem is to detect cracks, with unknown orientation, based on a physical model. In Paper IV, the same problem is considered, but instead of employing a physical model for the crack echoes, a phenomenological model is used.

The problem of detecting a family of signals contaminated by Gaussian noise leads to the composite hypothesis test

$$\begin{aligned} H_0 : \bar{Y} &= \bar{V} \\ H_1 : \bar{Y} &= \bar{s}(\theta) + \bar{V}, \end{aligned} \quad (2.20)$$

where  $\bar{s}(\theta)$  is a known vector-valued function of  $\theta$ , which is a single or a set of unknown parameters taking values in some space  $\Lambda$ .

For a given  $\theta$ , the signal,  $\bar{s}(\theta)$ , in (2.20) is completely known. Thus, the likelihood ratio for (2.20), conditioned on  $\theta$ , can be obtained in the same fashion as in the previous section by substituting  $\bar{s}$  in (2.8) for  $\bar{s}(\theta)$  yielding

$$L(\bar{y}|\theta) = \exp\left\{\bar{s}(\theta)^T \Sigma_V^{-1} \bar{y} - \frac{1}{2} \bar{s}(\theta)^T \Sigma_V^{-1} \bar{s}(\theta)\right\}. \quad (2.21)$$

There are different strategies when dealing with composite hypothesis tests, such as (2.20), some of which are mentioned in Appendix A, and the applicability of these different approaches depends mainly on the a priori knowledge available. The expression in (2.21) forms the basis for the Bayes, the NP, and the generalized likelihood ratio test (GLRT) strategies, which are those considered in this thesis.

If  $\theta$  is assumed to be a realization of a random variable  $\Theta$ , having the known prior pdf  $p_\Theta$ , then the unconditional likelihood ratio for (2.20) can be obtained from (2.6) as

$$L(\bar{y}) = E_{\bar{S}}\{L(\bar{y}|\bar{S})\} = E_{\bar{S}(\Theta)}\{L(\bar{y}|\bar{S}(\Theta))\} = E_\Theta\{L(\bar{y}|\Theta)\}. \quad (2.22)$$

By using (2.21) in (2.22) and explicitly writing out the expectation integral gives

$$L(\bar{y}) = \int_{\theta \in \Lambda} \exp\left\{\bar{s}(\theta)^T \Sigma_V^{-1} \bar{y} - \frac{1}{2} \bar{s}(\theta)^T \Sigma_V^{-1} \bar{s}(\theta)\right\} p_\Theta(\theta) d\theta, \quad (2.23)$$

which is the NP and Bayes optimal detection statistic for (2.20).

If the a priori pdf  $p_\Theta$  is unknown other types of tests have to be employed, e.g. the GLRT. The GLRT detection statistic can be expressed as

$$T(\bar{y}) = \max_{\theta \in \Lambda} \{L(\bar{y}|\theta)\}. \quad (2.24)$$

This detection statistic is of significant practical interest since it does not require a priori knowledge of the parameter distribution, which is often hard to obtain. Moreover, a detector based on the statistic in (2.24) has been shown to have very competitive performance compared to the optimal NP and Bayes detectors for several problems [12], which also is the conclusion drawn in Paper III where it is employed to the problem of detecting cracks of unknown orientation.

It is generally mathematically intractable to obtain closed form solutions for the likelihood ratio in (2.23). The difficulty lies in solving the expectation integral for arbitrary signal models and parameter pdfs. Although for some special cases closed form solutions are attainable, one is illustrated in the example below. The detector in this example is used in the phenomenological model based approach to detect cracks presented in Paper IV and summarized in Chapter 3.

---

#### EXAMPLE 2.1: THE NONCOHERENT DETECTOR

---

Consider the hypothesis problem in (2.20) with a signal of the form

$$s_n(\theta) = a_n \sin(2\pi f_c(n-1)T_s + \theta), \quad n = 1, \dots, N \quad (2.25)$$

where  $a_n$ ,  $f_c$ , and  $T_s$  are the envelope, carrier frequency, and sampling time, respectively, all of which are assumed to be known. Moreover,  $\theta$  is the phase of the sinusoidal carrier and is assumed to be unknown and stochastic with a uniform distribution over  $[0, 2\pi]$ . Hence, by using (2.23) the likelihood ratio for this problem can be expressed as

$$L(\bar{y}) = \frac{1}{2\pi} \int_0^{2\pi} \exp\left\{\bar{s}(\theta)^T \Sigma_V^{-1} \bar{y} - \frac{1}{2} \bar{s}(\theta)^T \Sigma_V^{-1} \bar{s}(\theta)\right\} d\theta. \quad (2.26)$$

where  $\bar{s}(\theta) = [s_1(\theta), s_2(\theta), \dots, s_N(\theta)]^T$ . In order to solve the integral in (2.26) the two terms in the exponential function have to be simplified.

First, consider the first term of the exponential function in (2.26). By using the trigonometric identity  $\sin(b + c) = \sin(b) \cos(c) + \cos(b) \sin(c)$  the signal  $\bar{s}(\theta)$  in (2.25) can be expressed as

$$\bar{s}(\theta) = \bar{s}_s \cos(\theta) + \bar{s}_c \sin(\theta), \quad (2.27)$$

where the components in  $\bar{s}_s$  and  $\bar{s}_c$  are  $s_{s_n} = a_n \sin(2\pi f_c(n-1)T_s)$  and  $s_{c_n} = a_n \cos(2\pi f_c(n-1)T_s)$ , respectively. This yields that the first term in (2.26) can be expressed as

$$\bar{s}^T(\theta) \Sigma_V^{-1} \bar{y} = \cos(\theta) \bar{h}_s^T \bar{y} + \sin(\theta) \bar{h}_c^T \bar{y} \quad (2.28)$$

where

$$\bar{h}_c = \bar{s}_c^T \Sigma_V^{-1} \quad \text{and} \quad \bar{h}_s = \bar{s}_s^T \Sigma_V^{-1}. \quad (2.29)$$

These two vectors are sometimes called in-phase and quadrature filters, respectively.

The second term in the exponential function in (2.26) is now considered. Since the covariance matrix,  $\Sigma_V$ , is symmetric and positive-definite a spectral decomposition yields

$$\Sigma_V = \sum_{k=1}^N \lambda_k \bar{u}_k \bar{u}_k^T = U \Lambda U^T, \quad (2.30)$$

where  $\lambda_k$  are the eigenvalues and  $\bar{u}_k$  the corresponding orthonormal eigenvectors. By using (2.30) the second term in the exponential function in (2.26) can be expressed as

$$\begin{aligned} \bar{s}^T(\theta) \Sigma_V^{-1} \bar{s}(\theta) &= \bar{s}^T(\theta) U \Lambda^{-1} U^T \bar{s}(\theta) \\ &= \sum_{m=1}^N \sum_{k=1}^N \sum_{n=1}^N \frac{1}{\lambda_n} U_{m,n} U_{k,n} s_m(\theta) s_k(\theta) \\ &= \sum_{m=1}^N \sum_{n=1}^N \frac{1}{\lambda_n} U_{m,n} U_{m,n} a_m^2 \sin^2(2\pi f_c(m-1)T_s + \theta) \\ &= \sum_{m=1}^N \sum_{n=1}^N \frac{1}{\lambda_n} U_{m,n} U_{m,n} a_m^2 \left[ \frac{1}{2} + \frac{1}{2} \cos(4\pi f_c(m-1)T_s + 2\theta) \right]. \end{aligned} \quad (2.31)$$

The third equality in (2.31) is due the orthogonality of the eigenvectors in  $U$  and the fourth equality is obtained with the trigonometric identity  $\sin^2(b) = 1/2 - 1/2 \cos(2b)$ . Furthermore, assuming that the square of the envelope  $a_1^2, \dots, a_N^2$  is slowly varying with respect to twice the carrier frequency yields

$$\sum_{m=1}^N \sum_{n=1}^N \frac{1}{\lambda_n} U_{m,n} U_{m,n} a_m^2 \frac{1}{2} \cos(4\pi f_c(m-1)T_s + 2\theta) \approx 0. \quad (2.32)$$

This is the before mentioned *narrowband approximation*. By employing the narrowband approximation to (2.31) the second term in the exponential function in (2.26) can be reduced to

$$\bar{s}^T(\theta) \Sigma_V^{-1} \bar{s}(\theta) \approx \frac{1}{2} \bar{a}^T \Sigma_V^{-1} \bar{a}, \quad (2.33)$$

where  $\bar{a} = [a_1, a_2, \dots, a_N]^T$ .

Finally, by using (2.33) and (2.29) in (2.26) the likelihood ratio takes the form

$$\begin{aligned} L(\bar{y}) &= \frac{1}{2\pi} \int_0^{2\pi} \exp\{\cos(\theta) \bar{h}_s^T \bar{y} + \sin(\theta) \bar{h}_c^T \bar{y} - \frac{1}{4} \bar{a}^T \Sigma_v^{-1} \bar{a}\} d\theta \\ &= \exp\{-\frac{1}{4} \bar{a}^T \Sigma_v^{-1} \bar{a}\} \frac{1}{2\pi} \int_0^{2\pi} \exp\{\cos(\theta) \bar{h}_s^T \bar{y} + \sin(\theta) \bar{h}_c^T \bar{y}\} d\theta \quad (2.34) \\ &= \exp\{-\frac{1}{4} \bar{a}^T \Sigma_v^{-1} \bar{a}\} I_0(r). \end{aligned}$$

Here  $I_0$  is the zeroth-order modified Bessel function of the first kind and

$$r = \sqrt{(\bar{h}_s^T \bar{y})^2 + (\bar{h}_c^T \bar{y})^2}. \quad (2.35)$$

Since the factor  $\exp\{-\frac{1}{4} \bar{a}^T \Sigma_v^{-1} \bar{a}\}$  in (2.34) is independent of the observations,  $\bar{y}$ , it can be included in the detection threshold when formulating a decision rule. Moreover, the Bessel function,  $I_0$ , is monotonically increasing yielding that  $r$  can replace the likelihood ratio as a detection statistic. Thus, the NP and Bayes optimal decision rule for the noncoherent detection problem is

$$\delta(\bar{y}) = \begin{cases} 1 & \text{if } r \geq \tau' \\ 0 & \text{if } r < \tau', \end{cases} \quad (2.36)$$

where  $\tau' = I_0^{-1}(\tau \exp\{\frac{1}{4} \bar{a}^T \Sigma_v^{-1} \bar{a}\})$ . It should be noted that this decision rule is derived based on the narrowband approximation and is thereby optimal for cases when (2.32) holds.

---

A detector for signals of the form (2.25) and based on the statistic in (2.35) is commonly called *noncoherent detector* or *envelope detector*. Similar to the coherent detector, the performance of the noncoherent detector can be treated analytically [5, 7, 8]. However, this is not generally the case for composite hypothesis tests, such as (2.20), where performance analysis has to be treated on a case by case basis.

### 2.1.3 Detection of Gaussian signals in Gaussian noise

In the two preceding sections the signal to be detected was assumed to be highly structured, either completely known or parametrically determined. In this section the statistical nature of the signal  $\bar{S}$  in (2.1) is modeled by a Gaussian random vector with a known mean  $\bar{\mu}_S$  and covariance matrix  $\Sigma_S$ , i.e.  $\bar{S} \sim \mathcal{N}(\bar{\mu}_S, \Sigma_S)$ . Moreover,  $\bar{V}$  and  $\bar{S}$  are also assumed to be independent. Under the foregoing assumptions, the distributions of the observation  $\bar{Y}$  in (2.1) can be described by  $\bar{Y} \sim \mathcal{N}(0, \Sigma_V)$  and  $\bar{Y} \sim \mathcal{N}(\bar{\mu}_S, \Sigma_V + \Sigma_S)$  under  $H_0$  and  $H_1$ , respectively. The likelihood ratio can thereby be expressed as

$$L(\bar{y}) = \frac{p_1(\bar{y})}{p_0(\bar{y})} = \frac{|\Sigma_V|^{1/2}}{|\Sigma_V + \Sigma_S|^{1/2}} \exp \left\{ \frac{1}{2} \bar{y}^T \Sigma_V^{-1} \Sigma_S (\Sigma_V + \Sigma_S)^{-1} \bar{y} + \bar{\mu}_S^T (\Sigma_V + \Sigma_S)^{-1} \bar{y} - \bar{\mu}_S^T (\Sigma_V + \Sigma_S)^{-1} \bar{\mu}_S \right\}. \quad (2.37)$$

The natural logarithm of the likelihood ratio in (2.37) gives the detection statistic

$$T(\bar{y}) = \frac{1}{2} \bar{y}^T \Sigma_V^{-1} \Sigma_S (\Sigma_V + \Sigma_S)^{-1} \bar{y} + \bar{\mu}_S^T (\Sigma_V + \Sigma_S)^{-1} \bar{y} + G, \quad (2.38)$$

where  $G = (1/2) \ln\{|\Sigma_V|/|\Sigma_V + \Sigma_S|\} - \bar{\mu}_S^T (\Sigma_V + \Sigma_S)^{-1} \bar{\mu}_S$  is independent of the observation  $\bar{y}$  and can thereby be included in the detection threshold  $\tau$ .

A well-known case of the Gaussian signal detection problem is detection of an amplitude modulated sinusoid, where the phase is a uniform random variable and the amplitude is a Rayleigh random variable [5, 12]. This case can be considered to fall into the categories of both parameterized signal detection and Gaussian signal detection but is treated in this section because the likelihood ratio is most easily obtained by using the analytical framework presented here. The classical detector [5, 12] for this problem is commonly called *quadrature matched filter* and has been, and still is, widely used in radar, sonar, and communication systems. In the example below a wideband version of the classical quadrature matched filter detector is derived. The detector in this example is also used in the phenomenological model based approach to detect cracks presented in Paper IV and summarized in Chapter 3.

---

**EXAMPLE 2.2: WIDEBAND QUADRATURE MATCHED FILTER DETECTOR**


---

Consider the hypothesis problem in (2.1) with a signal of the form

$$S_n = Aa_n \sin(2\pi f_c(n-1)T_s + \Theta), \quad n = 1, \dots, N, \quad (2.39)$$

where the amplitude  $A$  is a Rayleigh distributed random variable, i.e.  $A \sim R(\sigma_A^2)$ , and the phase angle  $\Theta$  of the sinusoid is a uniformly distributed random variable, i.e.  $\Theta \sim U[-\pi, \pi]$ . Moreover, assume that  $\sigma_A$ , the carrier frequency  $f_c$ , the sampling interval  $T_s$ , and the envelope  $\bar{a} = [a_1, \dots, a_N]$  are all known.

By using the trigonometric identity  $\sin(b+c) = \sin(b)\cos(c) + \cos(b)\sin(c)$  the signal can be expressed as

$$S_n = A_1 a_n \sin(2\pi f_c(n-1)T_s) + A_2 a_n \cos(2\pi f_c(n-1)T_s), \quad (2.40)$$

where  $A_1 = A \cos(\Theta)$  and  $A_2 = A \sin(\Theta)$ . The stochastic variables  $A_1$  and  $A_2$  can be shown [51] to be independent identically distributed (i.i.d.) zero mean Gaussian with variance  $\sigma_A^2$ , i.e.  $A_i \sim N(0, \sigma_A^2)$ ,  $i = 1, 2$ . Hence, the signal in (2.40) is zero mean Gaussian with 2 degrees of freedom. A vector representation of the signal is

$$\bar{S} = \mathcal{S} \begin{pmatrix} A_1 \\ A_2 \end{pmatrix}, \quad (2.41)$$

where

$$\mathcal{S} = \begin{pmatrix} 0 & a_1 \\ a_2 \sin(2\pi f_c T_s) & a_2 \cos(2\pi f_c T_s) \\ \vdots & \vdots \\ a_N \sin(2\pi f_c(N-1)T_s) & a_N \cos(2\pi f_c(N-1)T_s) \end{pmatrix}. \quad (2.42)$$

This yields the explicit expression for the signal covariance matrix as

$$\Sigma_S = E\{\bar{S}\bar{S}^T\} = \sigma_A^2 \mathcal{S}\mathcal{S}^T. \quad (2.43)$$

The natural logarithm of the likelihood ratio can now be straightforwardly obtained by using (2.43) in (2.38) yielding

$$\ln\{L(\bar{y})\} = \frac{\sigma_A^2}{2} \bar{y}^T \Sigma_V^{-1} \mathcal{S}\mathcal{S}^T (\Sigma_V + \sigma_A^2 \mathcal{S}\mathcal{S}^T)^{-1} \bar{y} + G, \quad (2.44)$$

where

$$G = \frac{1}{2} \ln \left\{ \frac{|\Sigma_V|}{|\Sigma_V + \sigma_A^2 \mathcal{S}\mathcal{S}^T|} \right\}. \quad (2.45)$$

The expression for the detection statistic in (2.44) can be reduced into a numerically efficient formulation by using the matrix inversion lemma [12]

$$(A + BCD)^{-1} = A^{-1} - A^{-1}B(DA^{-1}B + C^{-1})^{-1}DA^{-1}. \quad (2.46)$$

In (2.44) let  $A = \Sigma_V$ ,  $B = \sigma_A \mathcal{S}$ ,  $D = \sigma_A \mathcal{S}^T$  and  $C = I_{2 \times 2}$ , where  $I_{2 \times 2}$  represents a  $2 \times 2$  identity matrix. The detection statistic can now be expressed as

$$\begin{aligned} & \ln\{L(\bar{y})\} \\ &= \frac{\sigma_A^2}{2} \bar{y}^T \Sigma_V^{-1} \mathcal{S} \mathcal{S}^T [\Sigma_V^{-1} - \Sigma_V^{-1} \sigma_A^2 \mathcal{S} (\sigma_A^2 \mathcal{S}^T \Sigma_V^{-1} \mathcal{S} + I_{2 \times 2})^{-1} \mathcal{S}^T \Sigma_V^{-1}] \bar{y} + G \\ &= \frac{\sigma_A^2}{2} \bar{y}^T H H^T \bar{y} - \frac{\sigma_A^2}{2} \bar{y}^T H Q H^T \bar{y} + G. \end{aligned} \quad (2.47)$$

Here  $Q$  is a  $2 \times 2$  matrix given by

$$Q = \sigma_A^2 \mathcal{S}^T \Sigma_V^{-1} \mathcal{S} (\sigma_A^2 \mathcal{S}^T \Sigma_V^{-1} \mathcal{S} + I_{2 \times 2})^{-1}, \quad (2.48)$$

and  $H$  is a  $N \times 2$  filter given by

$$H = \Sigma_V^{-1} \mathcal{S} = [\bar{h}_s \ \bar{h}_c]. \quad (2.49)$$

It should be noted that  $H$  contains the in-phase and quadrature filters, also defined for the noncoherent detector in (2.29).

In the derivation of the classical *quadrature matched filter*, which also is called *square-law envelope detector*, the  $2 \times 2$  matrix  $Q$  in (2.48) is approximated to be diagonal [5, 12]. This simplification is based on the assumption of narrowband signals [5, 12], with a condition equivalent to the narrowband approximation in (2.32), and thus not satisfied for wideband transient signals, i.e. envelopes  $\bar{a}$  of short time duration. Since no approximations are employed in Example 2.2, a detector based on the statistic in (2.47) is optimal also when the envelope  $\bar{a}$  has short time duration.

## 2.2 Signal detection in continuous time

In the case of discrete time signal detection the mathematical toolbox required to treat the various problems considered was that of ordinary probability calculus.

The main reason for this is that the observation space is  $\mathbb{R}^N$ , thus the probability densities or families of densities under the two hypotheses are on  $\mathbb{R}^N$  and can be integrated by means of the regular Riemann integral to give probabilities.<sup>3</sup> However, when facing continuous time detection problems the observations are realizations of a random variable indexed by time as a continuous parameter. The observation space is then a set where each element is a continuous time waveform, i.e. a *function space*. Thus, to treat continuous time detection problems requires the notion of probability densities in function spaces and methods of integration of in such spaces. This section is not claimed to be a comprehensive treatment on this subject but covers some selected issues of interest for Paper I and Paper II, which utilizes the continuous time formalism. Rigorous and comprehensive presentations can be found in [8, 53].

The hypothesis problem for signal detection in continuous time, corresponding to (2.1), can be expressed as

$$\begin{aligned} H_0 : Y_t &= V_t, & 0 \leq t \leq T \\ H_1 : Y_t &= S_t + V_t, & 0 \leq t \leq T, \end{aligned} \quad (2.50)$$

where  $\{S_t; t \in [0, T]\}$  is the signal to be detected and  $\{V_t; t \in [0, T]\}$  represents an additive noise which here is assumed to be white Gaussian with spectral height  $N_0/2$ . The autocovariance function for the white Gaussian noise is

$$C_V(t, u) = E\{V_t V_u\} = \frac{N_0}{2} \delta(t - u), \quad t, u \in \mathbb{R}, \quad (2.51)$$

where  $\delta$  denotes the Dirac delta function. In the discrete time setting the more general case of colored Gaussian noise was considered. This more general case can also be treated in the continuous time formalism by means of, for example, the Karhunen-Loève expansion [8], but is omitted in this brief presentation.

An NP an Bayes optimal decision rule for the hypothesis problem in (2.50) can be described by

$$\delta(Y_0^T) = \begin{cases} 1 & \text{if } L(Y_0^T) \geq \tau \\ 0 & \text{if } L(Y_0^T) < \tau, \end{cases} \quad (2.52)$$

where  $Y_0^T$  denotes the observed signal in the time interval  $[0, T]$  and  $L(Y_0^T)$  is the likelihood ratio. Since the likelihood ratio in the continuous time setting is  $L(Y_0^T) = p_1(Y_0^T)/p_0(Y_0^T)$ , the pdfs are required to be defined on a space of functions which will be denoted  $\Omega$ . This demands a generalization of the concept

---

<sup>3</sup>There do exist some “exotic” cases even for  $\mathbb{R}^N$  where more general integration techniques are required [52].

of pdfs to incorporate also function spaces, which is established by the Radon-Nikodym derivative [8, 53]. Given a probability measure  $P$  on an arbitrary space  $\Omega$  the corresponding pdf  $p$  can be expressed by the Radon-Nikodym derivative as

$$p = \frac{dP}{d\mu}. \quad (2.53)$$

Here  $\mu$  is a so-called  $\sigma$ -finite measure on  $\Omega$  that dominates  $P$ , i.e.  $\mu \gg P$ . A thorough presentation of measures and generalized integration can be found in [52].

Based on the Radon-Nikodym derivative in (2.53) the likelihood ratio for (2.50) can be formally expressed. Let the probability measures for the observation under  $H_0$  and  $H_1$  be denoted  $P_0$  and  $P_1$ , respectively, and the corresponding pdfs be denoted  $p_0$  and  $p_1$ , respectively. This yields the likelihood ratio as the Radon-Nikodym derivative of  $P_1$  with respect to  $P_0$  according to

$$L(Y_0^T) = \frac{p_1(Y_0^T)}{p_0(Y_0^T)} = \frac{dP_1(Y_0^T)}{d\mu(Y_0^T)} \bigg/ \frac{dP_0(Y_0^T)}{d\mu(Y_0^T)} = \frac{dP_1}{dP_0}(Y_0^T). \quad (2.54)$$

It should be noted that the measure  $\mu$  in (2.53) does not need to be explicitly defined in order to express the likelihood ratio in (2.54).

The same hierarchy of detection problem that was mentioned for the discrete time case is also applicable for continuous time detection problems and is for (2.50) dependent on the statistical properties of the signal  $S_t$ . The subsections below considers the cases when  $S_t$  is known and deterministic as well as parameterized.

### 2.2.1 Detection of deterministic signals in Gaussian noise

The scenario considered here is when  $S_t$  in (2.50) is deterministic and known i.e.  $S_t = s_t$ . The most common<sup>4</sup> and also the simplest formulation of the likelihood ratio is obtained by first rewriting the hypotheses in (2.50), with  $S_t = s_t$ , into an equivalent form given by

$$\begin{aligned} H_0 : X_t &= W_t \\ H_1 : X_t &= \int_0^t s_u du + W_t. \end{aligned} \quad (2.55)$$

Here  $X_t = \int_0^t Y_u du$  and  $W_t = \int_0^t V_u du$ . The stochastic process  $\{W_t; t \in [0, t]\}$  is a so-called Wiener process which is a Gaussian process with zero mean and autocovariance

$$C_W(t, u) = \frac{N_0}{2} \min\{t, u\}, \quad (t, u) \in [0, T]^2. \quad (2.56)$$

---

<sup>4</sup>Another approach to obtain the likelihood ratio is based on the Kahrunen-Loève transformation and Grenander's theorem [8].

The likelihood ratio for (2.55) is given by the Cameron-Martin formula [8] and can be expressed as

$$L(X_0^T) = \exp \left\{ \frac{2}{N_0} \int_0^T s_t dX_t - \frac{1}{N_0} \int_0^T s_t^2 dt \right\}. \quad (2.57)$$

Thus a Bayes or NP optimal detector for (2.55) is obtained by constructing a decision rule on the form (2.52) where the the likelihood ratio is given by (2.57).

The reason for reformulating the original hypotheses in (2.50) into the equivalent form in (2.55) lies in that the Cameron-Martin formula for the likelihood ratio is based on Pitcher's theorem [8]. Pitcher's theorem presents an expression for the likelihood ratio when the additive stochastic process is continuous and of bounded variation. The Gaussian white noise in the original hypotheses in (2.50) does not have bounded variance since  $E\{V_t^2\} = C_V(t, t) = (N_0/2)\delta(t - t)$ , which is the motivation for the reformulation. However, the Wiener process in the reformulated hypotheses (2.55) has bounded variance since  $E\{W_t^2\} = C_W(t, t) = (N_0/2)t$ , and thus allows the likelihood ratio to be obtained via Pitcher's theorem.

The equation in (2.57) bears a clear resemblance to the corresponding discrete time formulation in (2.8). It should be noted though, that the first integral in (2.57) is not a regular Riemann integral due to the randomness of  $X_t$ . This integral is a so-called *mean-square Stieltjes integral* and because of the randomness defined in a stochastic sense as the mean square limit [8].

### 2.2.2 Detection of parameterized signals in Gaussian noise

A continuous time equivalent to the discrete time parameterized signal detection problem can be expressed by the hypotheses

$$\begin{aligned} H_0 : X_t &= W_t \\ H_1 : X_t &= \int_0^t s_u(\theta) du + W_t, \end{aligned} \quad (2.58)$$

where  $s_t(\theta)$  is a known function of the unknown parameters  $\theta$ .

In the discrete time formulation the likelihood ratio in (2.22) is obtained by taking the expectation, with respect to  $\theta$ , of the conditional likelihood ratio. An equivalent approach is also applicable in the continuous time case where the conditional likelihood ratio for (2.58) is given by the Cameron-Martin formula in (2.57) by substituting  $s_t$  for  $s_t(\theta)$  yielding

$$L(X_0^T|\theta) = \exp \left\{ \frac{2}{N_0} \int_0^T s_t(\theta) dX_t - \frac{1}{N_0} \int_0^T s_t^2(\theta) dt \right\}. \quad (2.59)$$

Just as in the discrete time case the conditional likelihood ratio in (2.59) is the quantity which constitutes the basis for the Bayes, the NP, and the GLRT detectors

considered in this thesis. The detection statistic for the GLRT is

$$T(X_0^T) = \max_{\theta \in \Lambda} \{L(X_0^T | \theta)\}, \quad (2.60)$$

and when the a priori pdf,  $p_\Theta$ , for  $\theta$  is known the Bayes and the NP test statistic is given by

$$L(X_0^T) = \int_{\theta \in \Lambda} \exp \left\{ \frac{2}{N_0} \int_0^T s_t(\theta) dX_t - \frac{1}{N_0} \int_0^T s_t^2(\theta) dt \right\} p_\Theta d\theta. \quad (2.61)$$

The detection statistics in (2.60) and (2.61) are both very similar to their discrete time counter parts with no significant differences apart from the mean-square Stieltjes integral.

### Wideband noncoherent detector

The formalism presented above is used in Paper I, where the problem of detecting a continuous time amplitude modulated sinusoid with unknown and uniform phase is treated. This so-called noncoherent detection problem was presented in a discrete time setting with a colored Gaussian noise in Example 2.1, where a solution based on the narrowband approximation was derived.

In the continuous time setting and when the noise is taken to be white Gaussian the hypotheses are described by (2.58), where the signal to be detected is given by

$$s_t(\theta) = a_t \sin(2\pi f_c t + \theta), \quad t \in [0, T]. \quad (2.62)$$

Here  $a_t$  is a known waveform representing the envelope,  $f_c$  is a known frequency, and  $\theta$  is an unknown uniformly distributed phase angle. The unconditional likelihood ratio (i.e. optimal detection statistic) is given by (2.61) with  $\Theta \sim U[0, 2\pi]$ , yielding

$$L(X_0^T) = \frac{1}{2\pi} \int_{-\pi}^{\pi} \exp \left\{ \frac{2}{N_0} \int_0^T s_t(\theta) dX_t - \frac{1}{N_0} \int_0^T s_t^2(\theta) dt \right\} d\theta. \quad (2.63)$$

The well-known noncoherent detector is based on an approximative solution to the likelihood ratio integral in (2.63) and is given by [8]

$$L(X_0^T) \approx e^{-\frac{\bar{a}^2}{2N_0}} I_0 \left( \frac{2r_1}{N_0} \right). \quad (2.64)$$

Here  $\bar{a}^2 = \int_0^T a_t^2 dt$  and  $r_1 = \sqrt{A_c^2 + A_s^2}$ , with  $A_c$  and  $A_s$  defined by

$$A_c \triangleq \int_0^T a_t \cos(2\pi f_c t) dX_t \quad \text{and} \quad A_s \triangleq \int_0^T a_t \sin(2\pi f_c t) dX_t. \quad (2.65)$$

To obtain (2.64) the narrowband approximation [8] is imposed, which requires that  $a_t^2$  is slowly varying relative  $4\pi f_c$ . However, the expression in (2.64) holds with equality if  $a_t^2$  is constant or a raised-cosine [8].

An analytical series expansion solution to the noncoherent detection problem, which does not rely on the narrowband approximation and is thus valid for any waveform of the envelope  $a_t$ , is derived in Paper I. The analytical series expansion solution is given by

$$L(X_0^T) = e^{-\frac{\bar{a}^2}{2N_0}} \left[ I_0 \left( \frac{2r_1}{N_0} \right) I_0 \left( \frac{r_2}{2N_0} \right) + 2 \sum_{l=1}^{\infty} I_{2l} \left( \frac{2r_1}{N_0} \right) I_l \left( \frac{r_2}{2N_0} \right) \cos(l\phi) \right]. \quad (2.66)$$

Here  $r_2 = \sqrt{B_c^2 + B_s^2}$ , with  $B_c$  and  $B_s$  defined by

$$B_c \triangleq \int_0^T a_t^2 \cos(4\pi f_c t) dt \quad \text{and} \quad B_s \triangleq \int_0^T a_t^2 \sin(4\pi f_c t) dt, \quad (2.67)$$

and  $\phi = 2\phi_1 + \phi_2$ , where  $\phi_1 = \tan^{-1}(A_c/A_s)$  and  $\phi_2 = \tan^{-1}(B_s/B_c)$ .

The advantage of a detector based on the general expression in (2.66) over the classical noncoherent detector with the detection statistic given by (2.64) is illustrated in Paper I for a particular envelope signal  $a_t$ . In this study Monte-Carlo simulations are used to compute the detector performance in terms of minimum probability of error and ROC curves for different bandwidths of the envelope signal and different SNRs. These results clearly show that the narrowband approximation yields a performance degradation for the classical noncoherent detector when the bandwidth of the envelope is large, i.e. the narrowband approximation does not hold. A similar behavior will of course also be obtained for other types of envelopes (except raised-cosine) for which the narrowband approximation does not hold.

### Multiple pulses with unknown arrival time

The continuous time formalism is also employed in Paper II, which treats the problem of detecting multiple transient signals, with unknown arrival times, contaminated by an additive white Gaussian noise. The hypotheses for this problem can be described by (2.58), where the signal to be detected is on the form

$$s_t = s_t(\theta_1, \dots, \theta_M, \tau_1, \dots, \tau_M) = \sum_{m=1}^M x_t(\theta_m, \tau_m), \quad t \in [0, T]. \quad (2.68)$$

Here  $M$  is the number of pulses,  $x_t(\theta, \tau)$  denotes a transient (pulse) which is nonzero in a finite time interval  $t \in [\tau, \tau + T_x]$ , where  $\tau$  is the time location (arrival

time),  $T_x$  is the duration time of the pulse, and  $\theta$  is a parameter vector determining the waveform of the pulse.

When deriving an expression for the likelihood ratio the following assumptions are imposed:

- The arrival times  $\tau_m$  are assumed to be independent realizations of a stochastic variable  $\Upsilon$  taking values in the set  $[0, T - T_x]$  with a known prior distribution  $P_\Upsilon$  and corresponding pdf  $p_\Upsilon$ .
- The total time occupied by the pulses is  $M \cdot T_x \ll T$ , i.e. the pulse durations are very short,  $T_x \ll \frac{T}{M}$ .
- The waveform parameters  $\theta_m$  are assumed to be independent realizations of a stochastic variable  $\Theta$  taking values in some set  $\Lambda$  with a known prior distribution  $P_\Theta$ .

The assumptions above can be found relevant in applications such as radar, sonar, and ultrasonic nondestructive testing (UNDT) where pulse-echo detection techniques are employed. In, for example, the UNDT application an impinged defect can generate several short pulses with arrival times that can be modeled as random due to their dependence on a potential defect's location, shape, and orientation. The UNDT application is further discussed in Paper IV and Chapter 3, where also the result from this section is employed in deriving detectors.

Under the foregoing assumptions, and when  $s_t$  contains a fixed number of pulses, it is shown in Paper II that the likelihood ratio can be expressed as

$$L(X_0^T | M) = \left[ \int_0^{T-T_x} L(Y_\tau^{\tau+T_x}) p_\Upsilon(\tau) d\tau \right]^M, \quad (2.69)$$

where  $L(X_\tau^{\tau+T_x})$  is the likelihood ratio for a single pulse with known arrival time i.e.  $L(X_\tau^{\tau+T_x}) = E_\theta \{L(X_0^T | \theta, \tau)\}$ . Moreover, since  $(\cdot)^M$  is monotone, a detection statistic, equally efficient in discriminating the hypothesis as the likelihood ratio in (2.69), is given by

$$\mathcal{T}(Y_0^T) = \int_0^{T-T_x} L(Y_\tau^{\tau+T_x}) p_\Upsilon(\tau) d\tau. \quad (2.70)$$

This expression is equivalent to the likelihood ratio for the case when  $s_t$  only contains a single pulse, i.e.  $M = 1$ .

A classical approach to obtain a detection statistic for the problem of detecting a transient signal with unknown arrival time is to compute the maximum likelihood

(ML) ratio over the time interval of interest. Thus the detection statistic is given by

$$\mathcal{T}(Y_0^T) = \max_{\tau \in [0, T-T_x]} \{L(Y_\tau^{\tau+T_x})\}. \quad (2.71)$$

As mentioned, a decision rule based on this statistic is known as a generalized likelihood ratio test (GLRT).

The advantage of a detector based on the expression in (2.70) over the GLRT, with the detection statistic given by (2.71), is illustrated in Paper II for a particular signal family. In this study Monte-Carlo simulations are used to compute the detector performance in terms of ROC curves for different noise strengths  $N_0/2$ . In general, regardless of the particular transient signal family, if the assumptions stated above are satisfied then a detector based on (2.70) can be expected to outperform the GLRT based on (2.71).

## 2.3 Detection of non-Gaussian signals

In the previous sections the problem of detecting a signal contaminated by additive Gaussian noise was considered. As mentioned, this standard problem formulation is applicable for a wide range of detection problems and can easily be treated mathematically due to the properties of Gaussianity and additivity.

In some situations the stochastic processes involved can not be modeled as Gaussian. Detection of non-Gaussian signals is a very wide area and is generally associated with several mathematical difficulties, some of which are overcome by introducing assumptions and simplifying models. Due to the mathematical complications, the solutions to the non-Gaussian detection problems has branched off into a set of special cases. An overview of several non-Gaussian signal detection problems is nicely presented in a tutorial paper by Garth and Poor [23]. A less general presentation is given in [54] which focuses on signal detection problems with an additive non-Gaussian noise.

In this section a discrete time non-Gaussian detection problem is considered, which is of interest for the studies in Paper V and Paper VI. For this problem the observations under  $H_0$  and  $H_1$  are modeled by a static nonlinear function of either only an i.i.d. Gaussian noise or a known deterministic signal contaminated by an additive i.i.d. Gaussian noise. Thus, the hypotheses can be expressed on the form

$$\begin{aligned} H_0 : Y_n &= g(V_n), \quad n = 1, \dots, N \\ H_1 : Y_n &= g(s_n + V_n), \quad n = 1, \dots, N, \end{aligned} \quad (2.72)$$

where  $g$  is a static nonlinear function,  $V_1, \dots, V_N$  are i.i.d. Gaussian random variables and  $\bar{s} = [s_1, \dots, s_N]^T$  is a known and deterministic signal to be detected.

Since the function  $g$  is nonlinear the resulting pdfs of  $\bar{Y} = [Y_1, \dots, Y_N]^T$  under the two hypothesis will be non-Gaussian.

If only one time instant is considered then the problem reduces to  $\mathbb{R}$  and the pdfs of  $Y_n$  under the two hypotheses can be obtained via the formula of probability densities through a nonlinearity [55]. Specifically, if  $Z = g(X)$  and the pdf of  $X$  is  $p_X$  then the pdf of  $Z$  can be expressed as

$$p_Z(z) = \sum_{m=1}^M \frac{p_X(a_z^{(m)})}{|g'(a_z^{(m)})|}, \quad (2.73)$$

where  $g'(x) = \frac{d}{dx}g(x)$  and  $\{a_z^{(m)}\}_{m=1}^M$  are the  $M$  roots to the equation  $z = g(x)$ .

Thus, by employing (2.73) the pdf of  $Y_n$  under  $H_0$  is

$$p_0(y_n) = \sum_{m=1}^M \frac{p_V(b_{y_n}^{(m)})}{|g'(b_{y_n}^{(m)})|}, \quad (2.74)$$

where  $\{b_{y_n}^{(m)}\}_{m=1}^M$  denotes the  $M$  roots, which satisfy  $y_n = g(b_{y_n}^{(m)})$ . Similarly, the pdf of  $Y_n$  under  $H_1$  becomes

$$p_1(y_n) = \sum_{k=1}^K \frac{p_V(c_{y_n}^{(k)})}{|g'(s_n + c_{y_n}^{(k)})|}, \quad (2.75)$$

where  $\{c_{y_n}^{(k)}\}_{k=1}^K$  denotes the  $K$  roots, which satisfy  $y_n = g(s_n + c_{y_n}^{(k)})$ . The likelihood ratio for (2.72) can thus be expressed by using (2.74) and (2.75) yielding

$$L(y_n) = \frac{p_1(y_n)}{p_0(y_n)} = \frac{\sum_{m=1}^M \frac{p_V(c_{y_n}^{(m)})}{|g'(s_n + c_{y_n}^{(m)})|}}{\sum_{k=1}^K \frac{p_V(b_{y_n}^{(k)})}{|g'(b_{y_n}^{(k)})|}}. \quad (2.76)$$

Moreover, since the noise samples  $V_1, \dots, V_N$  are assumed i.i.d. the likelihood ratio for the whole signal, i.e. all samples  $n = 1, \dots, N$ , can be expressed as

$$L(\bar{y}) = \prod_{n=1}^N L(y_n). \quad (2.77)$$

Closed form expressions for the likelihood ratio in (2.77) is generally difficult to find since analytical expressions for the pdfs of  $Y_n$  under the two hypotheses can be hard to obtain. The tractability of the problem depends mainly on the structure of the nonlinearity  $g$  and the pdf of the noise  $p_V$ . However, the formula for transformation of pdfs in (2.73) can be utilized to obtain numerical representations for the pdfs under the two hypothesis and thereby the likelihood ratio. This numerical approach is taken in Paper V and Paper VI where the performance of an optimal detector for a static nonlinear sensor is evaluated.

## Defect detection in ultrasonic nondestructive testing

TO utilize accurate signal models is often beneficial in reaching a signal processing objective such as detection. This chapter is intended to give a brief presentation of the signal models, for the UNDT defect detection application, employed in this thesis. The model of the received signal includes modeling of the transducer, the defect echo, and the material clutter noise. In particular, the defects are assumed to be crack-like and reside in an elastic solid such as steel or copper. In modeling the crack echo two different approaches are taken where one is based on an advanced physical model and the other is a simple phenomenological model based on qualitative reasoning of the involved scattering mechanisms. Equipped with the models mentioned above the defect detection problem can be solved within the framework of optimal signal detection presented in Chapter 2.

This chapter begins in Section 3.1 with a short background on elastodynamic wave propagation and scattering. Section 3.2, is devoted to the modeling of the transducer. The two crack echo models are presented in Section 3.3, and in Section 3.4, the clutter noise model is presented. Finally, in Section 3.5 the defect detection problem is cast as a composite binary hypothesis test and the signal detection approaches that have been used in Papers III and Paper IV are summarized.

### 3.1 Elastodynamic preliminaries

The equations governing elastodynamic wave motions are the equation of motion and the stress-strain constitutive relationship [56]. These expressions provide the basis for obtaining explicit mathematical models for many of the processes in-

volved in an UNDT measurement, such as transmission, propagation, scattering, and reception.

The equation of motion, expressed in Cartesian tensor notation and with the Einstein summation convention, for an isotropic elastic solid, without body forces, at some point  $\bar{x}$  may be written as [14]

$$\rho \frac{\partial^2 u_k(t, \bar{x})}{\partial t^2} = \frac{\partial \tau_{lk}(t, \bar{x})}{\partial x_l}. \quad (3.1)$$

Here,  $\rho$  is the density of the medium,  $u_k$  is the particle displacement,  $\tau_{lk}$  is the symmetric stress tensor, and the subindices denote the  $x, y, z$ -dimension. The constitutive equation can be expressed as [14]

$$\tau_{lk}(t, \bar{x}) = C_{lkmn} \varepsilon_{mn}(t, \bar{x}), \quad (3.2)$$

where  $C_{lkmn}$  denotes the stiffness constants for the material and  $\varepsilon_{mn}$  is the material strain. Moreover, for small displacements the strain can be approximated by [14]

$$\varepsilon_{mn}(t, \bar{x}) = \frac{1}{2} \left( \frac{\partial u_m(t, \bar{x})}{\partial x_n} + \frac{\partial u_n(t, \bar{x})}{\partial x_m} \right). \quad (3.3)$$

The particle displacement,  $u_k$ , in the equation of motion (3.1) have three spatial degrees of freedom and can be decomposed into two dominating and fundamentally different wave components [14]. The wave component associated with the particle displacements in the propagation direction is called pressure waves or P-waves and the component with displacements orthogonal to the propagation direction is referred to as shear waves or S-waves. These wave modes have different wave speeds, for example, in metals the P-waves travels approximately twice as fast as the S-waves [14]. Other wave modes that occur in elastic wave propagation and scattering are; Rayleigh waves, Lamb waves, and leaky waves. The different wave modes can exist simultaneously in an elastodynamic medium and depend on the propagation direction and mode conversions at boundaries in the medium.<sup>1</sup>

It is often a formidable task to accurately model the scattered field from an inhomogeneity in an elastic solid. Analytical closed form solutions only exist for a few special cases. Generally, scattering problems are solved by introducing the ansatz [14]

$$u_k(t, \bar{x}) = u_k^{(in)}(t, \bar{x}) + U_k(t, \bar{x}), \quad (3.4)$$

where  $u_k$  is the total displacement field,  $u_k^{(in)}$  is the incident field generated by the transmitting transducer and  $U_k$  is the scattered field from a inhomogeneity in the elastic solid. The scattered field,  $U_k$ , is obtained by using the ansatz in (3.4) and then solving the equation of motion (3.1) when imposing boundary conditions representing the scatterer.

---

<sup>1</sup>A mode conversion occurs when one wave mode is transformed into another.

### 3.2 Modeling of the piezoelectric transducer

Piezoelectric materials possess the ability to convert electrical energy to mechanical energy and vice versa, due to a coupling between mechanical motion and time-varying electric fields. This feature makes piezoelectric materials very useful for constructing ultrasonic transducers. A schematic of a typical piezoelectric transducer is presented in Figure 3.1. The electric field is applied via the electrodes, which are attached on both sides of the piezoelectric crystal.

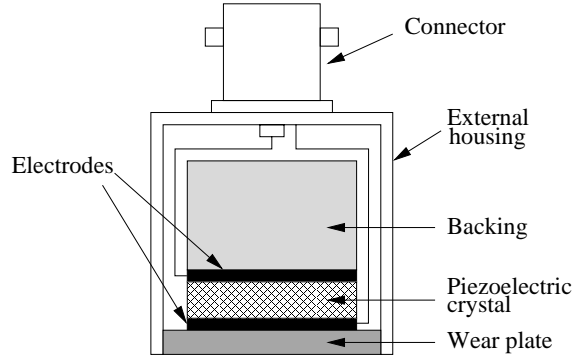


Figure 3.1: Schematic of a piezoelectric transducer.

In the transmission phase an electric excitation signal  $s_e^{(in)}(t)$ , generally in the form of a short pulse, induces a damped vibration in the piezoelectric crystal. The vibrations generate longitudinal waves that propagate both backward into the *backing*, where they are absorbed, and forward into the acoustic medium.

A piezoelectric transducer can often be modeled as a linear time invariant (LTI) system [14] with an electro-acoustic impulse response  $\beta_{ea}(t)$  (in [14] the particle velocity is used whereas here the particle displacement will be used, which is simply related to the velocity through time differentiation). The particle displacement,  $u(t)$ , normal to the transducer face (the normal displacement) is then described as

$$u(t) = \beta_{ea}(t) * s_e^{(in)}(t), \quad (3.5)$$

where  $*$  denotes convolution. The model in (3.5) can be generalized by introducing a spatial weighting function  $a(\bar{x}_{S_T})$ , where  $\bar{x}_{S_T}$  is a point on the transducer surface  $S_T$ . The normal displacement at the point  $\bar{x}_{S_T}$  then becomes

$$u(\bar{x}_{S_T}, t) = a(\bar{x}_{S_T}) u(t). \quad (3.6)$$

In this thesis the transducer is modeled as a so-called piston transducer which means that the weighting function  $a(x_{S_T})$  is uniform over  $S_T$ .

Moreover, in order for the mechanical motion, generated by the piezoelectric crystal, to propagate into the test specimen, the transducer needs to be in physical contact with the object. The most common approach is to apply a coupling gel or a layer of water as an interface between the transducer and the medium but in some applications the transducers are welded to the test object.

In the reception phase a displacement at every point on the face of the receiving transducer induces a spatially distributed stress throughout the piezoelectric crystal, which collectively give rise to an electric field over the electrodes. Thus, the voltage signal measured by a receiving transducer can be modeled as being proportional to the spatial average of the normal displacement over the transducer surface [57]

$$\langle u \rangle(t) = \int_{\bar{x} \in S_T} u(t, \bar{x}) d\bar{x}. \quad (3.7)$$

In a similar fashion as in the transmission phase, the piezoelectric crystal can be considered to have an acousto-electrical impulse response  $\beta_{ae}(t)$ . Hence, the received voltage signal can be described as [57]

$$x(t) = \beta_{ae}(t) * \langle u \rangle(t). \quad (3.8)$$

When specifying the properties of a piezoelectric transducer used for UNDT applications it is common to define an overall impulse response, which includes the effects of both transmission and reception [14]. The overall impulse response is often referred to as the transducers efficiency factor and is defined as

$$\beta(t) = \beta_{ae}(t) * \beta_{ea}(t) * s_e^{(in)}(t). \quad (3.9)$$

The benefit of introducing the overall impulse response in (3.9) is that the model for the received signal can be formulated in such a way that the reception and transmission of the transducer, and the wave propagation and scattering can be treated separately. Thus, in order to obtain the scattered signal response the efficiency factor in (3.9) is convolved with the combined impulse responses for the wave propagation and scattering.

The efficiency factor, expressed in the frequency domain, that has been used in Paper III and Paper IV is given by [58]

$$\tilde{\beta}(\omega) = \begin{cases} \sin^2 \left( \pi \frac{|\omega| - \omega_1}{\omega_2 - \omega_1} \right), & \omega_1 \leq |\omega| \leq \omega_2, \\ 0, & \text{otherwise,} \end{cases} \quad (3.10)$$

where the upper and lower frequencies are  $f_2 = \omega_2/2\pi = 6.68$  MHz and  $f_1 = \omega_1/2\pi = 1.32$  MHz, respectively. Hence, the center frequency of the probe is 4 MHz and the -3 dB bandwidth is 2.68 MHz, yielding a relative bandwidth of 67%. Figure 3.2 shows this efficiency factor in both the time- and the frequency domain.

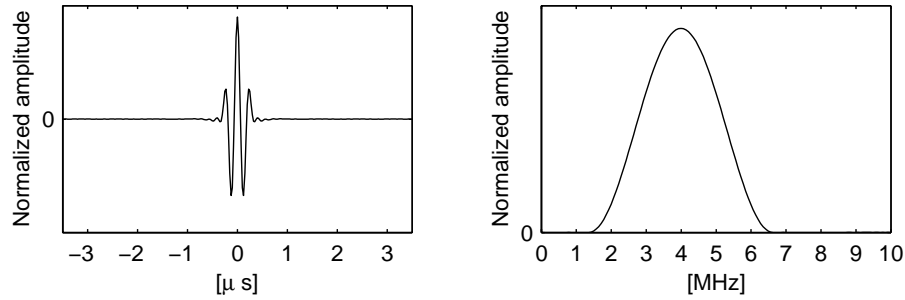


Figure 3.2: The transducer efficiency factor in (3.10) plotted in the time domain (left) and the frequency domain (right).

### 3.3 Modeling of the crack echo

The UNDT defect detection problem in this thesis considers the special case of detecting a crack residing in an elastic solid by means of a pulse-echo measurement configuration. In order to employ the signal detection framework, presented in Chapter 2, an explicit model of the crack echo is required. This section presents the two models for crack echoes, which have been used in Paper III and Paper IV.

#### 3.3.1 Physical model in the frequency domain

The physical model for the crack echoes adopted in this thesis has been developed by Mattsson *et al.* [58, 59, 60, 61]. This model is based on the so-called electromechanical reciprocity theorem [14, 62] and is formulated in the frequency domain by considering harmonic waves. The work by Mattsson *et al.* [58, 59, 60, 61] also resulted in a numerical package, which in a modified form has been used in this thesis to compute crack echo signals. This section will briefly present the electromechanical modeling approach and the modification made to the original numerical package.

The electromechanical reciprocity theorem [14] presents a relation between two different electromechanical states of the same body in terms of the electromagnetic and elastodynamic fields. This theorem was for the first time applied to the problem of elastic wave scattering in an ingenious paper by Auld [62] where a methodology applicable to several UNDT problems is presented. The set-up considered in the approach by Auld is that of an elastic body with two piezoelectric transducers attached. Moreover, in order to apply the electromechanical

reciprocity theorem the two different states of the considered volume must be defined. In the approach by Auld, the first state corresponds to the solution when one of the transducers is excited by an electromagnetic wave, which carries power  $P$  and is of frequency  $\omega$ , *in the absence of the defect*. The second state corresponds to the solution when the other transducer is excited by an electromagnetic wave with the same frequency and power, but *in the presence of the defect*. Auld derives an expression for the reflection coefficient, at the receiving transducer, due to the scatterer. The reflection coefficient, in Cartesian tensor notation, is given by [62]

$$\delta\Gamma(\omega) = \frac{i\omega}{4P} \int_{\bar{x} \in S_F} [u_k^{(1)}(\omega, \bar{x})\tau_{kl}^{(2)}(\omega, \bar{x}) - u_k^{(2)}(\omega, \bar{x})\tau_{kl}^{(1)}(\omega, \bar{x})]n_l^{(S_F)} d\bar{x}, \quad (3.11)$$

where  $i = \sqrt{-1}$ ,  $P$  is a constant representing the feeding power to the firing transducer,  $u_k^{(b)}$  and  $\tau_{kl}^{(b)}$  are the displacement and stress, respectively, and  $b = \{1, 2\}$  denotes the state. Moreover, the integration in (3.11) is performed over the surface of the defect here denoted  $S_F$  and  $\bar{n}^{(S_F)}$  denotes the inward-directed normal to  $S_F$ . From a signal processing point of view the reflection coefficient in (3.11) is simply a frequency domain expression of the impulse response of the defect observed at the receiving transducer.

As mentioned in the previous section, the electrical signal from the receiving transducer generated by a defect echo is obtained by convolving the transducer efficiency factor in (3.9) with the impulse response of the defect. In the frequency domain this operation corresponds to a multiplication. Thus, the electrical signal in the frequency domain can be expressed as

$$\tilde{s}(\omega) = \tilde{\beta}(\omega)\delta\Gamma(\omega). \quad (3.12)$$

For the pulse echo set-up considered in this thesis there is only one transducer present but the approach by Auld is still applicable by simply letting the position for the two transducers coincide. The problem geometry as well as the crack specific parameters are depicted in Figure 3.3. The crack defect is modeled as open and strip-like with an infinite length in the  $Y$ -direction. Moreover, the boundary conditions at the crack, expressed in the primed coordinate system in Figure 3.3, are taken to be so-called spring boundary conditions [61]

$$\begin{aligned} u_k(x', y', 0^+) - u_k(x', y', 0^-) &= 0, & |x'| > w/2, \forall y' \\ K_{kl}[u_l(x', y', 0^+) - u_l(x', y', 0^-)] &= w n_l^{(z')} \tau_{lk}(x', y', 0^-), & |x'| \leq w/2, \forall y' \\ n_i^{(z')} \tau_{lk}(x', y', 0^+) - n_i^{(z')} \tau_{lk}(x', y', 0^-) &= 0, & \forall x', \forall y'. \end{aligned} \quad (3.13)$$

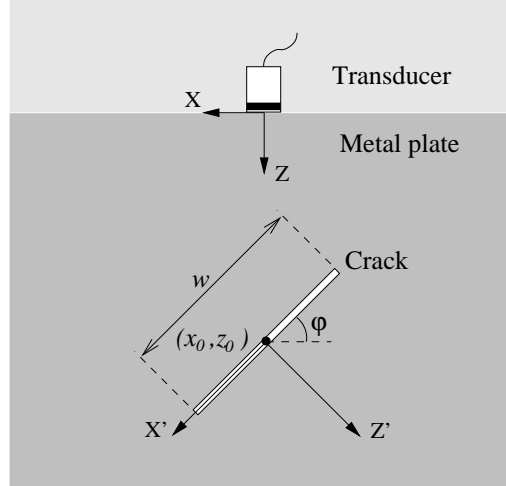


Figure 3.3: The geometry of the strip-like crack model showing the parameters specifying the crack width  $w$ , center location  $(x_0, z_0)$ , and angular orientation  $\varphi$  with respect to the  $X$ -axis. A primed coordinate system  $(X', Y', Z')$  is attached to the crack with the origin at the crack center.

Here  $n^{(z')}$  is a normal to the surface  $z' = 0$  and  $K_{kl}$  are the spring constants [61]

$$(K_{kl}) = \begin{pmatrix} K_{11} & 0 & 0 \\ 0 & K_{22} & 0 \\ 0 & 0 & K_{33} \end{pmatrix}. \quad (3.14)$$

By using the boundary conditions in (3.13) and the ansatz in (3.4) the reflection coefficient in (3.11) is reduced to [61]

$$\delta\Gamma(\omega, \theta) = \frac{i\omega}{4P} \int_{-\infty}^{\infty} \int_{-w/2}^{w/2} \Delta U_k^{(2)} \tau_{lk}^{(1)} n_l^{(z')} dx' dy'. \quad (3.15)$$

Here  $\Delta U = U(x', y', 0^+) - U(x', y', 0^-)$  is the so-called crack opening displacement (COD) and  $\theta$  contains the defect related physical parameters such as the crack width  $w$ , location  $x_0, z_0$ , and angular orientation  $\varphi$  (where  $x_0, z_0$  and  $\varphi$  correspond to the position and the orientation of the primed coordinate system).

In the numerical package by Mattsson *et al.* [58, 59, 60, 61], the expression in (3.15) is solved one frequency at a time for a predefined set of frequencies. The time domain signal, for a given transducer efficiency factor  $\tilde{\beta}(\omega)$ , is then obtained by performing an inverse Fourier transformation of (3.12). However, it was found that the supposedly constant feeding power to the transmitting

probe, i.e.  $P$  in (3.15), was indirectly varied as a function of frequency in the original numerical package. Instead of assigning a specific feeding power,  $P$ , to the transmitting transducer a constant displacement amplitude,  $U_0$ , is assigned at the surface,  $S_T$ , of the transducer. Since the displacement is uniform over the face of the transducer it is acting as a piston source. The feeding power to a piston transducer that is required to maintain a displacement amplitude,  $U_0$ , independent of the displacement frequency,  $\omega$ , is proportional to [14]

$$P \propto c\rho\omega^2U_0^2, \quad (3.16)$$

where  $c$  is the sound velocity and  $\rho$  is the density of the wave propagation medium. Thus, from (3.16) it is clear that assigning a constant displacement amplitude  $U_0$  implies a feeding power  $P$  that increases with  $\omega^2$ . This behavior results in crack echo signals that are significantly up-shifted in frequency, see right column in Figure 3.4 where signals corresponding to a crack with different angular orientations are displayed. The original computer package was therefore modified by introducing a frequency scaling of the assigned displacement amplitude for the transmitting transducer according to

$$U_0(\omega) \propto \frac{1}{\omega} \sqrt{\frac{P}{c\rho}}, \quad \omega \neq 0, \quad (3.17)$$

where  $P$  is kept constant.

Simulated crack echo signals with the constant feeding power modification are presented in the left column in Figure 3.4. These echo signals are computed for a strip-like crack with different angular orientations  $\varphi$  (see Figure 3.3) and with a probe efficiency factor given by (3.10). From Figure 3.4 it can clearly be seen that the echo from a crack with  $\varphi = 45^\circ$  and  $\varphi = 90^\circ$  contains several pulses. The first and the second pulses are reflections of the P-wave from the cracks near-tip and far-tip, respectively. The other pulses, which arrives later in time, are due to the slower propagating mode converted waves [58].

### 3.3.2 Phenomenological model in the time domain

In the previous section the physical principles governing elastodynamic wave motions were utilized to obtain an advanced numerical model of the crack echo. In this section the crack echo is represented by a simple phenomenological model in the form of an explicit mathematical expression based on qualitative reasoning of the involved scattering mechanisms. This model is employed in Paper IV, and is inspired by the impulse-response method by Lh emery, who has published a series of theoretical and application oriented papers on the subject [63, 64, 65, 66].

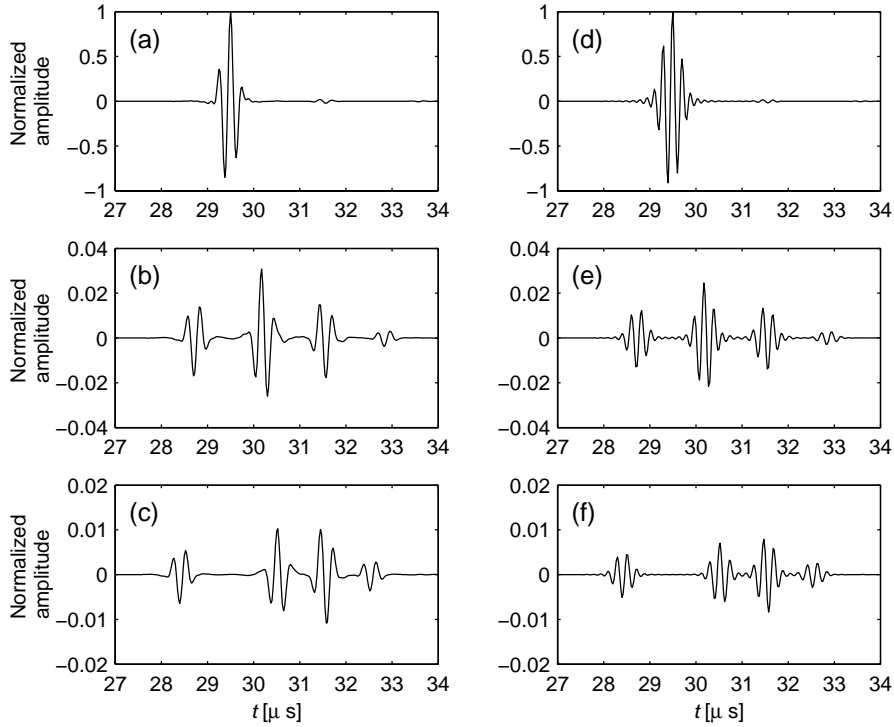


Figure 3.4: Crack echoes for different angular orientations  $\varphi = 0$  (upper row),  $\varphi = 45^\circ$  (middle row) and  $\varphi = 90^\circ$  (last row), computed with the original numerical package (d)-(f) and the modified version (a)-(c).

Although the impulse-response method is also based on fundamental physical principles its formulation allows approximations to easily be introduced. This is a great advantage since, apart from the obvious desire that the model should represent the crack echo accurately, another main objective is that the model is tractable for deriving detectors.

The impulse-response method is formulated in the time domain, in contrast to the modeling approach in the previous section. A defect echo signal can thereby be expressed as [63]

$$s(t; \theta) = \beta(t) * h(t; \theta), \quad (3.18)$$

where  $\beta(t)$  is the transducer efficiency,  $h(t; \theta)$  is the impulse response of the defect and  $\theta$ , as before, represents the underlying physical parameters such as shape, location, orientation etc. A general approach to derive the impulse response for a defect of complex geometry and with different acoustical impedances can be found in [66].

In [65] Lh emery studies the special case of a so-called penny shaped crack and presents a signal processing method for defect discrimination. Lh emery shows that the impulse response for a penny shaped crack consist of two components separated in time. The one appearing first in time is the contribution from the crack tip closest to the receiving transducer and the second is from the far tip. The crack defect impulse response can then be described by

$$h(t; \theta) = h_{\text{near tip}}(t; \theta) + h_{\text{far tip}}(t; \theta). \quad (3.19)$$

The occurrence of separate signal components, indicated by (3.19), can also be observed in the simulated crack echo responses in Figure 3.4, where also a few more mode converted pulses appears. Based on these simple observations the expression in (3.19) is extended to include  $M$  components. This yields

$$h(t; \theta) = \sum_{m=1}^M h_m(t; \theta), \quad (3.20)$$

where  $h_1(t; \theta)$  and  $h_2(t; \theta)$  are the near-tip and far-tip impulse responses respectively. The remaining terms in (3.20) represent the mode converted contributions in the crack impulse response.

Instead of deriving a physically based expression for each  $h_m(t; \theta)$  in (3.20) according to [66] a simple parametric model is postulated. Since the transducer is assumed to generate a transient wave-pulse the efficiency factor  $\beta(t)$  will have a bandpass character. Thus, each signal component consisting of  $\beta(t) * h_m(t; \theta)$  will also be bandpass and can thereby be represented by an amplitude modulated sinusoid [13]

$$\beta(t) * h_m(t; \theta) \approx \begin{cases} A_m a_m(t - \tau_m) \sin(\omega_m(t - \tau_m) + \phi_m), & t \in [\tau_m, \tau_m + T_a] \\ 0, & \text{otherwise} \end{cases}$$

$$\tilde{\theta}_m = [A_m \ \omega_m \ \tau_m \ \phi_m]. \quad (3.21)$$

Here  $\tau_m$  is the arrival time,  $A_m$  is the amplitude,  $\omega_m$  is the carrier frequency,  $\phi_m$  is the phase angle,  $a_m(t)$  is the envelope and  $T_a$  is the time duration of the envelope. The phenomenological crack scattering model then becomes

$$s(t; \theta) \approx s(t; \tilde{\theta}_1, \dots, \tilde{\theta}_M, a_1, \dots, a_M) = \sum_{m=1}^M x[t; \tilde{\theta}_m, a_m(t)], \quad (3.22)$$

where  $x[t; \tilde{\theta}_m, a_m(t)]$  is given by (3.21). Note that the physical parameter  $\theta$  has been replaced by a set of ‘‘unphysical’’ parameters,  $\tilde{\theta}_1, \dots, \tilde{\theta}_M$ , and the envelopes  $a_1(t), \dots, a_M(t)$ .

### 3.4 Modeling of clutter noise in metals

Polycrystalline materials, such as stainless steel and copper, consist of densely packed crystals or grains, which are randomly configured throughout the material. Therefore, in an UNDT scenario, when an acoustic pulse is emitted into a material the pulse will be scattered by a myriad of micro-structures causing the received signal to exhibit a random behavior. This signal is commonly called clutter.

It has been shown that the clutter signal from materials can be modeled as a colored Gaussian process when the number of grains is large [46, 47]. Due to this property, clutter models in UNDT studies are often modeled as colored Gaussian processes [26, 49, 50, 67]. One evident dilemma with this approach is to find out how the noise process should be colored. An approach to overcome this difficulty is to derive a physical model based on the material micro-structural properties. Such a clutter model has been put forward by Yalda *et al.* [38] and Margetan *et al.* [68].

The clutter noise model used in this thesis (Paper III and Paper IV), is a modification of the model by Yalda *et al.* [38], which considers an immersion testing pulse-echo set-up with a focused transducer. The new model, derived in Paper III and briefly presented here, is modified in the following aspects:

- The configuration is that of pulse-echo contact testing.
- The transducer is modeled as unfocused.
- Approximations are introduced to reduce the computational complexity.

The backscattered noise is assumed to be dominated by single scattering of the incident wave field by the individual grains. Based on this assumption the basic idea in this modeling approach is that the clutter noise is a superposition of the backscattered field from all grains isonified by the transmitting transducer.

By specifying the time interval within which the clutter noise signal is to be computed will impose restrictions on the depth coordinate. This *time window of interest* (TWOI) together with the beam pattern for the transducer yields a *spatial region of interest* (SROI) within which the backscattering from grains are to be modeled. The geometry of the problem is depicted in Figure 3.5.

In the model by Yalda *et al.* [38] a clutter noise realization is obtained by adding the backscattered field from all grains in the SROI. To alleviate much of the computational complexity the SROI is here first decomposed into  $N$  sub-regions  $\text{SROI}_n$ , which are slices perpendicular to the propagation direction of the incident wave, see Figure 3.5. The backscattered contribution from all grains within the  $\text{SROI}_n$  can then be represented by a frequency and depth dependent random variable  $Q_n(\omega)$ . The statistical properties of  $Q_n(\omega)$  are derived in Paper III, where it

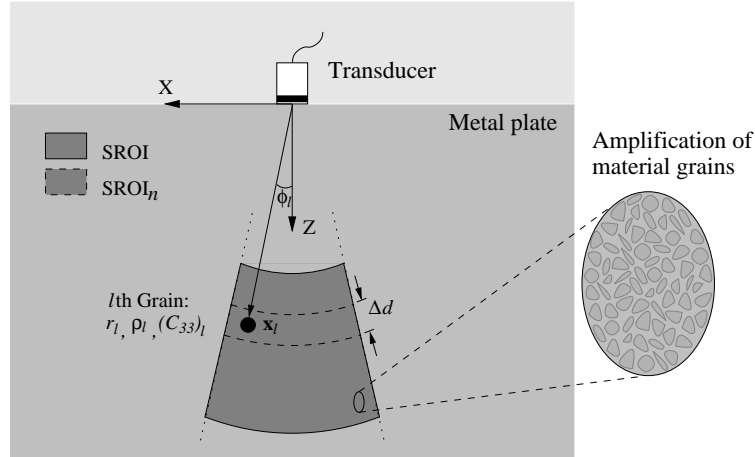


Figure 3.5: Sketch over the clutter noise model geometry illustrating the SROI and the  $l$ :th grain residing in the  $n$ :th sub region,  $SROI_n$ .

is shown, based on the central limit theorem, that  $Q_n(\omega)$  can be modeled as a zero mean Gaussian random variable. The frequency domain clutter noise signal can be expressed as

$$\tilde{v}(\omega) = \tilde{\beta}(\omega) \frac{\omega^2}{4\pi\rho c^4} \sum_{n=1}^N \frac{\exp\{2(j\frac{\omega}{c} - \alpha)R_n\}}{R_n} Q_n(\omega), \quad (3.23)$$

where  $\alpha$  is the material attenuation coefficient,  $R_n$  is the distance from the transducer to the center of the  $n$ :th slice.

The discrete time clutter noise realizations used in Paper III and Paper IV were computed by a numerical implementation of (3.23) under the assumption of a large number of grains. In this implementation a clutter noise realization,  $\bar{v} = [v(1), \dots, v(N)]^T$ , is obtained by an inverse discrete Fourier transformation of  $[\tilde{v}(\omega_1), \dots, \tilde{v}(\omega_N)]$  computed from (3.23) at  $N$  equidistant frequencies. Since the frequency domain clutter signal in (3.23) consists of linear combinations of Gaussian random variables, its inverse Fourier transform,  $\bar{v}$ , will also be Gaussian.

A realization of a typical clutter noise signal for a stainless steel with a probe efficiency factor given by (3.10) is depicted in Figure 3.6 in both the time and the frequency domain.

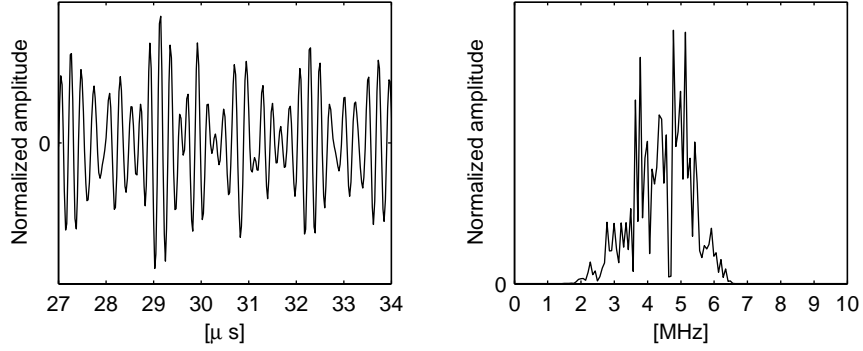


Figure 3.6: A clutter noise realization in the time domain (left) and the corresponding discrete Fourier transform (right).

### 3.5 Signal detection applied to nondestructive testing

The framework of parameterized signal detection, presented in Section 2.1.2, is suitable for treating the defect detection problem. In a typical UNDT situation, a potential defect can have different locations, orientations, and shapes, all of which will affect the backscattered wave-field and thereby the measured signal. These defect related physical attributes, which for example are represented by  $\theta$  in (3.15), can often be considered a priori unknown from one inspection to another. The uncertainty about the defect related physical attributes can be modeled by considering  $\theta$  to be a realization of a stochastic variable  $\Theta$  with the pdf  $p_{\Theta}$ . Thus, the uncertainty about  $\theta$  is transformed into an uncertainty about the defect echo  $\bar{s}$ . The ensemble of the defect echo signals for all possible values of  $\theta$  may be represented by

$$\mathcal{S} = \{ \bar{s}(\theta) \in \mathbb{R}^N \mid \theta \in \Lambda \}, \quad (3.24)$$

where  $\Lambda$  is the set where  $\theta$  takes its values.

In a testing situation the defect echo,  $\bar{s}(\theta)$ , is drawn from the signal family  $\mathcal{S}$  in (3.24), according to the pdf  $p_{\Theta}(\theta)$ . Moreover, by omitting multiple reflections the clutter noise can be considered both as additive and independent of the defect generated signal. Thus, the defect detection problem can be cast as the composite hypothesis test

$$\begin{aligned} H_0 : \bar{Y} &= \bar{V} \\ H_1 : \bar{Y} &= \bar{s}(\Theta) + \bar{V}, \end{aligned} \quad (3.25)$$

where  $\bar{V} \sim \mathcal{N}(0, \Sigma_V)$  represents the clutter noise.

As shown in Section 2.1.2, a decision rule for (3.25) can be formulated as

$$\delta(\bar{y}) = \begin{cases} 1 & \text{if } T(\bar{y}) \geq \tau \\ 0 & \text{if } T(\bar{y}) < \tau. \end{cases} \quad (3.26)$$

Here  $\tau$  is a user defined threshold and  $T$  is a detection statistic given by either the likelihood ratio in (2.23), for the NP and Bayes optimal detector, or the maximum likelihood ratio in (2.24) for the generalized likelihood ratio test (GLRT).

The particular problem considered in Paper III and Paper IV is to detect a strip-like crack residing in an elastic solid. Equipped with the signal models presented in Sections 3.3.1 and 3.3.2 a few approaches to compute a detection statistic are presented in the following sections.

### 3.5.1 Physical model based crack echo detector

Instead of pursuing an analytical approach in deriving a detector for strip-like cracks, the likelihood ratio in (2.23) can be computed numerically. This is simply achieved by a discretization of the pdf  $p_{\Theta}$  in (2.23) at  $M$  sample points  $\theta_m$ , and generating  $\bar{s}(\theta_m)$  by means of the computerized mathematical model of the crack scattering described in Section 3.3.1. Thus, the numerical approximation of the likelihood ratio reads

$$L(\bar{y}) = \int_{\theta \in \Lambda} L(\bar{y}|\theta) p_{\Theta}(\theta) d\theta \approx \sum_{m=1}^M L(\bar{y}|\theta_m) P_{\theta_m}, \quad (3.27)$$

where  $P_{\theta_m} = p_{\theta}(\theta_m)\Delta\theta$  and  $\Delta\theta$  is the volume around each sampling point. The conditional likelihood ratio in (3.27) is

$$L(\bar{y}|\theta_m) = \exp \left\{ \bar{s}(\theta_m)^T \Sigma_V^{-1} \bar{y} - \frac{1}{2} \bar{s}(\theta_m)^T \Sigma_V^{-1} \bar{s}(\theta_m) \right\}. \quad (3.28)$$

The NP and Bayes optimal detector for (3.25) can be implemented as a non-linear filter bank based on (3.28) and (3.27), which is depicted in Figure 3.7 as a block diagram.

If the a priori pdf  $p_{\Theta}$  is not known, which is often the case in a practical situation, the GLRT approach can be adopted. A numerical approximation of the GLRT detector in (2.24) can straightforwardly be obtained based on the same filter bank, given by (3.28), that was used for the NP and Bayes optimal detector. Thus, the GLRT detection statistic is

$$T(y) = \max_m \{L(y|\theta_m)\}. \quad (3.29)$$

The corresponding block diagram for the GLRT detector is depicted in Figure 3.8.

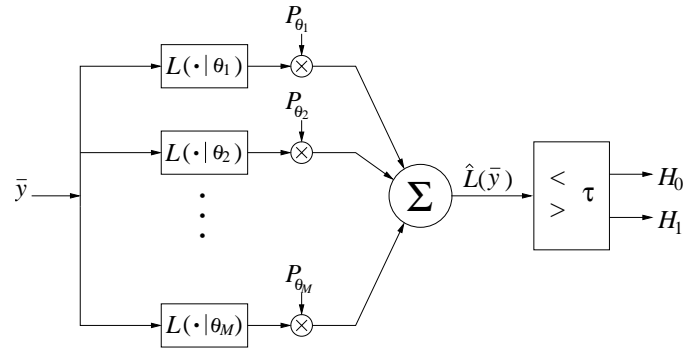


Figure 3.7: Block diagram of the NP and Bayes optimal detector

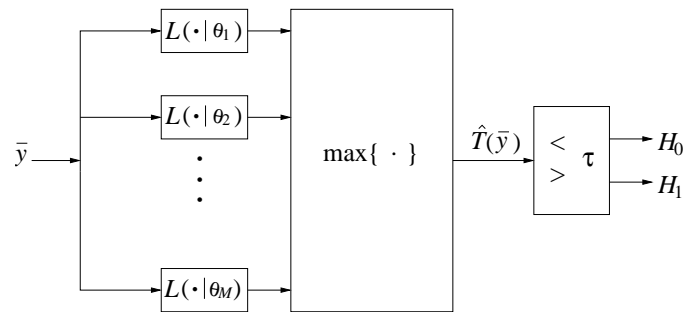


Figure 3.8: Block diagram of the GLRT detector

In Paper III the detection approaches described above are exemplified by assuming that the cracks position  $(x_0, z_0)$ , width  $w$ , and the constants  $K_{ij}$  are known while the angular orientation  $\varphi$  is unknown, see Figure 3.3 and the boundary conditions in (3.13). Thus, in this case  $\theta$  in (3.28) and (3.29) corresponds to the angular orientation  $\varphi$  of the crack. One should note that a fundamental limitation of the filter bank implementation of the detectors described above is the computational complexity. For a problem with  $K$  unknown parameters which need to be discretized into  $M$  different intervals, the number of filters in the filter bank is  $M^K$ , i.e. the number of filters grows exponentially with the number of parameters  $K$ . Thus, except for problems with few unknown parameters, one has to consider sub-optimal family detectors with lower complexity.

### 3.5.2 Phenomenological model based crack echo detector

The phenomenological signal model in Section 3.3.2 has been employed in Paper IV to obtain low complexity detectors for crack defects. This signal model consists of superpositions of pulses given by (3.21). Since the statistical variability of the underlying physical parameters of the cracks were represented by the stochastic variable  $\Theta$  in (3.25), the arrival time and waveform parameters in (3.21) are also modeled as stochastic. The problem of detecting several pulses with unknown arrival time is studied in Paper II, where an approximation of the NP and Bayes optimal detection statistic is given. This result is applied in Paper IV to the crack echo detection problem. In order to obtain a simple detection statistic, of low computational complexity, the following assumptions are imposed:

- The number of pulses are assumed to be fixed and the stochastic parameters of the pulses are assumed to be statistically independent.
- The carrier frequencies are assumed to be equal and deterministic but unknown for all pulses and will be denoted  $\omega_c$ .
- The discrete time envelopes for all pulses are assumed to be known and equal and denoted  $\bar{a} = [a(1), \dots, a(N_a)]^T$ , where  $N_a$  is the number of samples of the envelope.
- The arrival times  $\tau_1, \dots, \tau_M$  are assumed to be realizations from independent identically distributed (i.i.d.) stochastic variables with a uniform distribution on the observation interval. In the discrete time representation this corresponds to a uniform probability mass function on  $[1, N - N_a]$ .
- The pulse durations are assumed to be short relative the acquisition time, i.e.  $N_a \ll N$ .

Under these assumptions the detection statistic takes the form (see Paper II)

$$T(\bar{y}) = \sum_{n=1}^{N-N_a} E_{A,\phi} \left\{ L_{\omega_c}(\bar{y}_n^{n+N_a} | A, \phi) \right\}, \quad (3.30)$$

where  $\bar{y}_n^{n+N_a}$  denotes the sub-vector of  $\bar{y}$  from  $n$  to  $n + N_a$  and

$$L_{\omega_c}(\bar{y}_n^{n+N_a} | A, \phi) = \exp \left\{ \bar{x}^T \tilde{\Sigma}_V^{-1} \bar{y}_n^{n+N_a} - \frac{1}{2} \bar{x}^T \tilde{\Sigma}_V^{-1} \bar{x} \right\}. \quad (3.31)$$

Here  $\tilde{\Sigma}_V$  is the covariance matrix (of size  $N_a \times N_a$ ) of the noise  $\bar{V}$  and

$$x(n; A, \phi, \omega_c) = Aa(n) \sin(\omega_c(n-1)T_s + \phi) \quad n = 1, \dots, N_a, \quad (3.32)$$

where  $T_s$  is the sampling time.

The assumptions listed above are not based on any detailed analysis of the statistical properties of the model parameters but rather imposed to obtain a mathematically tractable problem. Clearly, the position, orientation, and size of a crack will affect the arrival times as well as the waveforms of the pulses via the intricate relationship between the underlying physical parameters and the parameters in (3.21). Due to the lack of knowledge concerning this intricate relationship and the statistical properties of a potential crack's physical parameters the assumptions listed above are intentionally conservative in the sense that they introduce very little a priori knowledge. By refining these assumptions to agree more with the underlying physical reality the detector will yield higher performance but become significantly more complex. In the following subsections three approaches to solve  $E_{A,\phi}\{L_{\omega_c}(\bar{y}_n^{n+N_a}|A, \phi)\}$  in (3.30) are pursued based on different assumptions of the statistical properties of the model parameters  $A$  and  $\phi$ .

### Case 1: Matched filter detector

By ignoring that  $A$  and  $\phi$  can exhibit any form of variability the problem reduces to detecting a deterministic pulse. This is equivalent to the coherent detection problem described in Section 2.1.1, with the likelihood ratio given by (2.8). Thus, under these simplified assumptions  $E_{A,\phi}\{L_{\omega_c}(\bar{y}_n^{n+N_a}|A, \phi)\}$  reduces to

$$L_{\lambda}(\bar{y}_n^{n+N_a}) = \exp\left\{\bar{x}^T(\lambda)\Sigma_V^{-1}\bar{y}_n^{n+N_a} - \frac{1}{2}\bar{x}^T(\lambda)\Sigma_V^{-1}\bar{x}(\lambda)\right\}, \quad (3.33)$$

where  $\lambda = [\omega_c \ A \ \phi]$  are some fixed parameters.  $\square$

### Case 2: Noncoherent detector

The previous case is here extended by allowing the phase  $\phi$  to have a uniform distribution, i.e.  $\phi \sim U[0, 2\pi]$ . This corresponds to the noncoherent detection problem, presented in Example 2.1, where the likelihood ratio is given by (2.34). Thus,  $E_{A,\phi}\{L_{\omega_c}(\bar{y}_n^{n+N_a}|A, \phi)\}$  can then be expressed as

$$L_{\lambda}(\bar{y}_n^{n+N_a}) = \exp\left\{-\frac{1}{4}\bar{a}^T\Sigma_v^{-1}\bar{a}\right\}I_0\left(\sqrt{(\bar{h}_s^T(\lambda)\bar{y}_n^{n+N_a})^2 + (\bar{h}_c^T(\lambda)\bar{y}_n^{n+N_a})^2}\right), \quad (3.34)$$

where  $\bar{h}_s(\lambda)$  and  $\bar{h}_c(\lambda)$  are given by (2.29) and depend on  $\lambda = [\omega_c \ A]$ . Recall that the likelihood ratio for the noncoherent detection problem was derived under the narrowband approximation. Since the defect echo pulses are relatively wideband it is questionable if the narrowband approximation is satisfied for these types of pulses.  $\square$

### Case 3: Wideband quadrature matched filter detector

The final case that has been considered is when both the pulse amplitude  $A$  and the phase  $\phi$  are modeled as random. The amplitude is here assumed to be Rayleigh distributed, i.e.  $A \sim R(\sigma_A)$ , with an unknown density parameter  $\sigma_A$ . As in the previous case, the phase is taken to be uniformly distributed. This is equivalent to the detection problem described in Example 2.2. The likelihood ratio for this problem is given in (2.47), which yields that  $E_{A,\phi}\{L_{\omega_c}(\bar{y}_n^{n+N_a}|A,\phi)\}$  can be expressed as

$$L_\lambda(\bar{y}_n^{n+N_a}) = \exp\{G_\lambda\} \times \exp\left\{\frac{\sigma_A^2}{2}(\bar{y}_n^{n+N_a})^T H_\lambda H_\lambda^T \bar{y}_n^{n+N_a} - \frac{\sigma_A^2}{2}(\bar{y}_n^{n+N_a})^T H_\lambda Q_\lambda H_\lambda^T \bar{y}_n^{n+N_a}\right\}, \quad (3.35)$$

where  $\lambda = [\omega_c \sigma_A]$ , and  $G_\lambda$ ,  $Q_\lambda$ , and  $H_\lambda$  now depend on  $\lambda$  and are given by (2.45), (2.48), and (2.49), respectively.  $\square$

The remaining problem is now to find appropriate values for the parameter  $\lambda$  in (3.33), (3.34), and (3.35). As mentioned, in previous UNDT studies [28, 29, 30], parametric detectors for defects have been optimized by using the SNRE in (1.7) as a criterion function. An alternative strategy is adopted here, which is simply based on finding the parameter  $\lambda^*$  that minimizes the probability of error

$$\lambda^* = \arg \min_{\lambda} \{P_E(\delta_\lambda)\}. \quad (3.36)$$

Here  $\delta_{\lambda^*}$  is on the form (3.26) with the detection statistic given by (3.30).

In Paper IV, the probability of error, for the three detectors presented above, is computed versus the various parameters in  $\lambda$ . From these simulations it can be concluded that it is feasible to optimize the detector parameters based on the minimum probability of error criterion even for quite small training data sets. Moreover, these results show that the detection performance is mainly dependent on the parameter specifying the carrier frequency  $\omega_c$ . Also presented in Paper IV are the ROCs for the proposed detectors, which are compared to the physical model-based optimal detector (Paper III). Moreover, since the wideband quadrature matched filter detector (Case 3 above) only shows a slight improvement in the ROCs compared to the noncoherent detector (Case 2 above) the crack echo pulses can be considered to satisfy the narrowband condition in this context. This is supported by the study in Paper I, where the effect of the signal bandwidth on the performance of the noncoherent detector is analyzed. However, even though the proposed detectors are based on quite ad hoc assumptions they result in only moderate performance degradation compared to the physical model-based optimal detector.

## Detectors in nonlinear sensor systems

THIS chapter is devoted to the problem of detecting signals acquired with a nonlinear sensor, for which three main topics are considered. The first is to derive an optimal detector for a static nonlinear sensor system and in particular to evaluate the detection performance as a function of the noise strength. This problem can be treated by means of the framework of non-Gaussian signal detection, presented in Section 2.4. As was pointed out in Section 1.2.2, detectability in nonlinear sensor systems could under certain circumstances be enhanced by noise. This phenomenon has been studied under the name of stochastic resonance (SR) [18, 19, 20, 21], which was illustrated in Example 1.1 by means of a dynamical system with a harmonic input signal. The SR phenomenon has also been studied in static (non-dynamical) systems [69, 70]. The second main topic is to propose a generally applicable quantifier for the SR phenomenon, which truly reflects the information processing capability of a system. The third topic concerns optimization of a tunable nonlinear sensor for detection, which is treated by employing the insights from the two above mentioned topics.

The nonlinear sensors that have been used in this thesis are the static SQUID and the static MR sensor, which are described in Sections 5.1 and 5.2, respectively. These sensors are used to illustrate the approaches taken for the three topics mentioned above, which are briefly outlined in Section 5.3.

## 4.1 The superconducting quantum interference device

The superconducting quantum interference device (SQUID) is an electromagnetic apparatus that converts magnetic flux variations into a voltage variation. The SQUID is the most sensitive magnetic sensor currently available, achieving a magnetic field resolution in the order of  $10^{-15}$  Tesla. A significant limitation of the practical usefulness of the SQUIDs is their sensitivity to both inherent and external noise. There are two main types of SQUIDs namely the rf (or AC) SQUID and the DC SQUID. The rf SQUID is the one studied in Paper V, and its fundamental components are depicted in Figure 4.1. This section will only give a brief description of the SQUID sensor, an in depth presentation of SQUIDs, their underlying physical mechanisms and operation can be found in [31].

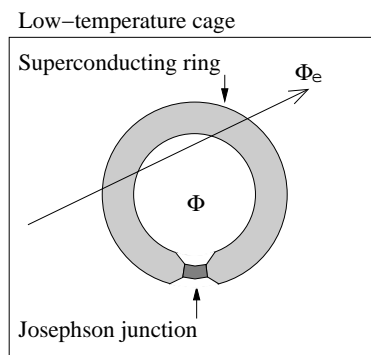


Figure 4.1: Simplified schematic of a SQUID sensor depicting the externally applied magnetic flux  $\Phi_e$  and the flux  $\Phi$  trapped in the superconductive ring.

A time varying external magnetic flux,  $\Phi_e(t)$ , is applied to the SQUID's superconductive ring, which is shielded by a low-temperature cage, see Figure 4.1. This external flux is here given by

$$\Phi_e(t) = \Phi_i(t) + \Phi_{DC} + \sigma\Phi_V(t), \quad (4.1)$$

where  $\Phi_i(t)$  is the input flux to be measured (detected),  $\Phi_{DC}$  is a known DC level applied to obtain a symmetric transfer characteristic,  $\Phi_V(t)$  is a noise disturbance of zero mean and unit variance, and  $\sigma$  is a noise strength parameter. The noise term  $\sigma\Phi_V(t)$  in (4.1) can often be modeled as Gaussian with a normalized autocorrelation given by

$$R(\tau) = \frac{1}{\sigma^2} E_t \{ \sigma\Phi_V(t) \sigma\Phi_V(t + \tau) \} = e^{-|\tau|/\tau_v}, \quad (4.2)$$

where  $\tau_v$  is the noise correlation time. Furthermore, the noise bandwidth  $\tau_v^{-1}$  is in many situations considerably larger than the bandwidth of input flux signal  $\Phi_i(t)$ , yielding that the noise can be approximated as being white [19].

The externally applied flux,  $\Phi_e$ , yields a magnetic flux through the superconductive loop (denoted  $\Phi$  in Figure 4.1), which evolves according to the dynamics determined by the superconductive properties of the ring and the Josephson junction. The dynamics of the magnetic flux through the superconducting loop can be described by [18, 19]

$$LC \frac{d^2}{dt^2} x(t) = -\tau_L \frac{d}{dt} x(t) - U'[x(t)] + x_e(t). \quad (4.3)$$

Here  $x(t) = \Phi(t)/\Phi_0$  is the normalized flux in the loop,  $x_e(t) = \Phi_e(t)/\Phi_0$  is the normalized external flux,  $\Phi_0 = \hbar/2e$  is the flux quantum,  $L$  is the inductance of the loop,  $C$  is the junction capacitance, and  $\tau_L = L/R_j$ , where  $R_j$  is the so-called normal state resistance of the junction. Moreover,  $U'(x) = \frac{d}{dx}U(x)$ , with the function  $U$  given by [18, 19]

$$U(x) = \frac{1}{2}x^2 - \frac{\beta}{4\pi^2} \cos(2\pi x), \quad (4.4)$$

where  $\beta = 2\pi L I_c / \Phi_0$ , and  $I_c$  is the so-called loop critical current. The parameter  $\beta$  determines the shape of the potential governing the dynamics of the SQUID.

In most practical applications the SQUID loop is shunted by a low resistance yielding that  $LC \ll \tau_L$  and thereby that the L.H.S. of (4.3) can be neglected [19]. Thus, in these cases the dynamics in (4.3) is reduced to

$$\tau_L \frac{d}{dt} x(t) = -U'[x(t)] + x_e(t). \quad (4.5)$$

Due to the modeling assumptions above the first order system in (4.5) bears a clear resemblance to the system studied in Example 1.1 (Chapter 1) with the exception of being multi-well. Several studies of various SR phenomenas in rf SQUIDs described by (4.5) have been published, many of which are devoted to signal detection [15, 16, 19, 20, 21].

A further simplification of the rf SQUID transfer characteristic in (4.5) can be made if the noise bandwidth,  $\tau_v^{-1}$ , not only is considered to be much larger than the bandwidth of the input flux signal  $x_i(t)$ , but also much less than  $\tau_L^{-1}$ , i.e.  $\tau_v \gg \tau_L$ . This is valid in many situations since  $\tau_L$  is typically in the order of  $10^{-10}$  to  $10^{-12}$  seconds which far exceeds the bandwidth of most real-world signals of interest. Thus, by setting  $\tau_L \frac{d}{dt} x(t) = 0$  the dynamics in (4.5) can be approximated by the quasi-static form [71]

$$U'[x(t)] = x_e(t). \quad (4.6)$$

The measured output voltage signal from the quasi-static rf SQUID is proportional to the so-called shielding flux  $x_s(t) = x(t) - x_e(t)$ . A non-dynamic transfer characteristic can now be obtained by solving (4.6) for  $x_s(t)$  as a function of  $x_i(t)$ . This has been done analytically [71, 72], in form of a Fourier-Bessel expansion when  $0 \leq \beta < 1$ , yielding

$$x_s(t) = \lim_{N \rightarrow \infty} \sum_{n=1}^N \frac{(-1)^n}{n\pi} J_n(n\beta) \sin[2\pi n(x_i(t) + x_{DC})], \quad (4.7)$$

where  $x_{DC} = \Phi_{DC}/\Phi_0$  and  $J_n$  denotes an  $n$ :th order Bessel function of the first kind. The quasi-static SQUID model in (4.7) has been reported [72] to exhibit SR like phenomenon, when altering the parameter  $\beta$ . However, in [72] no SNR enhancement was found when altering the noise strength parameter  $\sigma$ . This model is also used in Paper V to exemplify the proposed information theoretic approach to quantify SR.

## 4.2 The magneto-resistive sensor

The magneto-resistive (MR) sensor utilizes the magneto-resistive effect in ferromagnetic transition metals in order to measure external magnetic fields. The essence of this effect is that the resistance in a ferromagnetic material is dependent on the angle between the internal magnetization and the direction of an applied current. When an external magnetic field is applied the internal magnetization is rotated, thereby changing the resistance. In Paper VI a so-called barber pole MR sensor is used to detect weak magnetic DC fields in a strong noisy background. In this work the transfer characteristic of the MR sensor is obtained experimentally due to difficulties to determine all the required physical parameters and also since the available mathematical models for MR sensors transfer characteristics are quite crude. The experimental procedure for acquiring the transfer characteristic is simply to apply external fields of known amplitude to the sensor and measure the sensors response. This section gives a brief presentation of the basic functionality of an MR sensor, a thorough description of the MR effect can be found in [31].

The basic element in an MR sensor is a thin film of a magneto-resistive alloy etched into a rectangular shape with electrodes attached at both ends. In order to linearize the sensor for small external fields so-called barber poles are etched on the thin film, see Figure 4.2. The barber poles are a series of strips of high electrical conductivity that force the current flow in the thin film into a direction determined by the inclination of the barber poles.

In ferromagnetic materials there are certain preferred directions for the magnetization, this is due to the materials crystal structure and orientations. The most

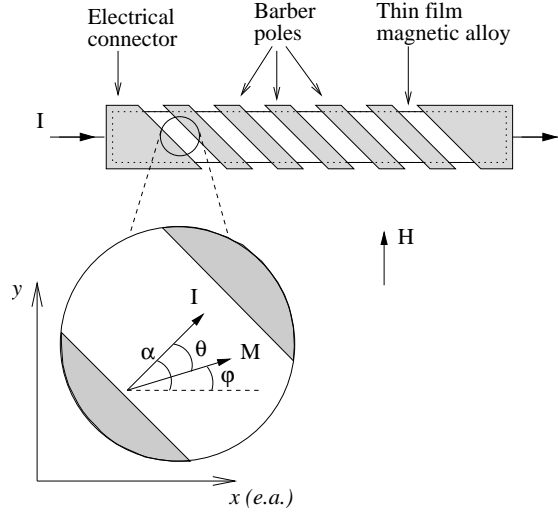


Figure 4.2: Schematic of an MR sensor with barber poles.

preferred direction is the so-called easy axis (e.a.), which in Figure 4.2 is assumed to be aligned with the  $x$ -direction. It has been shown that the resistance of the MR element can be described by [31]

$$R(\theta) = R_{\perp} + \Delta R \cos^2(\theta). \quad (4.8)$$

Here  $\theta$  is the angle between the internal magnetization,  $M$ , and the direction of the applied current,  $\Delta R = R_{\parallel} - R_{\perp}$ , where  $R_{\perp}$  and  $R_{\parallel}$  are the resistances perpendicular and parallel, respectively, to the  $x$ -direction. Under the influence of an external magnetic field,  $\vec{H} = [H_x \ H_y]^T$ , the direction of the magnetization  $M$  will rotate, which is represented by the angle  $\varphi$  between the e.a. and  $M$ . An approximate relation between the external field  $\vec{H}$  and  $\varphi$  for an *ellipsoidal*-shaped thin film is given by [31]

$$\sin(\varphi) = \frac{H_y}{H_0 + H_x / \cos(\varphi)}, \quad (4.9)$$

where  $H_0$  is the so-called characteristic field which is material dependent. Following [31], rough approximations of MR sensors' transfer characteristics can be expressed in terms of the resistance by using (4.8) and (4.9), and assuming that the  $x$ -component of the external field is  $H_x = 0$ . The  $y$ -component of the external field is here assumed to be given by

$$H_y(t) = H_s(t) + \sigma H_V(t), \quad (4.10)$$

where  $H_s(t)$  is the magnetic field to be measured (detected),  $H_V(t)$  is an ambient zero mean unit variance white Gaussian noise disturbance, and  $\sigma$  is a noise strength parameter.

For an elliptic MR element without barber poles  $\alpha \approx 0$ , which yields that  $\theta \approx \varphi$  (see Figure 4.2). Thus, by using (4.8) and (4.9) the resistance can be expressed as a function of the  $y$ -component of the external field according to

$$R(H_y) = R_0 - \Delta R \left( \frac{H_y}{H_0} \right)^2, \quad (4.11)$$

where  $R_0 = R_{\perp} + \Delta R$ . Figure 4.3 depicts the resistance  $R$  as a function of the external field  $H_y$  normalized by  $H_0$ .

The resistance for an elliptic MR element with barber poles, inclined so that  $\alpha = 45^\circ$ , can be expressed as [31]

$$R(H_y) = R_0 - \Delta R \frac{H_y}{H_0} \sqrt{1 - \left( \frac{H_y}{H_0} \right)^2}. \quad (4.12)$$

A typical behavior of the transfer characteristic in (4.12) is depicted in Figure 4.3, where it can clearly be seen that  $R(H_y)$  can be well approximated as linear for  $H_y/H_0$  close to zero. However, if the sensor is intended to operate in a very noisy environment then the external field can not be confined to small amplitudes only, thereby violating the classical operating conditions. In these situations a wider domain of the MR sensor transfer characteristic will be utilized yielding that the sensor must be considered both nonlinear and non-bijective.

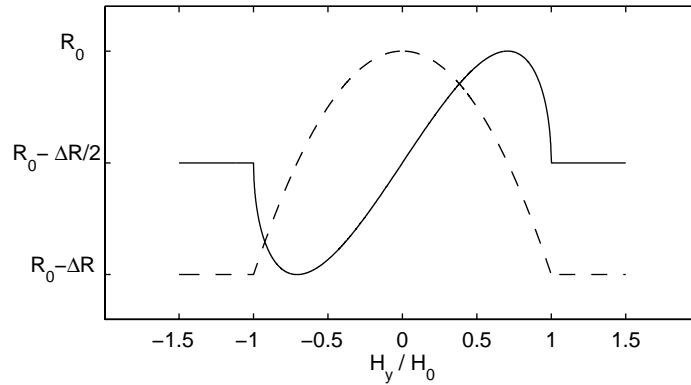


Figure 4.3: Typical transfer characteristics of an MR sensor expressed in terms of the MR elements resistance as a function of the external fields  $y$ -component. The resistance is plotted for an MR element without barber poles (dashed) and with barber poles (solid).

### 4.3 Optimal detectors in static nonlinear sensor systems

The problem of detecting a known signal contaminated by additive noise and measured by means of a static nonlinear sensor is considered. Moreover, the sensor's static nonlinear transfer characteristic, below denoted  $g$ , is assumed to be known yielding that the problem can be expressed as a binary hypothesis test on the form

$$\begin{aligned} H_0 : Y_n &= g(\sigma V_n), \quad n = 1, \dots, N \\ H_1 : Y_n &= g(s_n + \sigma V_n), \quad n = 1, \dots, N. \end{aligned} \quad (4.13)$$

Here,  $\bar{s} = [s_1, \dots, s_N]^T$  is the sampled signal to be detected,  $\sigma$  is a noise strength parameter and  $V_1, \dots, V_N$  are noise samples, which are assumed to be i.i.d. Gaussian with zero mean and unit variance.

The hypotheses in (4.13) can be directly associated with those in (2.72) yielding an optimal detector on the form

$$\delta(y) = \begin{cases} 1 & \text{if } L(\bar{y}) \geq \tau \\ 0 & \text{if } L(\bar{y}) < \tau, \end{cases} \quad (4.14)$$

where the likelihood ratio is given by

$$L(\bar{y}) = \prod_{n=1}^N \sum_{m=1}^M \frac{p_V(c_{y_n}^{(m)})}{|g'(s_n + c_{y_n}^{(m)})|} \bigg/ \sum_{k=1}^K \frac{p_V(b_{y_n}^{(k)})}{|g'(b_{y_n}^{(k)})|}. \quad (4.15)$$

In the following two sections the particular problems covered in Paper V and Paper VI, are briefly presented.

#### 4.3.1 Detectability in nonlinear sensor systems

In this section, the performance of a sensor-detector system, in terms of detectability as a function of the noise strength, is considered. As mentioned previously, these types of studies have been conducted under the name of stochastic resonance (SR), where various kinds of SNR measures, computed on the output of the sensor, has been used to reflect the performance as a function of the noise strength  $\sigma$ . The deflection ratio or *generalized signal-to-noise ratio* can be used to express many of the various definitions of SNRs by appropriately choosing<sup>1</sup> the function  $G$  below. The deflection ratio is defined by [8, 40]

$$d_{\Delta}(p_0, p_1) \triangleq \frac{(E_1 \{G(\bar{Y})\} - E_0 \{G(\bar{Y})\})^2}{\text{Var}_0 \{G(\bar{Y})\}}, \quad (4.16)$$

<sup>1</sup>For example, a connection between the deflection ratio in (4.16) and the SNR in (1.11), which has been used in several SR studies, is derived in [73].

where  $p_0$  and  $p_1$  are the pdfs of  $\bar{Y}$  under  $H_0$  and  $H_1$ , respectively, and  $\text{Var}_0\{G(\bar{Y})\}$  denotes the variance of  $G(\bar{Y})$  under  $H_0$ . However, unless  $G$  in (4.16) is given by the likelihood ratio in (4.15), the SNRs are not adequate for evaluating the performance of a nonlinear sensor with respect to hypothesis testing (for details see Appendix B). In such situations alternative measures must be employed which incorporate the whole probabilistic structure of the problem at hand.

From an information theoretic perspective, the problem of assessing performance of a signal transformation, such as performed by a sensor, can be seen as evaluating how much relevant information that is preserved after the signal has been processed. The hypotheses of the underlying signal in (4.13), i.e. before the influence of the sensor, can be described by

$$\begin{aligned} H_0 : X_n &= \sigma V_n, \quad n = 1, \dots, N \\ H_1 : X_n &= s_n + \sigma V_n, \quad n = 1, \dots, N. \end{aligned} \quad (4.17)$$

The ability to discriminate between  $H_0$  and  $H_1$  in (4.17) is determined by the pdfs of  $\bar{X} = [X_1, \dots, X_N]^T$  under  $H_0$  and  $H_1$ , which shall be denoted  $\tilde{p}_0$  and  $\tilde{p}_1$ , respectively. Likewise, the ability to discriminate between  $H_0$  and  $H_1$  in (4.13) depends on the corresponding pdfs of  $\bar{Y}$ , i.e.  $p_0$  and  $p_1$ , which are determined by  $g$  as well as  $\tilde{p}_0$  and  $\tilde{p}_1$ . Moreover, the optimal performance for discriminating between the hypotheses in (4.17) gives the upper limit for the hypothesis test in (4.13), which is achievable if  $g$  in (4.13) is sufficient for the binary hypothesis problem in (4.17), i.e. sufficient for  $\{\tilde{p}_0, \tilde{p}_1\}$ . A brief discussion on sufficient statistics can be found in Appendix B.

Instead of following the conventional SR approach, by computing some kind of SNR, an alternative route is taken where the so-called  $f$ -divergences are used to compute a performance measure based on the pdfs of the sensor output signal. The  $f$ -divergences are described by [39, 40, 41]

$$d_f(p_0, p_1) = h\left(\int_{\bar{y} \in \mathbb{R}^N} f\left(\frac{p_1(\bar{y})}{p_0(\bar{y})}\right) p_0(\bar{y}) d\bar{y}\right), \quad (4.18)$$

where  $h$  is an increasing function on  $\mathbb{R}$  and  $f$  is a convex<sup>2</sup> real function on  $\mathbb{R}_+$ , i.e.  $[0, \infty]$ . The properties for the  $f$ -divergences are summarized in Appendix B, where it is pointed out that these measures, in contrast to the SNRs, can be used to evaluate if a given signal transformation is sufficient with respect to  $\{\tilde{p}_0, \tilde{p}_1\}$ .

The basic idea for evaluating the information processing capability of a sensor, is to compute  $d_f(p_1, p_0)$  as a function of the noise strength  $\sigma$  and examine if the divergence exhibits a local maximum for increased noise strength  $\sigma$ . It should

---

<sup>2</sup>A function is said to be convex if for any two points  $A$  and  $B$  on the curve  $y = f(x)$ , the chord between  $A$  and  $B$  lies above the curve.

be noted that the hypothesis problem in (4.17) is equivalent to the coherent detection problem described in Section 2.1.1, where it is shown that the detection performance is monotonically dependent on  $d$  in (2.15), which for (4.17) reduces to  $d = \bar{s}^T \bar{s} / \sigma^2$ . This yields that  $d_f(\tilde{p}_0, \tilde{p}_1)$  is monotonically dependent on  $d$ , whereas the behavior of  $d_f(p_0, p_1)$  not only depends on  $d$  but also on  $g$ .

For the particular problem studied in Paper V,  $g$  is the static SQUID transfer characteristic in (4.7) and the hypotheses in (4.13) are reduced to only include a single time sample since  $\bar{s}$  is taken to be a known DC signal  $\mu$ . Moreover, the detection performance for the SQUID sensor-detector system is evaluated in terms of  $d_f(p_0, p_1)$  for increasing values of the noise strength  $\sigma$  while simultaneously scaling the DC level  $\mu$  so that  $d = \mu^2 / \sigma^2$  is kept constant. The particular  $f$ -divergence measure that is used in this study is the so-called Kolmogorov variational distance<sup>3</sup>. In addition to the Kolmogorov variational distance the performance is also expressed in terms ROC curves and minimum achievable probability of error for the optimal detector in (4.14). Based on these performance measures it is shown that the detectability in a static SQUID sensor system can be enhanced by increasing the noise strength  $\sigma$ . However, such a noise enhanced detection performance will not occur if  $g$  in (4.13) is bijective and the detector is optimal. As a conclusion it can be stated that a necessary requirement for noise enhanced information processing performance of a nonlinear system is that the system is non-bijective.

The use of  $f$ -divergences as quantifier for SR, which was proposed in Paper V, are applied to a dynamical system, similar to the system in Example 1.1, in a paper by Robinson *et al.* [74]. In [74] it is shown that the detectability does not exhibit enhancement when increasing the noise strength. This result is in conflict with the generally accepted notion of SR and is simply due to the fact that the system is bijective. It represents an interesting example of how the SNR measures, that traditionally has been used to quantify SR, does not suffice in describing the information processing capability of a nonlinear system.

### 4.3.2 Sensor optimization for detection

In most practical detection scenarios the strength of the ambient noise can not be altered, which was the case considered in the previous section. A more practically relevant problem is tuning of a sensor's transfer characteristic in order to improve the detectability in a given measurement environment. The hypotheses for this problem can be expressed as

$$\begin{aligned} H_0 : Y_n &= g_\beta(\sigma V_n), \quad n = 1, \dots, N \\ H_1 : Y_n &= g_\beta(s_n + \sigma V_n), \quad n = 1, \dots, N. \end{aligned} \quad (4.19)$$

---

<sup>3</sup>The Kolmogorov variational distance is given by (4.18) with  $h(z) = z$  and  $f(z) = |\pi_1 z - \pi_0|$ .

where  $\beta$  is some parameter by which the sensor transfer function may be modified.

If  $g_\beta$  is bijective for all possible parameter settings it will clearly be sufficient for all inference problems since the inverse,  $g_\beta^{-1}$ , exist for all  $\beta$ . However, if  $g_\beta$  is not bijective for any  $\beta$  it is not immediately clear if  $g_\beta$  is sufficient for a particular inference problem. Therefore, when facing an inference problem which is to be solved based the statistic  $g_\beta(X)$  the success could be crucially dependent on the choice of  $\beta$ . This naturally leads to the problem of finding a parameter setting so the function either becomes bijective or preserves as much relevant information as possible concerning the particular inference problem. As mentioned earlier, in the detection performance studies by Hibbs *et al.* [15] and Rouse *et al.* [16], the sensor is tuned to operate in the SR regime where the quantifier (the tuning criterion function) is the SNR in (1.11). Due to the weakness of the SNR measure the approach taken here is instead based on the  $f$ -divergences as a tuning criterion function. Thus, the optimal setting for  $\beta$  in (4.19) is given by

$$\beta^* = \arg \max_{\beta} \{d_f(p_0, p_1)\}. \quad (4.20)$$

This approach simply strives to find  $\beta$  that maximizes the divergence between the pdfs of the sensor output under  $H_0$  and  $H_1$ , i.e.  $p_0$  and  $p_1$  respectively.

The SQUID sensor and the MR sensor, presented in the previous sections, are used in Paper V and Paper VI to illustrate the sensor tuning approach by means of  $f$ -divergences. In these studies the objective is to operate the sensors in a noisy environment where it can not be guaranteed that the sensors are confined to operate in their linear regime.

In paper V, the Kolmogorov variational distance is displayed versus the static SQUID nonlinearity parameter  $\beta$  in (4.7). This result shows that, for a given noise strength  $\sigma$ , the Kolmogorov variational distance, and thereby the detectability, essentially increases monotonically with increasing  $\beta$ .

In paper VI, a similar study based on the MR sensor is performed, where the Kolmogorov variational distance and the Kullback-Leibler divergence<sup>4</sup> are used as optimization criteria. In this paper the sensor tuning is performed by simply injecting a known DC signal at the sensor input. Thus, the transfer function in (4.19) is given by  $g_\beta(X) = g(\beta + X)$ , where  $\beta$  is the known DC tuning and  $g$  is the experimentally determined transfer function, which resembles the transfer function in (4.12). From this study it is shown that both divergence measures display distinct local maxima, which indicate that by properly choosing  $\beta$ , the MR sensor can be tuned to improve the detectability for a given measurement environment.

---

<sup>4</sup>The Kullback-Leibler divergence is given by (4.18) with  $h(z) = z$  and  $f(z) = -\ln\{z\}$ .

# Chapter 5

## Concluding remarks and future work

THIS chapter will give some general comments and remarks on the insights that have been gained in this thesis in addition to the specific conclusions that are presented in the papers and throughout the previous chapters. Also briefly discussed in this chapter are some possible directions for future work.

As mentioned in the introduction, the main objective of this thesis is to contribute to the engineering quest by explicitly derive and apply optimal detectors for special, practically relevant problems. The particular problems in focus were to detect transient signal families as well as signals acquired with nonlinear sensors. This quest lead, for example, to the study of detecting multiple pulses with unknown arrival times, which is applicable to the UNDT application, even though the underlying assumptions may not be fully satisfied. This quest also lead to the study of detection of wideband signals, since, for example, the pulses generated from an UNDT system can exhibit a rather wideband characteristic. However, the pulses from an UNDT system will, more often than not, be narrow enough for the narrowband approximation to hold, yielding that the classical noncoherent and quadrature matched filter detectors can not be ruled out for these types of applications. Still, the use of the analytical solutions to the wideband noncoherent and quadrature matched filter detectors might be applicable in situations where a stationary harmonic signal source is located in a Gaussian noise environment and the measured signal is obtained by a mobile sensor that travels by the source with a high speed. This scenario can, for example, occur in air-borne surveillance systems.

The main conclusion regarding the UNDT defect detection problem is that the framework of composite hypothesis testing is appropriate since it can treat the oc-

currence of defects of various shapes and orientations. Moreover, a suitable approach to obtain detectors for this problem is to employ the solution techniques for detection of parameterized signals, where the signals can be represented either by a physical model or a phenomenological model. If sufficient *a priori* knowledge is available the physically model based strategy has the benefit of being optimal and can be used for a wide variety of defect types as long as a physical model is accessible. On the other hand, the phenomenological model based approach has the benefit of reducing the computational complexity and also that the assumptions regarding the signal models are explicit. Thus, any reduction in performance relative to the optimal performance can be directly traced to the imposed modeling assumptions. Any detection approach where the modeling assumptions are implicit, such as split spectrum processing (SSP), makes parameter tuning and interpretations of performance behavior less obvious.

The most urgent direction for future work is to perform real data experiments, where the proposed detector strategies can be employed and the validity of both the physical and the phenomenological defect echo models investigated. An obstacle in such a study, which is of significant importance, is to find a practically realizable approach to estimate detector performance, for example in the form of ROC curves. Another important direction for future work is to extend the statistical hypothesis testing problem to include multidimensional signals, acquired e.g. with a sensor array.

Throughout the thesis, and in most practical applications, the ultrasonic excitation pulse has been *a priori* determined without a detailed consideration to the particular detection problem at hand. An interesting aspect of pulse-echo detection problems, not only applicable to UNDT but also to sonar and radar, is to determine the most appropriate pulse to transmit in order to maximize detectability.

The framework of optimal signal detection is also suitable for detection problems when the signals are acquired with nonlinear sensors. However, this problem departs from the analytically tractable case of Gaussian signal detection and thereby requires either more advanced analytical treatment or retreating to numerical solution techniques. The main conclusion for the nonlinear sensor-detector application is that the stochastic resonance (SR) phenomena can be treated by utilizing concepts from both optimal signal detection and information theory. In particular, by quantifying the SR effect in terms of the  $f$ -divergences yields that the phenomenon can truly be interpreted as a noise enhanced gain of the systems information throughput. Apart from detection, another interesting problem is signal/parameter estimation in nonlinear sensor systems.

# Background on binary hypothesis testing

In this Appendix the binary hypothesis testing problem is treated in some more detail to give the reader additional insight into the role of the likelihood ratio as well as some of the optimality criteria used to design detectors.

The Appendix is introduced in Section A.1 with a brief presentation of simple and composite hypothesis tests. The Bayesian and Neyman-Pearson optimality criterion are described in Section A.2 and Section A.3, respectively, followed by the generalized likelihood ratio strategy in Section A.3. Finally, in Section A.4, some common approaches for evaluating detector performance are presented.

## A.1 Simple and composite binary hypothesis testing

Binary hypothesis testing is concerned with deciding among two possible statistical hypothesis, denoted  $H_0$  and  $H_1$  respectively, by processing the outcomes,  $y$ , of a stochastic variable  $Y$  taking values in some space  $\Omega$ . When the stochastic variable  $Y$  is assumed to have two possible probability distributions  $P_0$  and  $P_1$  under  $H_0$  and  $H_1$ , respectively, the hypotheses can be expressed as

$$\begin{aligned} H_0 : Y &\sim P_0 \\ H_1 : Y &\sim P_1. \end{aligned} \tag{A.1}$$

The test in (A.1) is sometimes known as *simple* since each of the two hypothesis correspond to only a single distribution for the observation, and  $H_0$  and  $H_1$  are commonly referred to as the *null* and *alternative* hypotheses, respectively.

In the case when several distributions can occur under either both or only one of the two hypothesis the test is commonly referred to as *composite*. This can be described by

$$\begin{aligned} H_0 &: Y \sim P_0 \\ H_1 &: Y \sim P_\theta, \end{aligned} \tag{A.2}$$

where  $\theta$  is a parameter used to index the family of distributions that can occur under the  $H_1$  hypothesis, i.e.  $\{P_\theta | \theta \in \Lambda\}$ , and  $\Lambda$  is some space where  $\theta$  takes its values.

The main objective of binary hypothesis testing is to formulate a decision rule which, based on an observation  $y$ , in some optimal fashion can discriminate between  $H_0$  and  $H_1$ . The discrimination is achieved by mapping the observation  $y$  into either 1 or 0 corresponding to  $H_1$  and  $H_0$ , respectively. Thus, the decision rule can be considered to partition the observation space  $\Omega$  into subsets  $\Omega_1$  and  $\Omega_0 = \Omega_1^c$ , where  $\Omega_1^c$  denotes the complement to  $\Omega_1$ , so that observations  $y \in \Omega_1$  and  $y \in \Omega_1^c$  yields 1 and 0, respectively. The decision rule can thereby be formulated as

$$\delta(y) = \begin{cases} 1 & \text{if } y \in \Omega_1, \\ 0 & \text{if } y \in \Omega_1^c. \end{cases} \tag{A.3}$$

The key problem in obtaining an optimal decision rule of the form (A.3) is to define in which sense the test is desired to be optimal and then partition the observation space accordingly. There are several strategies that can be employed to obtain a decision rule, the applicability of which are mainly dependent on the type of test and the amount of a priori knowledge that is available. In this thesis the strategies that has been exclusively used are Bayes', Neyman-Pearson's and the generalized likelihood ratio. These strategies are briefly described below.

## A.2 Bayesian optimality

In this presentation of the Bayesian optimal decision rule, the simple hypothesis testing problem in (A.1) is considered and the *a priori* probabilities for  $H_0$  and  $H_1$ , here denoted by  $\pi_0$  and  $\pi_1$ , respectively, are assumed to be known. However, an analogous treatment can be employed for the composite hypothesis test in (A.2) by assuming that the parameter  $\theta$  is a random quantity,  $\Theta$ , with a known *a priori* probability distribution  $Q$  and the corresponding pdf  $q$ . Based on the *a priori* knowledge, the composite hypothesis test in (A.2) can then be transformed into a simple test by [8]

$$p_1(y) = E_\theta\{p_\theta(y)\} = \int_{\theta \in \Lambda} p_\theta(y)q(\theta) d\theta, \tag{A.4}$$

and letting the probability distribution  $P_1$  correspond to the probability density  $p_1$ .

The Bayes optimal decision rule for (A.1) is defined as the one that minimizes, over all decision rules, a criterion function known as Bayes risk. The Bayes risk is intended to assign an overall cost for all possible permutations of deciding between  $H_0$  and  $H_1$  when either of them is true. The first step in constructing an expression for the Bayes risk is by defining a so-called *conditional risk* as the average cost incurred by the decision rule,  $\delta$ , when one of the hypothesis is true. The conditional risk can be expressed as

$$R_j(\delta) = C_{1j}P_j(\Omega_1) + C_{0j}P_j(\Omega_0), \quad j = 0, 1 \quad (\text{A.5})$$

where  $C_{ij}$  are positive numbers representing the cost of choosing  $H_i$  when in fact  $H_j$  is true. The Bayes risk, for some given priors  $\pi_0$  and  $\pi_1$ , is then obtained as the average of the conditional risk in (A.5), yielding

$$r(\delta) = \pi_0 R_0(\delta) + \pi_1 R_1(\delta). \quad (\text{A.6})$$

Thus, the Bayesian strategy for finding a decision rule can be expressed as

$$\min_{\delta} \{r(\delta)\}. \quad (\text{A.7})$$

By using (A.5) and the identity  $P_j(\Omega_1) = 1 - P_j(\Omega_0)$ , the Bayes risk in (A.6) can be expressed as

$$\begin{aligned} r(\delta) &= \pi_0 C_{00} + \pi_1 C_{01} + \pi_0 (C_{10} - C_{00}) P_0(\Omega_1) + \pi_1 (C_{11} - C_{01}) P_1(\Omega_1) \\ &= \pi_0 C_{00} + \pi_1 C_{01} \\ &\quad + \int_{y \in \Omega_1} \pi_0 (C_{10} - C_{00}) p_0(y) - \pi_1 (C_{01} - C_{11}) p_1(y) dy, \end{aligned} \quad (\text{A.8})$$

where  $P_j(\Omega_1) = \int_{\Omega_1} p_j(y) dy$  is used in the second equality. By assuming that  $C_{11} < C_{01}$  and  $C_{00} < C_{10}$ , the region  $\Omega_1$  that minimizes  $r$  becomes

$$\Omega_1 = \left\{ y \in \Omega \mid \pi_1 (C_{01} - C_{11}) p_1(y) \geq \pi_0 (C_{10} - C_{00}) p_0(y) \right\}. \quad (\text{A.9})$$

The region in (A.9) can also be expressed as

$$\Omega_1 = \left\{ y \in \Omega \mid \frac{p_1(y)}{p_0(y)} \geq \tau \right\}, \quad (\text{A.10})$$

where

$$\tau = \frac{\pi_0 (C_{10} - C_{00})}{\pi_1 (C_{01} - C_{11})}. \quad (\text{A.11})$$

Moreover, the expression for  $\Omega_1$  in (A.10) consists of the quantity

$$L(y) = \frac{p_1(y)}{p_0(y)}, \quad (\text{A.12})$$

which is known as the likelihood ratio. Thus, the Bayes optimal decision rule for (A.1) can be expressed as

$$\delta(y) = \begin{cases} 1 & \text{if } L(y) \geq \tau \\ 0 & \text{if } L(y) < \tau, \end{cases} \quad (\text{A.13})$$

and is commonly known as a likelihood ratio test.

A noteworthy special case of the Bayes risk criterion occurs when the cost assignment is uniform, i.e.  $C_{ij} = 0$  if  $i = j$  and  $C_{ij} = 1$  if  $i \neq j$ . The Bayes risk then reduces to

$$r(\delta) = P_E(\delta) = \pi_0 P_0(\Omega_1) + \pi_1 P_1(\Omega_0), \quad (\text{A.14})$$

which is the average probability of error. Hence, in this case the Bayes optimality criterion is a minimum probability of error scheme.

### A.3 Neyman-Pearson optimality

The Neyman-Pearson (NP) optimal decision rule is defined by the one that maximizes the probability of detection, over all decision rules satisfying an imposed false-alarm constraint. Hence, the NP criterion for obtaining a decision rule can be expressed as

$$\max_{\delta} \{P_D(\delta)\} \text{ when } P_F(\delta) \leq \alpha, \quad (\text{A.15})$$

where  $P_D(\delta)$  and  $P_F(\delta)$  denotes the probability of detection and probability of false alarm, respectively, given the decision rule  $\delta$  and the false alarm constraint  $\alpha$ . The Neyman-Pearson optimality criterion is a very operationally attractive criterion since the trade off between detectability and false alarm is placed in the hands of the designer in a way that is easy to relate to the final outcome.

When deriving an expression for the NP decision rule, the simple hypothesis test in (A.1) will be considered, but as in the Bayesian case an analogous treatment can be employed for the composite hypothesis test in (A.2). The probability of false alarm and the probability of miss for the test in (A.1) given a decision rule  $\delta$ , i.e. acceptance region  $\Omega_1$ , can be expressed as

$$P_F(\delta) = P_0(\Omega_1) = \int_{y \in \Omega_1} p_0(y) dy, \quad (\text{A.16})$$

and

$$P_D(\delta) = P_1(\Omega_1) = \int_{y \in \Omega_1} p_1(y) dy. \quad (\text{A.17})$$

The acceptance region  $\Omega_1$ , i.e. decision rule, can be obtained by means of Lagrange multipliers, with the constraint  $P_F(\delta) \leq \alpha$ . Hence, the criterion to be maximized can be expressed as

$$r(\delta) = P_D(\delta) + \lambda(P_F(\delta) - \alpha) \quad (\text{A.18})$$

where  $\lambda$  is the Lagrange multiplier. By expressing the probabilities in (A.18) in terms of the integrals in (A.16) and (A.17) the expression in (A.18) reads

$$r(\delta) = \int_{y \in \Omega_1} [p_1(y) + \lambda p_0(y)] dy - \lambda \alpha. \quad (\text{A.19})$$

For this expression to be maximized, all  $y$  such that the integrand  $p_1(y) + \lambda p_0(y) \geq 0$  should be included in  $\Omega_1$ . Thus, the acceptance region  $\Omega_1$  becomes

$$\Omega_1 = \left\{ y \in \Omega \mid p_1(y) + \lambda p_0(y) \geq 0 \right\} = \left\{ y \in \Omega \mid \frac{p_1(y)}{p_0(y)} \geq -\lambda \right\}, \quad (\text{A.20})$$

where, again, the likelihood ratio occurs. Since,  $L(y) = p_1(y)/p_0(y) \geq 0$  the Lagrangian multiplier must satisfy  $\lambda \leq 0$ . Thus, by introducing  $\tau = -\lambda$ , the NP optimal decision rule for (A.1) can be expressed as

$$\delta(y) = \begin{cases} 1 & \text{if } L(y) \geq \tau \\ 0 & \text{if } L(y) < \tau. \end{cases} \quad (\text{A.21})$$

Moreover, the threshold  $\tau$  has to be chosen so that the constraint  $P_F(\delta) \leq \alpha$  is satisfied. By using (A.21) the imposed false alarm constraint can be expressed as

$$P_F(\delta) = \int_{\tau}^{\infty} p_L(L|H_0) dL = \alpha, \quad (\text{A.22})$$

where  $p_L(\cdot|H_0)$  denotes the pdf for the likelihood ratio (detection statistic) under  $H_0$ . Thus, by solving (A.22) for  $\tau$  yields the detection threshold.

## A.4 The generalized likelihood ratio strategy

In the case of a composite hypothesis test, such as (A.2), both the Bayes and the NP strategies considers  $\theta$  to be a random quantity  $\Theta$  with a known *a priori* distribution  $Q$  in order to transform the composite test into that of a simple test via

(A.4). Based on this knowledge these two approaches yielded clear cut optimization strategies. However, in many practical situations there is only limited a priori knowledge available for the distribution of  $\Theta$ . In these situations the integral in (A.4), which transformed the composite test into that of a simple test, can not be solved, yielding that other detection strategies has to be considered.

One approach is to postulate an ignorant (uniform) prior distribution for  $\Theta$  and then proceed and treat the problem within the Bayesian or NP framework. The obvious drawback with this approach is if the postulated distribution for  $\Theta$  deviates much from the true distribution which can result in detection performance significantly lower than the optimal.

Other ways to cope with the problem of unknown distribution of  $\Theta$ , when facing a composite hypothesis, are the uniformly most powerful (UMP) test, locally most powerful (LMP) test and the generalized likelihood ratio test (GLRT) [8, 12]. In many cases these techniques suffer less from the performance degradation that can occur when postulating an ignorant prior for  $\Theta$ . The test that has been employed in this thesis, is the GLRT which is based on the maximum likelihood (ML) ratio as detection statistic. Thus the GLRT statistic for the composite hypothesis test in (A.2) is

$$T_{\text{GLRT}}(y) = \frac{\max_{\theta} \{p_{\theta}(y)\}}{p_0(y)} = \max_{\theta \in \Lambda} \{L(y|\theta)\}, \quad (\text{A.23})$$

where  $L(y|\theta) = p_{\theta}(y)/p_0(y)$  is the conditional likelihood ratio. The GLRT detector can thereby be described by

$$\delta(y) = \begin{cases} 1 & \text{if } \max_{\theta} \{L(y|\theta)\} \geq \tau \\ 0 & \text{if } \max_{\theta} \{L(y|\theta)\} < \tau. \end{cases} \quad (\text{A.24})$$

Although the GLRT is not associated with any optimality criterion it is a very intuitive approach since among all  $\theta$  the GLRT uses the maximum likelihood estimate in forming the detection statistic. Moreover, the GLRT has proved to yield competitive detection performance, compared to the optimal, for several examples of composite hypothesis tests [12].

## A.5 Detector performance evaluation

The generic structure of the detectors presented in the previous sections can be described by the decision rule

$$\delta(y) = \begin{cases} 1 & \text{if } T(y) \geq \tau, \\ 0 & \text{if } T(y) < \tau, \end{cases} \quad (\text{A.25})$$

where  $T(y)$  is the detection statistic, which could be either the likelihood ratio in the case of the Bayes and NP test or the GLRT statistic. In fact, any monotone function of the likelihood ratio can also serve as detection statistic equally efficient in discrimination between the hypothesis as the likelihood ratio. Thus, a detection statistic given by

$$\tilde{T}(y) = f(L(y)), \quad (\text{A.26})$$

with  $f$  being any continuous monotone function, would also yield optimal performance. This is a very convenient property which can be used when implementing detectors but also when analytically evaluating detection performance. When constructing a decision rule based on a transformed statistic it is also required that the threshold is modified accordingly in order to maintain the desired false alarm rate (in case of the NP test) or the risk (in case of the Bayes test). Since  $f$  is monotone its inverse exist and the modified threshold can thus be obtained by

$$\tau' = f^{-1}(\tau). \quad (\text{A.27})$$

The decision rule in (A.25) can be viewed as consisting of two components. The first is the computation of the detection statistic and the second is the threshold operation of the detection statistic. Figure A.1 is a schematic presentation of the building blocks in a threshold decision rule.

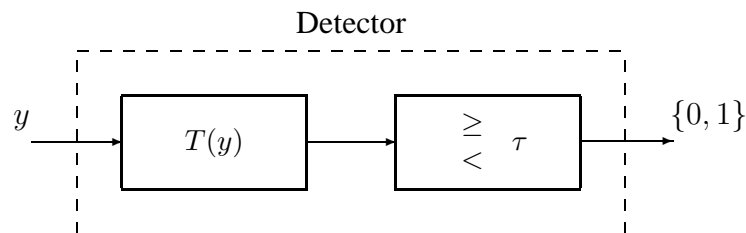


Figure A.1: Block structure of a threshold detector

The detection performance of a given detector can be evaluated in several different ways depending of the type of problem that is considered, the end objective of the evaluation and the optimality criterion that has been employed. In the case of an NP detector the performance is commonly presented by means of the so-called receiver operating characteristic (ROC) curves. This type of evaluation displays the probability of detection versus the probability of false alarm. The probability of detection and false alarm in (A.17) and (A.16), respectively, were expressed as integrals over  $\Omega$ . It is often a formidable task to perform such integrations, so instead these probabilities can be expressed based on the optimal decision rule in

(A.25). The probability of detection is thus given by

$$P_D(\delta) = \int_{\tau}^{\infty} p_T(T|H_1) dT, \quad (\text{A.28})$$

and the probability of false alarm is

$$P_F(\delta) = \int_{\tau}^{\infty} p_T(T|H_0) dT, \quad (\text{A.29})$$

where  $p_T(T|H_0)$  and  $p_T(T|H_1)$  are the pdf's of the detection statistic under  $H_0$  and  $H_1$ , respectively. When conducting a performance evaluation several ROC curves are often computed for different scenarios of varying degree of detection difficulty. Each ROC curve is then associated, or labeled, with some type of measure intended to represent the difficulty of the considered problem. Measures used to label ROC curves are for example signal-to-noise ratio or simply the energy of the noise.

In the case of a Bayes detector the performance is simply given by the value of the Bayes risk in (A.6). Also in this case the risk is often associated with a measure indicating the underlying detection difficulty. A quantity of particular interest in several detection problems is the minimum achievable probability of error which is given by the Bayes risk with a uniform cost assignment. The expressions in (A.28) and (A.29) can also be employed to obtain the minimum achievable probability of error by using the threshold  $\tau = \pi_0/\pi_1$  and the expression in (A.14), yielding

$$P_E(\delta) = \pi_0 P_F(\delta) + \pi_1 [1 - P_D(\delta)]. \quad (\text{A.30})$$

For most detection problems analytical performance evaluations are mathematically intractable. The cause for this is twofold; the first difficulty is to obtain the pdfs of the detection statistic under the two hypothesis and secondly, even if these pdfs could be obtained, it is difficult to perform the integrations in (A.28) and (A.29). Another way to formulate  $P_D(\delta)$  and  $P_F(\delta)$ , which is very useful when numerically computing the detector performance is by means of the expressions

$$P_D = E_1\{\delta(Y)\} = \int_{y \in \Omega} \delta(y) p_1(y) dy, \quad (\text{A.31})$$

and

$$P_F = E_0\{\delta(Y)\} = \int_{y \in \Omega} \delta(y) p_0(y) dy. \quad (\text{A.32})$$

These expressions can be employed to numerically evaluate the performance of a detector by means of Monte-Carlo simulations. In the Monte-Carlo approach a number of observations,  $y$ , are randomly generated for both  $H_0$  and  $H_1$ . These observations are then presented to the detector and the resulting outcomes are averaged according to (A.31) and (A.32).

# Appendix **B**

## Sufficient statistics and statistical distance measures

Statistical inference problems in the context of signal processing are concerned with extracting information from information bearing signals. The inference problem for both the transient signal family and the nonlinear sensor application considered in this thesis is that of detection. In both these applications signals are processed either by sensor transfer functions or by functions generating detection statistics. The ambition is that these transformations produces a so-called sufficient statistic, which preserves all relevant information available in the original signal that is useful for hypothesis testing. The amount of relevant information for hypothesis testing can be quantified by means of statistical distance measures.

This Appendix is introduced with a brief presentation of sufficiency in Section B.1, followed in Section B.2 by a presentation of a few statistical distance measures and their relating properties.

### **B.1 Sufficient statistics**

Although the concept of sufficiency in this thesis is only needed in the context of detection it will first be described in a general setting and then translated into the special case of binary hypothesis testing.

Suppose that  $Y$  is a stochastic variable taking values in an observation space  $\Omega$ , and that the distribution of  $Y$  is a member of a family of distributions indexed by  $\xi$  which takes values in some set  $\Lambda$ . Moreover, let the family of distributions be denoted  $\{P_\xi | \xi \in \Lambda\}$ . Then consider the situation when inferences are to be made about  $\xi$  when an observation  $y$  of  $Y$  are available. Note that  $\xi$  affects  $Y$  only

through its probability distribution  $P_\xi$  and, conversely, the statistical behavior of  $Y$  reflects the state of  $\xi$ . Thus, all available information about  $\xi$  is contained in the raw observation  $y$ .

If inferences about  $\xi$  were to be made on  $y$  directly, all information would be utilized and the results would be optimal. On the other hand, if inferences about  $\xi$  were to be made based on a function  $G(y)$  of the observation  $y$  the result will depend heavily on the properties of the function  $G$ . If  $G(Y)$  preserves all the information in  $Y$  about  $\xi$ ,  $G(Y)$  is said to be a sufficient statistic for  $\{P_\xi | \xi \in \Lambda\}$ . This may simply be expressed as  $G(Y)$  is sufficient for  $\xi$  when  $\{P_\xi | \xi \in \Lambda\}$  is understood. Thus, a statistical inference problem can be solved by either analyzing  $Y$  directly or, equally well, based on  $G(Y)$  if it is a sufficient statistic for  $\xi$ .

### Definition B.1 Sufficiency

Let  $G$  be a function which maps members from some space  $\Omega$  into some arbitrary set  $\Gamma$  thus

$$G : \Omega \rightarrow \Gamma. \quad (\text{B.1})$$

Assume that  $Y \in \Omega$  is a stochastic variable with a probability distribution belonging to the family of distributions  $\{P_\xi | \xi \in \Lambda\}$  on  $\Omega$ , thus

$$Y \sim P \quad \text{when} \quad P \in \{P_\xi; \xi \in \Lambda\}. \quad (\text{B.2})$$

The function  $G(Y)$  is said to be a sufficient statistic for  $\{P_\xi; \xi \in \Lambda\}$  if the distribution of  $Y$  conditioned on  $G(Y)$  does not depend on  $\xi \in \Lambda$ .

Note that all bijective functions  $G$  are obviously sufficient for  $\xi$  since the inverse  $G^{-1}$  exist. Hence, there exist many sufficient statistics for any given statistical inference problem. However, in many applications it is desirable to reduce the dimensionality of the original observation  $Y$  while maintaining the information about  $\xi$ . This leads to the concept of minimal sufficiency. A minimal sufficient statistic is the most compact representation of the observation without destroying information about  $\xi$ .

It is difficult to obtain and identify non-trivial sufficient statistics for a given statistical inference problem in general and minimal sufficient statistics in particular. The Fisher-Neyman factorization theorem [8] provides means to find a sufficient statistic (although not minimal) useful for several inference problems. Consider Definition B.1 of sufficiency and suppose the distribution  $P_\xi$  has a corresponding pdf  $p_\xi$ . The Fisher-Neyman factorization theorem then states that  $G(Y)$  is sufficient for  $\xi$  if and only if there exist some functions  $a$  and  $b_\xi$  such that the pdf  $p_\xi$  can be expressed as

$$p_\xi(y) = b_\xi(G(y))a(y), \quad \forall y \in \Omega \quad \text{and} \quad \forall \xi \in \Lambda. \quad (\text{B.3})$$

The problem of finding a sufficient statistic for  $\xi$  given  $p_\xi$  then reduces to finding some functions  $a$  and  $b_\xi$ , which factorizes  $p_\xi$  according to (B.3).

In binary hypotheses testing the objective is to optimally discriminate between two hypotheses based on an observation  $y$  of  $Y$ . Recall, that this problem could be described by

$$\begin{aligned} H_0 : Y &\sim P_0 \\ H_1 : Y &\sim P_1. \end{aligned} \tag{B.4}$$

Thus, in the light of the definition of sufficiency the family of probability distributions of  $Y$  in (B.2) is reduced to  $\{P_0, P_1\}$ , i.e.  $\xi \in \{0, 1\}$ . Moreover, if an optimal decision is to be made based on a function of the observation, such as  $G$  in (B.1), the function has to be sufficient for  $\{P_0, P_1\}$ , i.e. preserve all information relevant for discriminating between  $P_0$  and  $P_1$ . An expression that computes the likelihood ratio for (B.4) is an example of a function of the observation which generates a detection statistic that is sufficient for  $\{P_0, P_1\}$ . This is illustrated by the following example by applying the Fisher-Neyman factorization theorem.

---

EXAMPLE B.1: SUFFICIENT STATISTIC FOR A SIMPLE HYPOTHESIS TEST

---

Consider the simple hypothesis testing problem in (B.4) and let the distributions  $P_0$  and  $P_1$  have the corresponding pdfs  $p_0$  and  $p_1$ , respectively. An optimal detection statistic, generated by some function of the observation  $y$ , must be sufficient for  $\xi$  when  $\xi \in \{0, 1\}$ .

The pdfs for the two hypothesis may be written on the form

$$p_\xi(y) = [p_1(y)]^\xi [p_0(y)]^{1-\xi}, \quad \xi \in \{0, 1\}. \tag{B.5}$$

Moreover, this expression may be factorized as

$$p_\xi(y) = \left[ \frac{p_1(y)}{p_0(y)} \right]^\xi p_0(y) = b_\xi(L(y))a(y) \tag{B.6}$$

where  $L(y) = p_1(y)/p_0(y)$  is the likelihood ratio,  $b_\xi(l) = l^\xi$  and  $a(y) = p_0(y)$ . Thus, according to the Fisher-Neyman factorization theorem  $L(Y)$  is a sufficient statistic for  $\xi$ .

---

In signal detection the observation space  $\Omega$  is, for example,  $\mathbb{R}^N$  or  $C([0, T])$  and for these cases the likelihood ratio significantly reduces the dimensionality of the problem into a detection statistic on  $\mathbb{R}$ .

## B.2 Statistical distance measures

In the previous section the somewhat abstract concept of sufficiency was discussed in order to point out that performance evaluations of signal transformations, in the context of hypothesis testing, should reflect sufficiency with respect to  $\{P_0, P_1\}$ . This section will present a number of statistical distance measures between two probability distributions, namely the so-called  $f$ -divergences and the deflection ratio. The  $f$ -divergences in particular, can be used to evaluate if a given signal transformation is sufficient with respect to  $\{P_0, P_1\}$ . This is not generally the case for the deflection ratio. However, the deflection ratio can be used to express many different definitions of SNRs and thereby appears either directly or indirectly in many detection studies [8].

The  $f$ -divergences are presented in Section B.2.1, followed in Section B.2.2 by a presentation of the deflection ratio.

### B.2.1 Information theoretic distance measures

A number of fundamental performance limits for binary hypothesis testing can be expressed in terms of the  $f$ -divergences, which has been introduced by Csiszár [41, 42] and independently by Ali and Silvey [39]. Some examples are the bound in Stein's lemma [75], the Chernoff bound [8, 75] and the bound on minimum achievable probability of error in Bayesian hypothesis testing. These bounds express how well one can perform certain aspects of a binary hypothesis test, such as the probability of detection or probability of false alarm. Several connections to performance limits for other statistical inference problems also exist and can be found in [8, 40, 75]. However, in this thesis the focus is on the connections to the minimum achievable probability of error.

The  $f$ -divergences is a class of measures which can be interpreted as expressing the dissimilarity or distance<sup>1</sup> between two pdfs. Intuitively this is an appropriate measure for a binary hypothesis test, since the larger the distance is between the pdfs under the two hypothesis the better the detectability and vice versa.

Let  $Y$  be a stochastic variable taking values in some set  $\Omega$  and let the statistical properties of  $Y$  be described by the two probability distributions  $P_0$  and  $P_1$  with corresponding pdfs  $p_0$  and  $p_1$ , respectively. The  $f$ -divergences can be described by

$$d_f(p_0, p_1) = h\left(E_0\left\{f\left(\frac{p_1(Y)}{p_0(Y)}\right)\right\}\right) = h\left(\int_{y \in \Omega} f\left(\frac{p_1(y)}{p_0(y)}\right) p_0(y) dy\right), \quad (\text{B.7})$$

---

<sup>1</sup>The word distance is not used in the strict sense that it has in metric spaces, it simply denotes how dissimilar two probability distributions are.

where  $E_0$  is the expectation over  $P_0$ ,  $h$  is an increasing function on  $\mathbb{R}$  and  $f$  is a continuous convex<sup>2</sup> real function on  $\mathbb{R}_+$ , i.e.  $[0, \infty]$ . Furthermore, the function  $f$  also satisfies

$$\begin{aligned} f(0) &= \lim_{u \rightarrow 0} f(u) \\ 0 \cdot f\left(\frac{0}{0}\right) &= 0 \\ 0 \cdot f\left(\frac{a}{0}\right) &= \lim_{\varepsilon \rightarrow 0} \varepsilon \cdot f\left(\frac{a}{\varepsilon}\right) = a \cdot \lim_{u \rightarrow \infty} \frac{f(u)}{u}. \end{aligned} \tag{B.8}$$

The conditions stated in (B.8) are imposed on  $f$  so that the expression in (B.7) can be computed for subsets of  $\Omega$  with zero probability for  $P_0$  as well as subsets of  $\Omega$  where both  $P_0$  and  $P_1$  are zero.

The properties of the  $f$ -divergences can be summarized by:

1. If  $X = G(Y)$  is a transformation  $\Omega \rightarrow \Gamma$  then

$$d_f(p_0, p_1) \geq d_f(\tilde{p}_0, \tilde{p}_1), \tag{B.9}$$

where  $p_0$  and  $p_1$  are the pdfs of  $Y$  and  $\tilde{p}_0$  and  $\tilde{p}_1$  are the corresponding pdfs of  $X = G(Y)$ , respectively.

2. The distance  $d(p_0, p_1)$  has its minimum when  $P_0 = P_1$  and maximum when  $P_0 \perp P_1$ , where  $\perp$  denotes orthogonality in the sense that  $P_0$  and  $P_1$  does not share any subsets of  $\Omega$  where both are nonzero.

Property 1 above is of significant importance since it constitutes an equivalence to the data processing inequality [75] and thus enables evaluation of sufficiency for  $G$  with respect to binary hypothesis testing, i.e.  $\{P_0, P_1\}$ . Sufficiency with respect to hypothesis testing is obtained when the distance between  $p_0$  and  $p_1$  is equal to the distance between  $\tilde{p}_0$  and  $\tilde{p}_0$ . Property 2 has an intuitive appeal since it reflects the notion of a distance by yielding a minimum if the pdfs are identical and a maximum when pdfs are completely dissimilar.

A common way to quantify the performance of a detector is by means of the minimum achievable probability of error. Due to the intractability to analytically compute the probability of error for general hypothesis testing problems several studies [8, 39, 76] about distance measures were driven by the search for its upper and lower bounds. In fact, the minimum achievable probability of error,  $P_E$ , can

---

<sup>2</sup>A function is said to be convex if for any two points  $A$  and  $B$  on the curve  $y = f(x)$ , the chord between  $A$  and  $B$  lies above the curve.

be included in the class of  $f$ -divergences in (B.7) by defining the distance  $d_E = 1 - P_E$ . The expression for  $P_E$  in (A.14) can be reformulated according to

$$\begin{aligned} P_E &= \pi_0 P_0(\Omega_1) + \pi_1 P_1(\Omega_0) = \int_{\Omega_1} \pi_0 p_0(y) dy + \int_{\Omega_0} \pi_1 p_1(y) dy \\ &= \int_{\Omega} \min\{\pi_0 p_0(y), \pi_1 p_1(y)\} dy = \int_{\Omega} \min\left\{\pi_0, \pi_1 \frac{p_1(y)}{p_0(y)}\right\} p_0(y) dy, \end{aligned} \quad (\text{B.10})$$

thus  $d_E$  expressed on the form (B.7) is obtained by  $h(x) = 1 - x$  and  $f(x) = \min\{\pi_0, \pi_1 x\}$ .

Below are two of the most well-known members of the  $f$ -divergences briefly presented.

### The Kolmogorov variational distance

The Kolmogorov variational distance can be expressed in slightly different ways and is known under many names, for example Kolmogorov divergence, Variational distance or  $d_{\mathcal{E}}$ -divergence. The Kolmogorov variational distance is obtained when  $h(x) = x$  and  $f(x) = |\pi_1 x - \pi_0|$  in (B.7) yielding

$$d_{\mathcal{E}}(p_0, p_1) = \int_{\Omega} \left| \pi_1 \frac{p_1(y)}{p_0(y)} - \pi_0 \right| p_0(y) dy = \int_{\Omega} |\pi_1 p_1(y) - \pi_0 p_0(y)| dy. \quad (\text{B.11})$$

Sometimes the expression in (B.11) is called the weighted Kolmogorov divergence since the a priori probabilities  $\pi_0$  and  $\pi_1$  are included. An unweighted version of (B.11) is obtained by  $h(x) = x$  and  $f(x) = |x - 1|$ .

Perhaps the most fundamental connection between the  $f$ -divergences and limits for inference is the relation between the minimum achievable probability of error in Bayesian hypothesis testing and the Kolmogorov variational distance. This relation is given by [40, 76]

$$P_E = \frac{1}{2} - \frac{1}{2} d_{\mathcal{E}}(p_0, p_1). \quad (\text{B.12})$$

This divergence measure was used in Paper V, with the objective to generalize the stochastic resonance effect by expressing it as a gain in information throughput, and in Paper VI by serving as an optimization criterion for sensor tuning.

### The Kullback-Leibler distance

The Kullback-Leibler (KL) distance is also known as the relative entropy or information divergence. This divergence measure is obtained by setting  $h(z) = z$  and

$f(z) = -\ln\{z\}$  in (B.7), yielding

$$d_{KL}(p_0, p_1) = \int_{\Omega} -\ln\left(\frac{p_1(y)}{p_0(y)}\right) p_0(y) dy. \quad (\text{B.13})$$

The Kullback-Leibler divergence can be used to place a lower bound on the minimum achievable probability of error according to [40]

$$e^{d_{KL}(p_0, p_1)} \leq 8P_E. \quad (\text{B.14})$$

It should be noted that this KL distance is not symmetric since  $d_{KL}(p_0, p_1) \neq d_{KL}(p_1, p_0)$  unless  $p_0 = p_1$ , and does thereby not behave like a distance in the conventional sense. However, it is possible to construct a symmetric distance measure by  $J(p_0, p_1) = d_{KL}(p_0, p_1) + d_{KL}(p_1, p_0)$  this distance measure is commonly called the Kullback's  $J$ -divergence.

The KL distance in (B.13) was used in Paper II by serving as an alternative to the Kolmogorov variational distance for the sensor tuning problem.

### B.2.2 The deflection ratio

One of the major disadvantages to the distance measures presented in the previous section is that they are often difficult to compute analytically for general pdfs. In such situations less rigorous distance measures can be employed, that are analytically more tractable and at least captures some of the main dissimilarities between the pdfs.

The signal-to-noise ratio is a widely used concept in many areas of signal processing. It is often used to quantify the detection difficulty when computed directly on the input signals, and as a measure of the detector performance when computed from the detection statistic. There are almost as many definitions of the SNR as there are researchers and the definitions are often tailor made for the particular problem under study. For example, in the stochastic resonance application presented in Chapter 1, a frequency domain SNR measure were used. As also mentioned in Chapter 1, a time domain SNR measure has been used for the split spectrum processing application. A measure that captures many of the various definitions of SNRs is the deflection ratio or *generalized signal-to-noise ratio*. The deflection ratio is defined by [8, 40]

$$d_{\Delta}(p_0, p_1) \triangleq \frac{(E_1\{G(Y)\} - E_0\{G(Y)\})^2}{\text{Var}_0\{G(Y)\}}, \quad (\text{B.15})$$

where  $G$  some function of the observation and  $\text{Var}_0\{G(Y)\}$  denotes the variance of the statistic  $G(Y)$  when  $Y \sim P_0$ .

In detection applications the deflection ratio can be interpreted to express the effectiveness of a detection statistic  $G$  in separating the two hypothesis. The difficulty to compute the deflection ratio in (B.15) obviously depends on the choice of the function  $G$  as well as the statistical properties of  $Y$ , i.e.  $P_0$  and  $P_1$ .

As mentioned, other SNR definitions can be described on the form (B.15). This is achieved by choosing the function  $G$  in some appropriate fashion. However, arbitrary  $G$  yields distance measures which do not necessarily reflect the dissimilarity between two pdfs adequately. This becomes clear by first reformulating (B.15) according to

$$\begin{aligned}
d_{\Delta}(p_0, p_1) &= \frac{\left[ \int_{\Omega} G(y)p_1(y) dy - \int_{\Omega} G(y)p_0(y) dy \right]^2}{\text{Var}_0\{G(Y)\}} \\
&= \frac{\left[ \int_{\Omega} G(y) \frac{p_1(y)}{p_0(y)} p_0(y) dy - \left( \int_{\Omega} G(y)p_0(y) dy \right) \left( \int_{\Omega} \frac{p_1(y)}{p_0(y)} p_0(y) dy \right) \right]^2}{\text{Var}_0\{G(Y)\}} \\
&= \frac{\left[ E_0 \left\{ G(Y) \frac{p_1(Y)}{p_0(Y)} \right\} - E_0\{G(Y)\} E_0 \left\{ \frac{p_1(Y)}{p_0(Y)} \right\} \right]^2}{\text{Var}_0\{G(Y)\}} \\
&= \frac{\text{Cov}_0^2 \left( G(Y), \frac{p_1(Y)}{p_0(Y)} \right)}{\text{Var}_0\{G(Y)\}}.
\end{aligned} \tag{B.16}$$

By means of the Cauchy-Schwartz inequality the square of the covariance can be bounded by  $\text{Cov}^2\{x, z\} \leq \text{Var}\{x\}\text{Var}\{z\}$ , with equality if  $x = z$ . Then the expression for the deflection ratio in (B.16) can be bounded by

$$d_{\Delta}(P_0, P_1) \leq \text{Var}_0 \left\{ \frac{p_1(Y)}{p_0(Y)} \right\} = d_{\chi^2}(p_1, p_0), \tag{B.17}$$

with equality if  $G(y) = \frac{p_1(y)}{p_0(y)}$ , i.e. if  $G$  is the likelihood ratio. The quantity  $d_{\chi^2}$  is a distance measure from the class in (B.7) with  $f(x) = (x - 1)^2$  and  $g(x) = x$  and thereby posses the properties for  $f$ -divergences. Thus for general  $G$ , i.e. various definitions of the SNR, the deflection ratio in (B.15) does not belong to the  $f$ -divergences and does thereby not inherit the desirable properties for  $f$ -divergences. This leads to the conclusion that the deflection ratio with an arbitrary  $G$  not necessarily can be used to adequately reflect if a detection statistic is sufficient for a given hypothesis test. This point is made in Paper III, where the deflection ratio, with  $G(z) = \|z\|^2$ , is used to evaluate and compare the performance of two detectors.

# Bibliography

- [1] R.A. Fisher, “On the mathematical foundations of theoretical statistics,” *Phil. Trans. Roy. Soc.*, vol. A 222, pp. 309–368, 1922.
- [2] J. Neyman and E. Pearson, “On the problem of the most efficient tests of statistical hypotheses,” *Phil. Trans. Roy. Soc.*, vol. A 231, no. 9, pp. 492–510, 1933.
- [3] N. Wiener, *Extrapolation, Interpolation and Smoothing of Stationary Time Series. With Engineering Applications*, J. Wiley, New York, 1949.
- [4] C.E. Shannon, “A mathematical theory of communication,” *Bell System Technical Journal*, vol. 27, pp. 379–423, 623–656, 1948.
- [5] H.L. Van Trees, *Detection, Estimation, and Modulation Theory, Part I*, J. Wiley, New York, 1968.
- [6] H.L. Van Trees, *Detection, Estimation, and Modulation Theory, Part III*, J. Wiley, New York, 1968.
- [7] H.A. Helstrom, *Detection and Estimation Theory*, J. Wiley, New York, 1968.
- [8] H.V. Poor, *An Introduction to Signal Detection and Estimation*, Springer, New York, 1994.
- [9] P.M. Woodward, *Probability and Information Theory, with Applications to Radar*, McGraw-Hill, New York, 1953.
- [10] A.W. Rihaczek, *Principles of High-Resolution Radar*, McGraw-Hill, New York, 1969.
- [11] R.O. Nielsen, *Sonar Signal Processing*, Artech House, London, 1991.

- [12] S.M. Kay, *Fundamentals of Statistical Signal Processing: Detection Theory*, Prentice Hall, New Jersey, 1993.
- [13] J.G. Proakis, *Digital Communications*, McGraw-Hill, New York, 1989.
- [14] L.W. Schmerr, *Fundamentals of Ultrasonic Nondestructive Evaluation: A Modeling Approach*, Plenum, New York, 1998.
- [15] A.D. Hibbs, A.L. Singsaas, E.W. Jacobs, A.R. Bulsara, J.J. Bekkedahl, and F. Moss, "Stochastic resonance in a superconducting loop with a josephson junction," *J. Appl. Phys.*, vol. 77, pp. 2582–2594, 1995.
- [16] R. Rouse, S. Han, and J.E. Lukens, "Flux amplification using stochastic superconductive quantum interference devices," *Appl. Phys. Lett.*, vol. 66, pp. 108–117, 1995.
- [17] A. Bulsara and L. Gammaitoni, "Tuning into noise," *Phys. Today*, vol. 49, no. 39, pp. 39–45, 1996.
- [18] L. Gammaitoni, P. Jung P. Hänggi, and F. Marchesoni, "Stochastic resonance," *Rev. of Mod. Phys.*, vol. 70, no. 1, pp. 223–287, 1998.
- [19] A. Bulsara and A. Zador, "Threshold detection of wideband signals: A noise-induced maximum in the mutual-information," *Phys. Rev. E*, vol. 54, no. 3, pp. 2185–2188, 1996.
- [20] V. Galdi, V. Pierro, and I. Pinto, "Evaluation of stochastic-resonance-based detectors of weak harmonic signals in additive gaussian noise," *Phys. Rev. E*, vol. 57, no. 6, pp. 6470–6479, 1998.
- [21] P. Jung, "Stochastic resonance and optimal design of threshold detectors," *Elsevier Phys. Lett A*, vol. 207, pp. 93–104, 1995.
- [22] S. Kay, "Can detectability be improved by adding noise?," *IEEE Sig. Proc. Lett.*, vol. 7, no. 1, pp. 8–10, 2000.
- [23] L.M. Garth and H.V. Poor, "Detection of non-gaussian signals: A paradigm for modern statistical signal processing," *IEEE Trans. Info. Theory*, vol. 82, no. 7, pp. 1061–1095, 1994.
- [24] I. Amir, N.M. Bilgutay, and V.L. Newhouse, "Analysis and comparison of some frequency compounding algorithms for the reduction of ultrasonic clutter," *IEEE Trans. Ultrason., Ferroelec., Freq. Contr.*, vol. 33, no. 4, pp. 402–411, 1986.

- [25] N.M. Bilgutay, U. Bencharit, R. Murthy, and J. Saniie, "Analysis of a non-linear diverse clutter suppression algorithm," *Ultrasonics*, vol. 28, pp. 90–96, 1990.
- [26] M.G. Gustafsson, "Nonlinear split spectrum processing using optimal detection," *IEEE Trans. Ultrason., Ferroelec., Freq. Contr.*, vol. 43, pp. 109–124, 1996.
- [27] V.L. Newhouse, N.M. Bilgutay, J. Saniie, and E.S. Furgason, "Flaw-to-grain echo enhancement by split-spectrum processing," *Ultrasonics*, vol. 20, pp. 59–68, 1982.
- [28] N.M. Bilgutay, U. Bencharit, and J. Saniie, "Enhanced ultrasonic imaging with split-spectrum processing and polarity thresholding," *IEEE Trans. Acoustics, Speech, and Signal Processing*, vol. 37, no. 10, pp. 1590–1592, 1989.
- [29] P. Karpur, P.M. Shankar, J.L. Rose, and V. L. Newhouse, "Split spectrum processing: optimizing the processing parameters using minimization," *Ultrasonics*, vol. 25, pp. 205–208, 1987.
- [30] P. Karpur, P.M. Shankar, J.L. Rose, and V.L. Newhouse, "Split spectrum processing: determination of the available bandwidth for spectral splitting," *Ultrasonics*, vol. 26, pp. 204–209, 1988.
- [31] W. Göpel, J. Hesse, and J.N. Zemel, *Sensors: A Comprehensive Survey*, VHC Publishers Inc., New York, 1989.
- [32] F. Chapeau-Blondeau, "Noise-enhanced capacity via stochastic resonance in an asymmetric binary channel," *Phys. Rev. E*, vol. 55, no. 2, pp. 2016–2019, 1997.
- [33] X. Godivier and F. Chapeau-Blondeau, "Stochastic resonance in the information capacity of a nonlinear dynamic system," *International Journal of Bifurcation and Chaos*, vol. 8, no. 3, pp. 581–589, 1998.
- [34] A. Longtin, "Stochastic resonance in neuron models," *Journal of statistical physics*, vol. 70, pp. 309–327, 1993.
- [35] M. Misono, T. Kohmoto, Y. Fukuda, and M. Kunitomo, "Noise-enhanced transmission of information in a bistable system," *Phys. Rev. E*, vol. 58, no. 5, pp. 5602–5607, 1998.

- [36] S. Mítaim and B. Kosko, "Adaptive stochastic resonance," *Proc. IEEE*, vol. 86, no. 11, pp. 2152–2183, 1998.
- [37] R.N. McDonough and A.D. Whalen, *Detection of Signals in Noise*, Academic Press, San Diego, 1995.
- [38] I. Yalda, F.J. Margetan, and R.B. Thompson, "Predicting ultrasonic grain noise in polycrystals: A Monte Carlo model," *J. Acoust. Soc. Am.*, vol. 99, no. 6, pp. 3445–3455, 1996.
- [39] S. Ali and D. Silvey, "A general class of coefficients of divergence of one distribution from another," *J. Royal. Stat. Soc. (ser. B)*, vol. 28, no. 1, pp. 131–142, 1966.
- [40] M. Basseville, "Distance measures for signal processing and pattern recognition," *Elsevier Science Publ., Signal Proc.*, vol. 18, pp. 349–369, 1989.
- [41] I. Csiszár, " $I$ -divergence geometry of probability distributions and minimization problems," *The Annals of Probability*, vol. 3, no. 1, pp. 146–158, 1975.
- [42] I. Csiszár, "Sanov property, generalized  $I$ -projection and a conditional limit theorem," *The Annals of Probability*, vol. 12, no. 3, pp. 768–793, 1984.
- [43] T. Kailath and H.V. Poor, "Detection of stochastic processes," *IEEE Trans. Info. Theory*, vol. 44, no. 6, pp. 2230–2259, 1998.
- [44] D.O. North, "An analysis of the factors which determine signal/noise discrimination in pulsed-carrier systems," *RCA Lab. Rep. PTR-6C*, 1943. (Reprinted in *Proc. IEEE*, vol. 51, pp.1016-1027, 1963).
- [45] H.L. Van Trees, *Detection, Estimation, and Modulation Theory, Part II*, J. Wiley, New York, 1968.
- [46] J.G. Abbott and F.L. Thurstone, "Acoustic speckle: Theory and experiment analysis," *Ultrasonic Imaging*, vol. 1, no. 3, pp. 303–324, 1979.
- [47] J.W. Goodman, "Some fundamental properties of speckle," *J. Opt. Soc. Am.*, vol. 66, no. 11, pp. 1145–1150, 1976.
- [48] R.B. Thompson and T.A. Gray, "A model relating ultrasonic scattering measurements through liquid-solid interfaces to unbounded medium scattering amplitudes," *J. Acoust. Soc. Am.*, vol. 74, no. 4, pp. 1279–1290, 1983.

- [49] M.G. Gustafsson and T. Stepinski, "Studies of split spectrum processing, optimal detection and maximum likelihood amplitude estimation using a simple clutter model," *Ultrasonics*, vol. 35, pp. 31–52, 1997.
- [50] K.D. Donohue, "Maximum likelihood estimation of A-scan amplitudes for coherent targets in media of unresolvable scatterers," *IEEE Trans. Ultrason., Ferroelec., Freq. Contr.*, vol. 39, no. 3, pp. 422–431, 1992.
- [51] A. Papoulis, *Probability, Random Variables and Stochastic Processes*, WCB/McGraw-Hill, Boston, 1991.
- [52] D.L. Cohn, *Measure Theory*, Birkhäuser, Boston, 1980.
- [53] P. Billingsley, *Probability and Measure*, J. Wiley, New York, 1979.
- [54] S.A. Kassam, *Signal Detection in Non-Gaussian Noise*, Springer-Verlag, New York, 1988.
- [55] J.S. Bendat, *Nonlinear System Analysis and Identification from Random Data*, J. Wiley, New York, 1990.
- [56] J.D. Achenbach, *Wave propagation in elastic solids*, North-Holland, Amsterdam, 1991.
- [57] X.M. Tang, M.N. Toksoz, and C.H. Cheng, "Elastic wave radiation and diffraction of a piston source," *J. Acoust. Soc. Am.*, vol. 87, no. 5, pp. 1894–1902, 1990.
- [58] J. Mattsson, *Modeling of scattering by cracks in anisotropic solids*, PhD thesis, Department of Mechanics, Chalmers University of Technology, Göteborg, Sweden, 1996.
- [59] J. Mattsson, A.J. Niklasson, and A. Eriksson, "3D ultrasonic crack detection in anisotropic materials," *Res. Nondestr. Eval.*, vol. 9, pp. 59–79, 1997.
- [60] J. Mattsson and A.J. Niklasson, "Ultrasonic 2D-SH crack detection in anisotropic solids," *J. Nondestr. Eval.*, vol. 16, pp. 31–41, 1997.
- [61] A.S. Eriksson, J. Mattsson, and A.J. Niklasson, "Modelling of ultrasonic crack detection in anisotropic materials," *NDT&E Inter.*, vol. 33, pp. 441–451, 2000.
- [62] B.A. Auld, "General electromechanical reciprocity relations applied to the calculation of elastic wave scattering coefficients," *Wave Motion*, vol. 1, no. 1, pp. 3–10, 1979.

- [63] A. Lhémery, “Impulse-response method to predict echo-responses from targets of complex geometry. Part I: Theory,” *J. Acoust. Soc. Am.*, vol. 90, no. 5, pp. 2799–2807, 1991.
- [64] A. Lhémery and R. Raillon, “Impulse-response method to predict echo-responses from targets of complex geometry. Part II. computer implementation and experimental validation,” *J. Acoust. Soc. Am.*, vol. 95, no. 4, pp. 1790–1800, 1994.
- [65] A. Lhémery and R. Raillon, “Impulse-response method to predict echo responses from targets of complex geometry. Part III: Application to nondestructive testing,” *J. Acoust. Soc. Am.*, vol. 95, no. 4, pp. 1801–1808, 1994.
- [66] A. Lhémery, “Impulse-response method to predict echo responses from defects in solids. Part I: Theory,” *J. Acoust. Soc. Am.*, vol. 98, no. 4, pp. 2197–2208, 1995.
- [67] F.S. Cohen, “Modeling of ultrasound speckle with application in flaw detection in metals,” *IEEE Trans. Sig. Proc.*, vol. 40, no. 3, pp. 624–632, 1992.
- [68] F.J. Margetan, R.B. Thompson, and I. Yalda-Mooshabad, “Backscattered microstructural noise in ultrasonic toneburst inspections,” *J. Nondestr. Eval.*, vol. 13, no. 3, pp. 111–136, 1994.
- [69] Z. Gingl, L.B. Kiss, and F. Moss, “Non-dynamical stochastic resonance: Theory and experiments with white and arbitrary colored noise,” *Europhys. Lett.*, pp. 191–196, 1995.
- [70] S.M. Bezrukov and I. Vodyanoy, “Stochastic resonance in non-dynamical systems without response thresholds,” *Nature*, vol. 385, pp. 319–321, 1997.
- [71] A. Barone and G. Paterno, *Physics and Applications of the Josephson Effect*, J. Wiley, New York, 1982.
- [72] M.E. Inchiosa, A.R. Bulsara, A. Hibbs, and B. Whitecotton, “Signal enhancement in a nonlinear transfer characteristic,” *Phys. Rev. Lett.*, vol. 80, no. 7, pp. 1381–1384, 1998.
- [73] J. Rung and J.W.C. Robinson, “A statistical framework for the description of stochastic resonance phenomenon,” in *STOCHAOS: Stochastic and Chaotic Dynamics in the Lakes*, pp. 409–416. AIP, Melville, New York, 2000.
- [74] J.W.C. Robinson, J. Rung, A.R. Bulsara, and M.E. Inchiosa, “General measures for signal-noise separation in nonlinear dynamical systems,” *Phys. Rev. E*, vol. 63, no. 1, pp. 1107–1117, 2001.

- [75] T.M. Cover and J.A. Thomas, *Elements of Information Theory*, J. Wiley, New York, 1991.
- [76] D.E. Boekee and J.C.A. Van Der Lubbe, "Some aspects of error bounds in feature selection," *Pattern Recognition*, vol. 11, pp. 353–360, 1979.